Bead-based chemistries to quantitate antibody responses to multiple *Plasmodium falciparum* and *Plasmodium vivax* antigens

Sonam Kaur Ghag

A dissertation

submitted in partial fulfillment of the

requirements for the degree of

Doctor of Philosophy

University of Washington

2019

Reading Committee:

Pradipsinh K. Rathod, Chair

Dustin Maly

Robert Synovec

Program Authorized to Offer Degree:

Chemistry

University of Washington

Abstract

Bead-based chemistries to quantitate antibody responses to multiple *Plasmodium falciparum* and *Plasmodium vivax antigens*

Sonam Kaur Ghag

Chair of the Supervisory Committee:
Professor Pradipsinh K. Rathod
Chemistry

Each year malaria impacts approximately 219 million people and causes over 400,000 deaths. The worldwide parasite burden remains high, even with the availability of efficacious antimalarial drugs and vector control tools such as insecticides and bed nets. Despite large investments in malaria vaccine development, there is currently no deployable vaccine for malaria. However, individuals who live in malaria endemic regions develop naturally acquired immunity (NAI). Thus, good vaccine candidates may be identified by studying serum antibody responses in malaria patients who live in endemic areas.

Protein arrays, which interrogate patient serum antibody binding to many proteins simultaneously, are the primary method of antigen prioritization. However, protein arrays are fabricated by generating unpurified malaria antigens in bacteria and directly spotting lysates onto slides without validation of correct antigen folding or purification. Results from protein arrays can be affected by the sample impurity where positive binding events may be masked by

background protein interactions or unrecognizable epitope presentation. Thus, technical improvements are needed to control protein production and protein exposure to patient sera. More recently, multiplexing bead-based assays have been applied to investigate malaria patient immune responses where spectrally distinct bead sets are coated with unique antigens of interest. For such assays, antigens traditionally are individually purified before coupling onto beads. To produce a more high-throughput method of patient immune response dissection using a large panel of antigens, bead-based chemistries were developed to modify multiplexing beads with a small linker molecule or with antigen capturing antibody. These modified beads capture malaria antigens directly from translation lysates, essentially purifying antigens in a single step. Both chemistries utilized the capture of recombinant antigens via a highly specific protein tag, HaloTag or C-tag. Although both systems successfully capture tagged antigens from translation lysates, the C-tag capture system proved to be more reliable and reproducible. Using recombinant malaria antigen merozoite surface protein 1 (MSP1)-coated beads and standard anti-MSP1 detecting antibodies, a 105-fold signal increase was observed in comparison to green fluorescence protein (GFP)-coated beads. Malaria patient sera responses to recombinant MSP1 were also measured. When assessed against MSP1-coated beads, serum from a high immune responsive patient gave an 8.5-fold increase in comparison to GFP-coated beads, while a low immune responsive patient gave a 2-fold increase. These results agree with previously reported protein microarray dissection of the same patient serum samples. The bead chemistries developed here make it possible to interrogate multiple malaria antigens simultaneously without demanding timely antigen purification. Furthermore, the multiplexing assay present antigen epitopes in a more accessible configuration while utilizing small amount of precious patient sera. The platform developed here will provide a high-throughput method of identifying specific

patient antibody-antigen binding events and has the potential to customize bead arrays to model populations with high antigenic variation.

Table of Contents

List of Figures and Schemes

Page

List of Tables

Page

Glossary

NAI- Naturally Acquired Immunity
MSP1- Merozoite Surface Protein 1
GFP- Green fluorescence protein
iRBCs- Infected red blood cells
SNPs- Single Nucleotide Polymorphisms
SP- Sulfadoxine-Pyrimethamine
ACTs- Artemesinin Combination Therapy Drugs
EMP1- Erythrocyte Membrane Protein 1
PE- Phycoerythrin
ELISA- Enzyme-Linked Immunosorbent Assay
EDC- 1-Ethyl-3-(3-dimethylaminopropyl)carbodiimide
Sulfo-NHS- N-hydroxysulfosuccinimide
GST- Glutathione S-transferase
MBP- Maltose Binding Protein
His Tag- Polyhistidine-tag
WGCF- Wheat Germ Cell Free system
TEV- Tobacco Etch Virus
AMA1- Apical Membrane Antigen 1
RH5- Reticulocyte Binding Homolog
MCS- Multicloning Site
AA- Amino Acid
SDW- Sterile Deionized Water
PP- Precision Protease
βme- 2-Mercaptoethanol
PBS- Phosphate Buffer Saline
LTQ- Linear Ion trap
3D7- *Plasmodium falciparum* isolate strain
POI- Protein of Interest
SMBP- Succinimidyl 4-(N-maleimidophenyl)butyrate
ESI- Electrospray Ionization
Fmoc- Fluorenylmethyloxycarbonyl protecting group
SAPE- Streptavidin, R-Phycoerythrin Conjugate
MFI- Mean Fluorescence Intensity
WG- Wheat Germ
MESA-ICEMR- Malaria Evolution in South Asia- International Center of Excellence for Malaria Research
WGS- Whole Genome Sequencing

Acknowledgments

The completion of this thesis dissertation would not have been possible without the help, support, and guidance of countless people. These past years were a unique journey and I learned so much more than just research and science. First, I would like to thank Dr. Pradip Rathod for all his guidance and support during my graduate school career. Pradip allowed me to join the lab and start a new project in which I was given ample space to try out my own ideas and grow as a researcher. I would also like to thank all the members of the Rathod Lab who have become a second family for me over the years. Each lab member has helped teach me new things and made coming to lab everyday a joy. Many lab members deserve a special acknowledgment as they were critical in helping me progress my project. From the very start Dr. Devaraja Mudeppa was a fantastic mentor in all things protein related. He is a master at using the wheat germ system for protein expression along with many other biochemical techniques. He taught me many of the basic skills I needed for my project and he helped me build a solid foundation of scientific skills. He was immensely patient with me and never turned me away when I came to him with questions. Dr. Sreekanth Kokkonda was an amazing mentor in all the organic synthesis work I did. He helped me develop synthesis schemes and always was available to talk when I needed help.

Finally, I must thank all of my friends and family who supported me throughout this process. There were times I was a complete mess and they were always there to keep my spirits up. I want to thank my parents for always emphasizing the importance of working hard and overcoming any challenges that come my way. I also want to thank my siblings, Sharan and Aman, for all their guidance, advice, and support from Monroe all the way to the end of this dissertation and beyond. Last, I want to thank my fiancé, Zain Babul, for being a constant

support in all my post workday melt downs. I cannot describe how much the non-science conversations and activities we did together helped keep me balanced.

Dedication

I would like to dedicate my dissertation to my parents, Amarjit Singh and Amarjit Kaur Ghag. Both their personal journeys took them from small villages in India to the other side of the world. They have worked tirelessly to give my siblings and I the life we are so fortunate to have, and they have always emphasized the importance of education. Without them I may not have ever thought to purse this doctorate and I cannot thank them enough.

Chapter 1: Introduction

Malaria

Global burden of malaria

Malaria threatens close to half the world's population. In 2017 alone there were an estimated 219 million cases of malaria.[1] Globally, malaria causes roughly 435,000 deaths and the most vulnerable populations are children under the age of five years as well as pregnant women.[2] Of the five malaria parasite species that cause human malaria: *Plasmodium falciparum*, *Plasmodium vivax*, *Plasmodium ovale*, *Plasmodium malariae*, and *Plasmodium knowlesi*, it is *Plasmodium falciparum* and *Plasmodium vivax* which cause the majority of cases and *Plasmodium falciparum* which is responsible for significantly more deaths.[3] Geographically, the disease has been restricted to parts of the world with suitable climates for transmission which also happen to be high poverty struck regions (Figure 1.1).[4] The highest burden of malaria cases occur in Africa and South East Asia (92% and 5% of cases respectively). Five countries alone account for half of all malaria cases worldwide: Nigeria (25%), Democratic Republic of the Congo (11%), Mozambique (5%), India (4%), and Uganda (4%).[1] In general, where malaria prospers, humans have prospered least. A comparison of gross domestic product (GDP) shows countries with high malaria endemicity have an average of 5.4X less GDP.[5] It is clear that underdeveloped countries with high poverty have a correlation with malaria prevalence due to the lack of free government provided bed nets, insufficient insecticide usage, and poor public health and infrastructure spending.[5]

History of malaria

Malaria can be traced back to many early civilizations through ancient writings and artifacts of the Egyptians, Chinese, and Indians of southeast Asia. The parasite likely spread in

the first century by traveling along the Nile and Mediterranean, eventually dispersing north to Greece and east to the Fertile Crescent. Here the parasite flourished with crowded settlements and standing water. In India and China, the population growth drove settlement to the more southern tropical regions that favored malaria.[6] Undoubtedly, the greatest effect was felt in Africa. Portuguese traders who entered the African coastal plains in the early 1500's were the first foreigners to confront the disease. The ailment was so tolling on newcomers the phrase "the White Man's Grave" became popular when describing West and Central Africa.[6] The parasite first was identified by French army doctor Charles Louis Alphonse Laveran in the late 1800's. By examining blood smears from soldiers under the microscope Laveran was able to distinguish crescent shaped bodies with small dots of pigments (now known to be the hemozoin byproduct of hemoglobin digestion by the parasite).[7] Laveran was the first to prove the disease was not caused by the "bad air" from swamps and marshes like many believed, but instead from a "germ."[7-8] The complete parasite cycle was understood thanks to the works of British scientist Ronald Ross and Italian scientist Giovanni Grassi. In 1895, Ross became the first person to show the presence of the parasite within an *Anopheles* mosquito after it had taken a blood meal.[9] Grassi later confirmed the parasites mosquito stage by transferring *Plasmodium vivax* to a healthy volunteer via mosquito bite.[8] Understanding how the parasite started using humans as a host was also of interest early on. In 1899 Laveran identified parasites in the blood of grivet monkeys which led to the discovery of parasites also present in the liver.[7] Until recently the closest known relative of *Plasmodium falciparum* was a chimpanzee parasite. These were assumed to have diverged at the same time as chimps and humans, over five million years ago. However, recent comparison of genomes has indicated human *Plasmodium falciparum* came

from a single linage of a gorilla parasite clade. Further, it is hypothesized that all known human strains may have resulted from a single cross-species transmission event.[10]

Malaria lifecycle

The malaria life cycle is quite complex and includes multiple different developmental stages each vastly unique from the other. The lifecycle starts with the bite of the female *Anopheles* mosquito (Figure 1.2). The mosquito bites the human host and during this bloodmeal it passes sporozoites to the hypodermis tissue.[11] These sporozoites travel to the liver where they exclusively invade hepatic cells. Inside the hepatocytes each sporozoite develops into tens of thousands of merozoites. Until these merozoites exit the liver cells the parasite is undetected by the hosts immune system, thus this stage is considered a dormant stage of the lifecycle. After departure from the liver stage the merozoites travel to the blood stream where their sole goal is to find and invade healthy red blood cells (RBCs).[12] Over multiple, two day life cycles, the invasion rupture and re-invasion of RBCs by the parasite can result in over 10^{12} parasitized erythrocytes in the bloodstream.[13] Merozoites rapidly invade erythrocytes and carry out a series of steps that morphologically change the RBC's structure. In *Plasmodium falciparum*, these infected red blood cells (iRBCs) are more prone to attachment to many different human host tissues and play a major role in the onset of severe malaria symptoms and cases.[14] A small subset of merozoites are predetermined to advance to the sexual forms of the parasite.[15] Here, mature male and female gametocytes are formed over a period of two weeks. When a mosquito bites this infected patient for a blood meal the mature gametocytes also get transferred. In the mosquito the sexual gametes merge and fertilize to create zygotes which mature into oocysts in the mosquito mid-gut.[16] The parasite then rapidly replicates and divides into thousands of sporozoites which migrate to the mosquito salivary glands. The lifecycle continues when an infected mosquito bites a new human

host.[13]

The blood stage of the parasite lifecycle is of significant importance to the disease progression within a human. Symptoms including fever, anemia, and lactic acidosis onset lead to the activation of the human innate immune response.[14] The blood stage is the best opportunity for the human immune response to recognize the parasite and guard itself by producing protective antibodies. Protection can be a challenge as the parasite utilizes a vast number of antigens during the invasion process. Merozoites are polarized cells in which the apical end contain organelles and structures such as the micronemes and rhoptries (Figure 1.3). These components comprise of numerous antigen proteins that facilitate invasion upon contact with RBCs.[17] Furthermore, morphological changes in RBCs are a result of an extensive parasite export network that aids in transport of adhesive proteins to the outside of the iRBC. These proteins help the iRBC bind to human tissue and delay parasite clearance. Parasite antigens involved in invasion and those exported to the outside of the iRBC are identified as foreign antigens by the host. The recognition of these parasite antigens can lead to a robust human immune response.

Current Treatments & Preventions

Antimalarial successes and challenges

Many of the early antimalarial treatments came from natural products that were accessible to ancient healers. The oldest known antimalarial comes from the bitter bark of a Cinchona tree native to South America. In the nineteenth century, the remedy was introduced to Europe and in 1820 French chemists isolated the active ingredient, quinine.[6] Quinine is a highly basic cinchona alkaloid which rapidly acts against intra-erythrocytic malaria parasites through a unknown mechanism of action. Currently quinine is still considered the second line of defense

when other treatments fail and resistance to the drug has been scarce and slow.[18] Search for a substitute to quinine has led to the next "gold standard" antimalarial in use after World War II, chloroquine. Chloroquine inhibits detoxification of the parasite's digestive vacuole after hemoglobin degradation.[19] However, in the late 1950's heavy use of chloroquine lead to resistance arising independently in four locations around the world.[6, 20] A single nucleotide polymorphism (SNP), K76T, in a gene which encodes a food vacuole transmembrane protein is the primary cause of chloroquine resistance.[21] In hopes of increasing efficacy a dual drug treatment was developed, Sulfadoxine-Pyrimethamine (SP). Components of this drug combination inhibit two different steps in the tetrahydrofolate biosynthesis. Again, resistance to SP appeared rapidly in southeast Asia and Africa due to SNPs in the gene encoding dihydrofolate reductase-thymidylate synthase.[21-23] After chloroquine failure mefloquine was introduced in Thailand as a first line defense against *Plasmodium falciparum*. Even with strict regulation of its use resistance was observed within six years of release and quickly spread to neighboring regions. Increased copy number in *pfmdr1*, a *P. falciparum* transmembrane transporter gene, has been the major determinant of resistance to mefloquine.[24] The current main line of defense against malaria is artemisinin combination therapy drugs (ACTs). The mode of action of artemisinin is still not fully understood, but it has been observed that the drugs cause oxidative stress and most likely effect multiple targets in the parasite.[25] However, delayed parasite clearance was observed around the Cambodia-Thailand border region in the early 2000's.[26-27] Although likely not the sole determinant of resistance, mutations in the propeller domain of the *P. falciparum* kelch gene have been associated with delayed parasite clearance.[26, 28-30] There is a clear pattern in which the parasite is capable of adapting and becoming resistant to each new drug treatment developed. This rapid spread of drug resistance has worsened the

burden of malaria and the emergence of resistance to ACTs now poses a great threat to the control of malaria and ultimate goal of malaria eradication.[31]

Other disease prevention strategies

Historically, vector management tools have contributed greatly to successful malaria control. The two most widely used and successful vector control methods are indoor residual spraying and long-lasting insecticidal bed nets and clothing. However, due to the emergence of insecticide resistance in mosquitos and growing concerns about health and environmental impacts of chemical controls new vector control methods are needed.[32] Some of these include, attractive toxic sugar baits and "eave tubes." Both approaches use the "attract and kill" strategy where mosquitos enter a tube trap and encounter a toxin that eliminates the mosquito. Also, the employment of selective microbial and plant-borne pesticides have shown to be effective agaisnt mosquito larvae.[33] The use of genetically modified mosquitos has become a new focus in the vector control field. One such example is the release of mosquitos carrying a dominate lethal mutation in endemic areas.[34] Although important, vector control is a merely a complement to drug and vaccine development.

Scope for a malaria vaccine and current vaccine pipeline

Vaccines are considered an important tool for disease control and eradication. The endless efforts put into developing a malaria vaccine stem from the observations that individuals who live in endemic regions eventually attain a naturally acquired immunity (NAI). Historical observations of such NAI were documented when early Europeans traveled to tropic regions and were highly susceptible to malaria in comparison to the indigenous population.[35] Those who live in endemic areas are constantly at risk for the disease (up to 1000 bites per year) and often can have high parasite loads but show minor to no symptoms.[35] Furthermore, the burden of disease in

these areas often falls on the youngest population or those with a compromised immune system while older children and adults are resistant to severe infections and death, though still susceptible to minor infection. Besides age, the degree of NAI can vary based on parasite prevalence which changes with season and number of previous clinical attacks.[35-37]

The mechanism of NAI has long been studied and it is evident that circulating antibodies play a major role in this protection. Passive transfer studies conducted in the 1960's showed that gamma globulin collected from recovered patients could be administered to infected children and reduced parasite counts to less than 1% of the initial infection. These early studies identified that the immune serums used for treatment had the greatest growth suppression on life cycle stages following schizogony.[38-40] However, present studies show circulating antibodies can block sporozoite, liver-stage, blood-stage, and sexual stages of the parasite and act as biomarkers of immunity.[37, 41] Additional components of NAI include release of cytokines that act against all stages of the parasite, cytotoxic T cell response that is directed at liver stage parasites, and memory B cell activation.[42-43] The usefulness of NAI has more recently been shown in studies where malaria naïve volunteers were inoculated with live sporozoites by laboratory mosquitos under controlled conditions. As a result, a dose dependent NAI protection was observed for up to a year in some volunteers.[43-45]

To date no FDA approved malaria vaccine has been released however there are numerous vaccines in the pipeline.[1] The most promising vaccine candidate has been a pre-erythrocyte vaccine, RTS,S. The vaccine is a hybrid which includes the carboxy terminus of *P. falciparum* circumsporozoite antigen and a hepatitis B surface antigen virus-like particle. Inoculation with the vaccine induces a humoral and cellular immune response that protects against sporozoites and liver stage schizonts. In phase 3 studies, a triple dose of the vaccine afforded protection of

39-50% and 23-30% in children age 5-17 months and 6-16 weeks, respectively.[46-47] The variation in short and long term efficacy and the high dose number makes alternative vaccine development necessary. The current malaria vaccine pipeline (Figure 1.4) is ever changing and quite diverse in regards to the targeted stage of the parasite lifecycle.[1] However, few new antigen targets have been identified for vaccine development and limited number of vaccines reach later phase trials. Thus, a more complete understanding of NAI is critical for understanding how the host protects itself against infection and disease. Vaccine development relies on mimicking the acquisition of NAI. By understanding which circulating host antibodies are most crucial for protection it is possible to prioritize antigen targets. This is more thoroughly discussed in the following sections.

Antigen Prioritization: Past and Current Methods

Early antigen discoveries

Malaria antigen prioritization based on protective immune responses has long been an area of interest to those who work on vaccines. However, identifying and characterizing immune reactive parasite antigens was, and continues to be, a challenge due to the antigenic diversity of malaria parasites. In the 1980s, the Freeman group from the Wellcome Laboratories in the UK helped pioneer antigen discovery using traditional biochemical assays. By fusing spleen cells from *P. yoelii* immune mice with cancerous myeloma cells the group was able to produce several monoclonal antibody-secreting hybridoma cell lines.[48-49] Using these secreted antibodies scientists were able to carry out indirect immunofluorescence against parasite cultures. The observation that some B cells produce antibodies against the infected erythrocyte membrane or the parasite antigen itself lead to the identification of specific antigen-antibody pairs.[50] Furthermore, target antigens could be purified and isolated using these monoclonal antibodies in

immunoprecipitation assays. Leading antigen candidates, including MSP1 and AMA1, were identified using these methods.[51-55] However, in this pre-genomic era only a subset of vaccine and diagnostic candidates were identified, representing less than 0.5% of the parasite genome.[56] With the publication of the *Plasmodium falciparum* genome in 2002 a new era of antigen identification ensued where potential antigens are ready to be unlocked.[57] What becomes important now is prioritization of these potential vaccine candidates and examination of the approaches used for such ranking.

Protein microarrays

Equipped with the entire parasite genome, having an efficient and quick way to screen thousands of antigen candidates became necessary. The development of automated micro-printing technology made the creation of protein microarrays possible.[58-59] Protein microarrays are ideally suited to investigate the humoral immune response and brought high-throughput and miniaturization capabilities to antigen prioritization. A single array slide can be printed with thousands of antigens of interest.[60] Once printed, each slide is hybridized with a single patient serum sample and an antigen-antibody response is detected if the serum sample contains antigen recognizing antibodies. The ability to express all the proteins of an infectious agent such as malaria allows for not only the prioritization but also the identification of novel antigens that would otherwise be undetectable using traditional biochemical techniques like 2D gels. The earliest reports of utilizing protein microarrays to identify malarial immunoreactive antigens of interest was in the late 2000's.[56] In these studies, and most subsequent works since, malarial antigens of interest are expressed using *E. coli* in vitro expression systems, lysates are directly printed on nitrocellulose slides, and probed with patient serums (Figure 1.5). These studies showed that such protein microarrays could classify characteristic immunoreactive antigen

profiles and identify the immunodominant antigens among thousands of proteins. With this new technology a variety of questions involving humoral immune responses in malaria patients become possible to investigate. The ability to probe thousands of antigens in parallel made it conceivable to compare immune responses of a single patient to large portions of the parasite genome. These arrays also made it possible to investigate within a family of highly polymorphic antibody targets. One such family is the *Plasmodium falciparum* Erythrocyte Membrane Protein 1 (PfEMP1) family of proteins. Protein microarrays have been used to compare sera profiles of children and adults against hundreds of recombinant PfEMP1-Duffy Binding Like domains, highly polymorphic domains which allow the parasite to evade host immune response.[61] Protein microarrays can also help identify major variations in differing areas of endemicity. For example, a study showed tremendous variations in the immune response to *Plasmodium falciparum* MSP1-19 antigen in two different Kenyan highland areas. This high degree of variation was thought to be caused by altitude, topography and other environmental conditions.[62] Although most of the early malarial protein microarray work was focused on African populations, similar studies have emerged from India. India is unique as it has two distinct species of the parasite, both highly infectious and both leading to unique NAI profiles. Using protein microarrays, it is possible to interrogate species-specific differences in elicited immune responses. Interestingly, NAI is acquired more rapidly in *P. vivax* than *P. falciparum*, possibly due to differing lifecycle progressions.[63] More recently, questions of disease progression and severity have been posed. Using protein arrays there is a possibility to identify biomarkers that may be associated with sever and cerebral malaria.[64]

Protein microarray drawbacks: Driving observations for current project aims

There are draw backs to the way protein microarrays have been used to study NAI. High priority malaria antigens have emerged from the decades of microarray work, many of which have been heavily studied as vaccine candidates. However, over the past few decades limited number of new antigens have been added to the vaccine candidate list and those that enter the pipeline often do not progress into late stages of development (Figure 1.4). Using protein microarrays, putative antigens that are the target of NAI have been identified yet no FDA approved vaccine has come from this work. We hypothesize several potential explanations for such results. First, in all major malarial NAI studies where protein arrays have been used the quality of the malaria antigens is questionable. In these studies antigens are expressed in *E.coli* cell-free expression systems and expressed lysates are directly spotted onto microarray slides without purification or assessment of correct folding. Select antigens may be checked for expression levels and proper folding, however many thousands of antigens on the microarray may not be assessed. Currently the most commonly used array slides are Fast Slides (Whatman). Slide chemistry utilizes a three-dimensional microporous nitrocellulose-based polymer that binds proteins in a noncovalent manner via non-specific adsorption.[65] Thus, in a complex biological mixture the amount of target protein immobilized can vary based on the amount of target protein expressed and the ratio of target protein to background proteins. Second, the antigens are adhered to the nitrocellulose slides using non-specific adsorption, where proteins have the capability of binding and presenting themselves in an endless number of orientations. This can lead to non-uniform protein presentation and subsequently non-uniform serum antibody binding among different patients.[66] Last, when antigens are spotted on an array, they are independently probed by antibodies. *In vivo*, antigen-antibody binding occurs in the presence of all other malarial

antigens and antibodies, not solely between one antigen and its binding partner. There may be important aspects of this binding phenomenon, such as cross reactivity or binding competition, that are being overlooked when interrogating a single antigen-antibody interaction at a time. An assay where multiple antigens are interrogated against a patient sample simultaneously would be more representative of *in vivo* antibody binding interactions and may lead to novel investigative findings.

Bead-based multiplexing

Advancements in technology have allowed for the emergence of a new method of antigen prioritization. The use of spectrally unique microspheres makes it possible to interrogate multiple antigens of interest simultaneously using a single patient sample. The principle components of bead-based multiplexing are flow cytometry, antibodies, and microspheres.[67-68] The development of microspheres dyed with fluorophores, next generation compact lasers, a wide selection of antibodies and dyes, readily available computers, and software of the late 1990's were all necessary for multiplexing assays. A key factor of multiplexing technology is the use of spectrally distinct microspheres. Luminex corporation developed xMap Technology in which polystyrene microspheres are internally dyed with precise amounts of two distinct fluorochromes. The microspheres are identical in all physical components, including size, and only differ in the amounts of the internal classification dyes. The dyes have unique emission profiles which produce spectral characteristics for individual microsphere regions (or bead sets).[69] Using these bead sets it is possible to carryout simultaneous detection of multiple analytes in a single well of a 96-well plate, reducing time labor and cost of an assay. Luminex also designed specialized instruments for multiplexing assays. The Luminex 200 (later purchased by BioRad and rebranded as the BioRad200) analyzes the beads in a sample one at a time,

similar to a flow cytometer. As a microsphere passes the imaging cell it is interrogated by two lasers: (1) a 635nm for internal dye excitation (2) a 532nm for surface reporter fluorophore R-Phycoerythrin (PE) excitation.[69] The excitation of the bead as well as any reporter dye leads to the identification of the bead set with its associated analyte and a positive binding event.

Multiplexing technology has the capability of addressing the same questions asked in microarray studies but with many added advantages. Preparation of bead sets with the desired antigens of interest is a single step procedure unlike spotting microarray slides which can be laborious. Also, multiplexing capabilities allow over 100 antigens to be simultaneously analyzed in a single well of a 96-well plate and only use a minute amount of patient sample. Furthermore, unlike protein microarrays multiplexing assays better mimic *in vivo* conditions as multiple antigens are present during the antigen-antibody binding. Lastly, a multiplex assay saves analysis time. A 96-well plate, which can be representative of 96 different patients, can be read within an hour. Due to these reasons much of the malaria field has shifted its methods to utilize multiplexing technologies over traditional protein microarrays.

Multiplex Platform

Multiplex assays used for the study of malarial antigens

Early small scale bead based assays were used in place of classic enzyme linked immunosorbent assays (ELISAs).[70] When working with multiple antigens ELISAs can be laborious and time consuming. Furthermore, ELISAs utilize a large amount of precious sample, as often low volume blood samples are obtained from a small finger prick. Early studies that compared ELISA and bead based multiplexing assays found both methods yielding similar findings, however a larger dynamic range was observed when using the multiplexing system.[70-74] Most bead-based studies report a small set of antigens, often focusing on three or four key targets

of NAI. The few reported multiplexing studies of malaria antigens have used patient samples mainly from Africa with a few studies using patient samples from South America and Southeast Asia however, no reports of such multiplexing assays have emerged from Indian patient samples.

Reported methods of multiplex studies all follow the standard protocols given in the Luminex bead coupling "cookbook".[75-78] Carboxylated bead sets are modified with purified antigens or antigen peptide fragments. Antigens are coupled to the beads using standard carbodiimide chemistry utilizing 1-Ethyl-3-(3-dimethylaminopropyl) carbodiimide (EDC) and N-hydroxysulfosuccinimide (Sulfo-NHS). One main disadvantage of this methods is that antigens must be first purified and then coupled to the beads. This adds a tremendous amount of time to the development of an assay. Malaria protein expression and purification has long been a bottleneck in antigen prioritization (discussed in detail in Chapter 2). Many malarial antigens which are targets of the NAI are surface exposed and membrane bound proteins which are challenging to isolate in pure forms. Second, protein capture using the standard EDC/Sulfo-NHS chemistry results in non-uniform presentation of the antigens which may result in variance in antigen-antibody binding each time new beads are modified. Also, carbodiimide chemistry coupling can lead to the complete loss of antigen epitope identification from protein unfolding post-carbodiimide capture. This is discussed in detail in Chapter 3 under "advantage of oriented linker."

Current multiplex chemistries and technical improvements possible

The popularity of multiplexing bead-based assays in malarial antigen discovery and prioritization has continued to grow over the last decade. The ability to interrogate multiple antigens in a single step using very small patient serum samples is highly appealing. However, the need to first purify each antigen from translation lysates and then couple to microspheres

makes the current approach unappealing for a high-throughput scheme. An alternative approach is to modify the multiplexing microspheres with a capture moiety that can pull out only the specifically labeled antigens of interest from a lysate mixture. Affinity based tags can be utilized for the design of such a system. Traditional tags such as glutathione S transferase (GST) or maltose binding protein (MBP) can offer high selectivity but due to their large size can alter protein function or compete with antigens of interest for patient sera antibodies therefore, smaller tags are favored. One such tag is hexa histidine (His Tag), however this tagging system is often insufficient in producing pure protein in a single step. Therefore, the need for a capture system that provides high affinity and selectivity while not interfering with binding of antibodies on the epitopes of the fused antigen remains.

Project aims

The aim of the following work is to address flaws in the current methods used to dissect antibody immune responses to malaria. Providing technical improvements of immune assays will help better prioritize antigen candidates and allow for additional disease related questions to be addressed. First, quality of antigens used for such studies needs to be better assessed. Antigens utilized must be expressed in full length and functional form and isolated in high purity. Additionally, methods of antigen immobilization need to be addressed to optimally present the correctly folded antigen of interest without masking or losing potential epitope binding sites. This requires a reliable chemistry to link antigens to the solid surface of choice. Furthermore, modifying this chemistry to allow for a gentle method of removal from solid surfaces could tell us how antigen structure is affected during immobilization procedures. The last improvement necessary is to have a system that could interrogate multiple antigens at a time as described above. Due to the vast number of possible malaria parasite antigen targets it would be highly

advantageous to interrogate multiple antigens in parallel while limiting the use of precious patient samples. The implementation of the listed technical improvements would not only save time and effort but also make it possible to develop a highly sensitive high-throughput method for investigation of NAI antigen targets.

Chapter 1 Figures

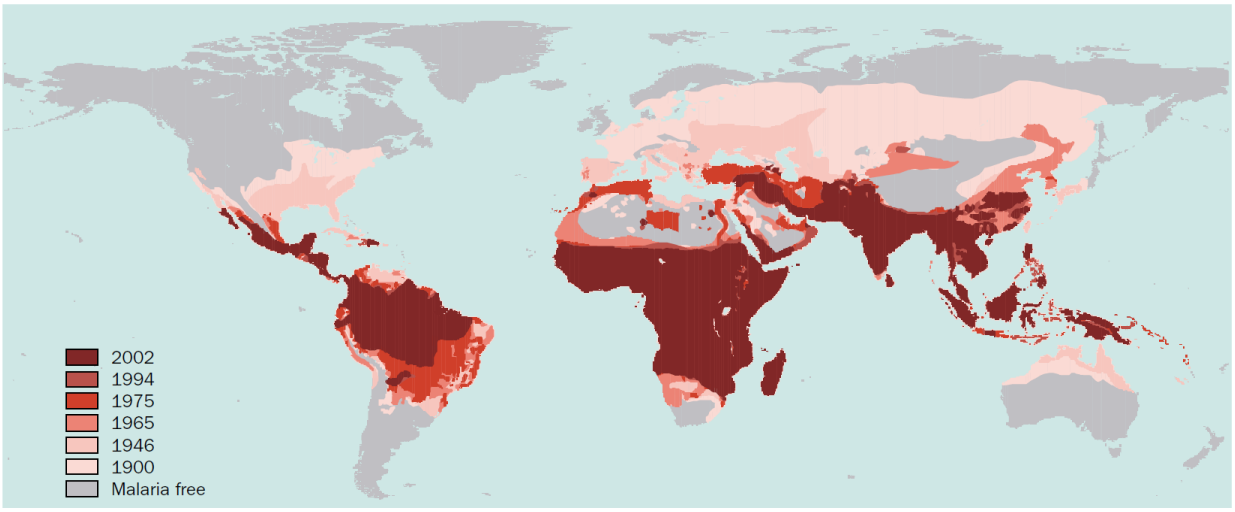

Figure 1.1 Global distribution of malaria over the years 1900-2002. Adapted from Snow, R. et. al. [4]

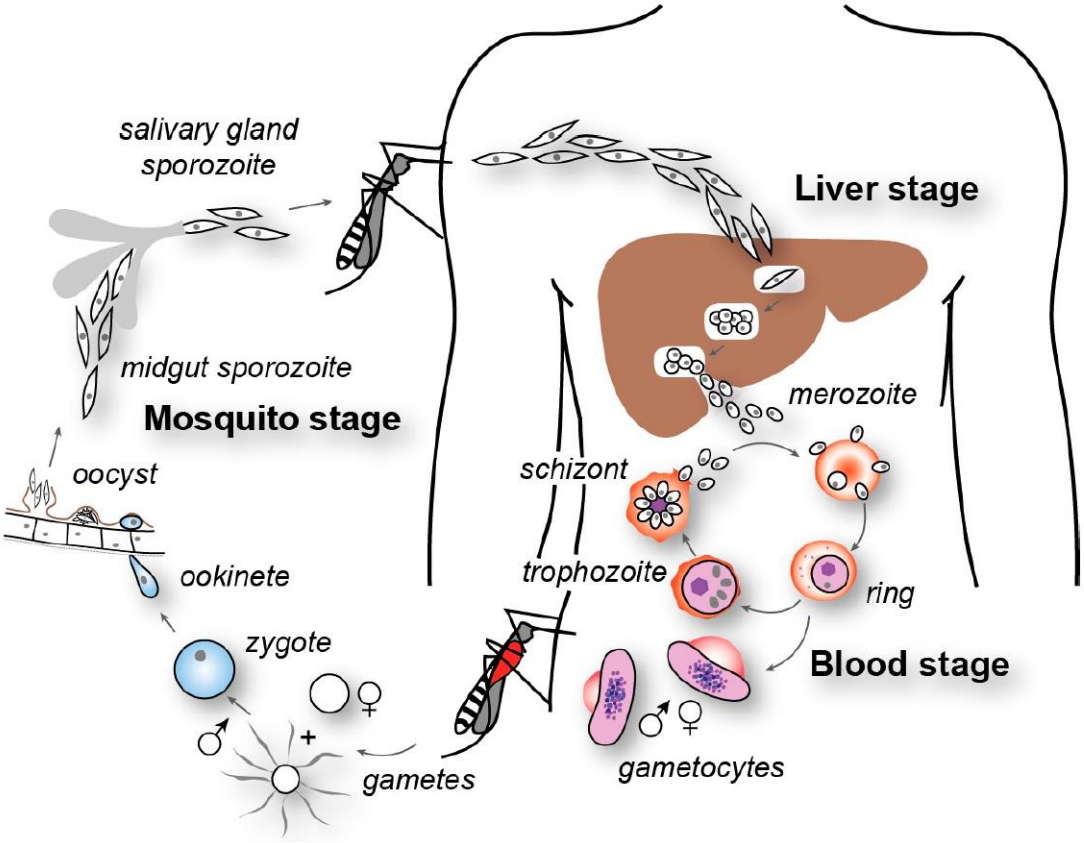

Figure 1.2 Malaria parasite lifecycle. Adapted from Baum, J. et. al.[14]

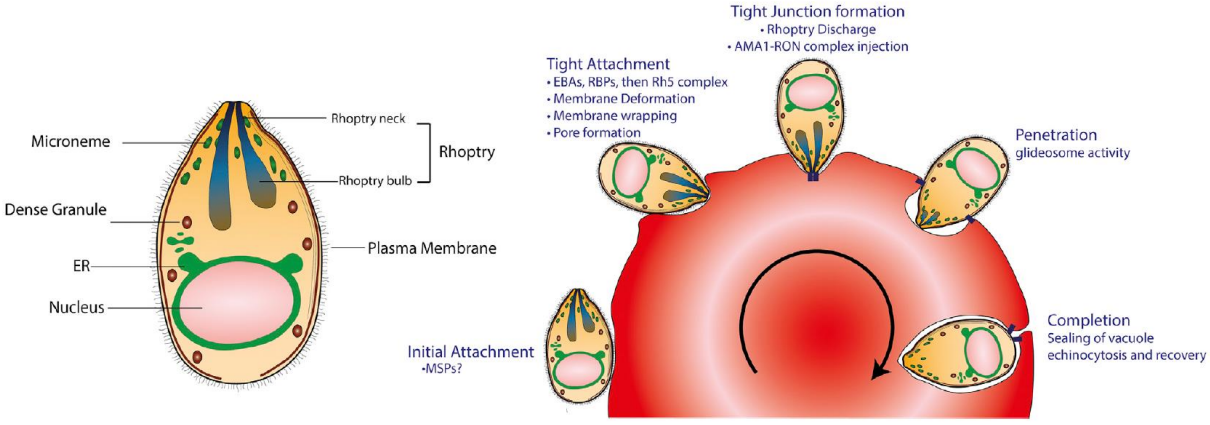

Figure 1.3 Erythrocyte invasion by merozoites. Adapted from Duraisingh, et. al.[12]

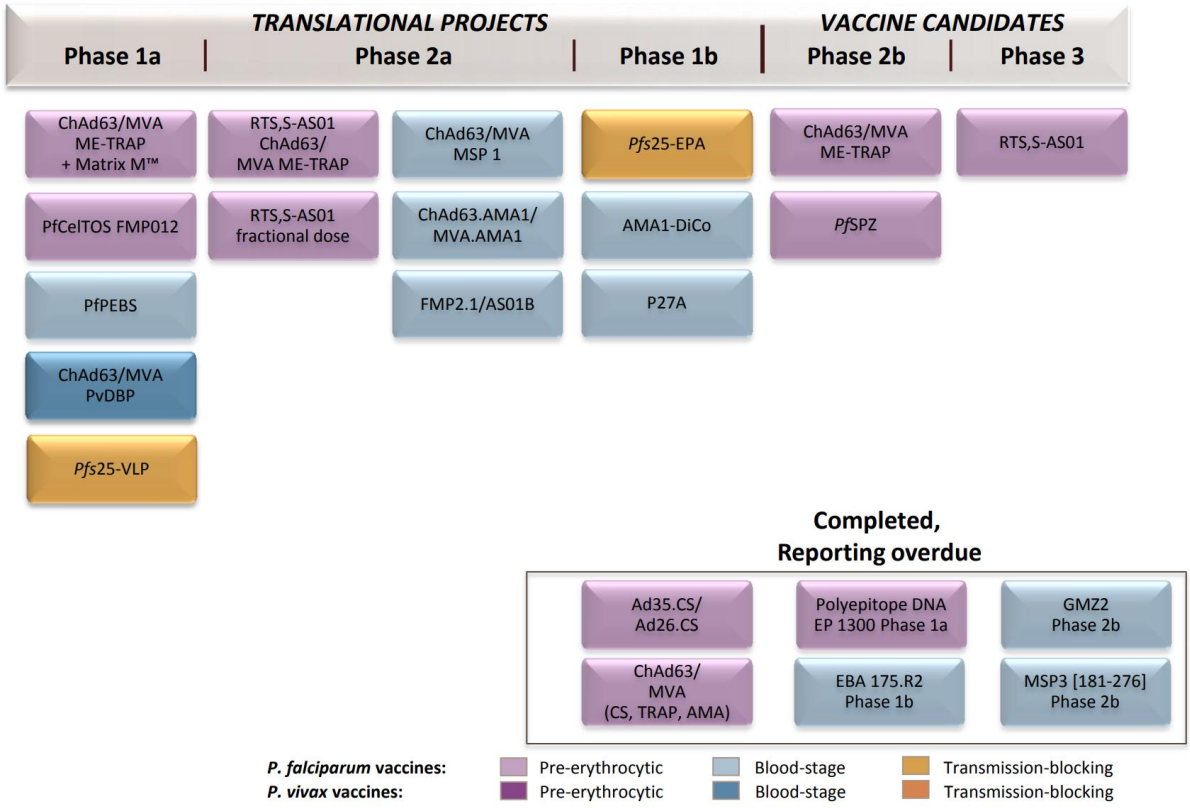

Figure 1.4 Current global malaria vaccine pipeline. Most recent pipeline as of April 2018. Adapted from WHO Malaria Report 2018.[1]

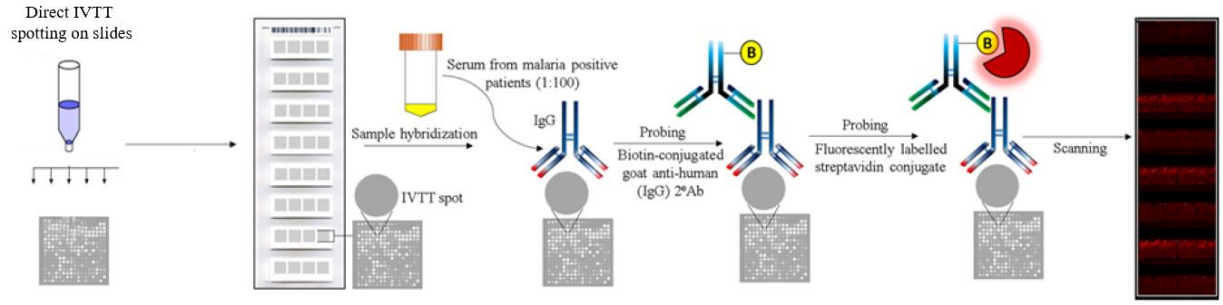

Figure 1.5 Schematic representation of traditional protein microarray experimentation and workflow. Antigens are expressed and directly spotted onto slides with no purification steps. A single slide contains thousands of antigen spots. Patient serums can then be hybridized on slides and read out with fluorescently labeled secondary antibodies. Finally, slides are scanned to produce an image with varying fluorescent signal responses based on patient antibody response. Adapted from Venkatesh et al. 2019.[79]

Chapter 2: Protein Expression and Purification

Malaria Antigen Expression and Purification

Protein expression

The most common method of protein expression is using *in vivo E. coli* translation. The robustness of this system makes it appealing for expression of a wide array of proteins. Due to its high translation rates with an average elongation rate greater than ten amino acids per second many researchers prefer the ease of using *E. coli* for protein expression.[80-81] However, expression of *Plasmodium* proteins in *E. coli* systems are not as successful as proteins from other organisms. In a study where 1000 *P. falciparum* genes were tested the *E.coli* system was only able to express 6.3 percent of the proteins in full-length and soluble form.[82] Many factors contribute to the inefficient expression of *Plasmodium* proteins: large gene length due to the presence of many low-complexity regions in the sequence, a heavily biased genome with 90% of the genome sequence being adenosine and thymine rich, and the lack of the correct folding machinery.[83-85] These factors can cause processing errors and ribosomal stalling which gives many unwanted truncated products. Furthermore the *E. coli* system is not equipped with the correct machinery to process and fold the multi-domain proteins of the eukaryotic *P. falciparum* which leads to the formation of insoluble products.

The Rathod lab has found that the most well-suited expression system for the translation of full length soluble *Plasmodium* proteins is the wheat-germ *in vitro* (cell-free) transcription translation system (WGCF system).[86-87] In wheat germ the important translation and transcription machinery is stored in the embryo. By physically grinding the wheat germ and combing with buffers a wheat germ extract (or wheat germ lysate) can be made. This wheat germ lysate is simply mixed with the mRNA of the desired protein of interest and translation occurs over an 18-

hour period. Due to the open nature of this system there is flexibility over reagents used in the translation that can help improve yield on a protein by protein basis. Wheat germ is also eukaryotic thus more capable of processing multi-domain proteins which significantly improves solubility.

Researchers from Japan have conducted multiple studies showing the successful expression of *P. falciparum* proteins, specifically challenging to express membrane proteins using the wheat germ cell free system. Out of 124 *P. falciparum* membrane proteins the Tsuboi group was able to successfully express 93.[88-90] The Rathod lab has also shown the successful expression of challenging to express proteins all showing significant functional activity.[86-87] Due to the effective expression of a large number of malarial proteins the wheat germ cell free system is ideal for expression of antigens to be used in the novel multiplexing assay.

Protein purification

A major bottleneck in vaccine development is the lack of reliable antigen expression and purification systems. Working with malarial antigen proteins can be challenging due to the inherent nature of the proteins. Many of the target antigens of NAI are membrane bound, high in cysteine composition, and contain multi-domains making it challenging to not only express correctly but also purify. Successful purification of malarial antigens has been shown using simple affinity fusion tags. The most reported tag for purification of *Plasmodium* proteins has been the Glutathione S-transferase (GST) tag.[89-90]

Despite marked increases in purity, GST purified antigens often need to undergo additional polishing steps. Commonly, antigen affinity purification leads to low yields thus adding additional steps of purification is not ideal. In efforts to develop a single step purification system that provides high quality and highly pure malaria antigens two new tagging systems

were implemented. The first is the HaloTag system which is based on covalent capture and the second is the CaptureSelect (C-tag) system which uses antibodies for the capture of a target peptide.

HaloTag purification

The HaloTag is a modified haloalkane dehalogenase that is designed to covalently bind to chloroalkane derivatives. Promega company engineered the tag from the bacterially encoded haloalkane dehydrogenase (DhaA) derived from a *Rhodococcus spp.*[91] The 34kDa wild type enzyme cleaves at the carbon-halogen bond of an aliphatic halogenated compound. Within the active site Asp106 displaces the terminal halogen by nucleophilic attack followed by a hydrolysis by His273 and a water molecule. To prevent the hydrolysis step and form a stable intermediate the His273 was mutated to a phenylalanine. This causes the covalently captured halogenated moiety to remain in the active site of the enzyme.[92-93] This covalent capture occurs within minutes and is highly specific leading to minimal off target capture events. This in turn makes it well suited for array studies where specific antigen-antibody interactions are of interest.

The purification workflow for HaloTagged antigens is shown in Figure 2.4. Magnetic beads modified with a HaloTag capture linker are purchased from Promega. These beads are mixed with the translation lysate of the fusion HaloTag antigen of interest and nonspecific background protein interactions from the lysate can be washed away. Due to the covalent interaction of the HaloTag with the haloalkane derivative the need for a cleavable site between HaloTag and antigen is needed. We use the Tobacco Etch Virus protease (TEV) which is a highly sequence specific cysteine protease. TEV protease recognizes the sequence ENLYFQ\S, (where \ denotes the cleavage site), and leaves only a single amino acid attached to the isolated protein.

C-tag purification

The CaptureSelect (C-tag) system utilizes a four amino acid tag (EPEA) fused to the C-terminus of the protein of interest. The C-tag has unique selectivity to a matrix coated with a 13kDa camelid antibody fragment.[94] The alanine residue is critical for binding and must be "free" for efficient capture by the matrix. The C-tag allows for high-selective capture and is shown to give exceedingly pure protein and high recovery in a single purification step.[95] The camelid antibody matrix is extremely stable and can be reused continually even under denaturing conditions. Elution of proteins from the matrix can be done under high salt concentrations at neutral pH, acidic conditions, or using a five amino acid peptide (SEPEA). The versatility in elution conditions and the highly specific nature of epitope binding makes the C-tag a valuable system for protein purification. To date, no reports have used the C-tag in the wheat germ cell free system for malaria protein purification.

The purification workflow for C-tagged antigens in shown in Figure 2.7. C-tag CaptureSelect resin is purchased from ThermoScientific. Wheat germ lysate translations of the fused C-Tag malaria antigens are captured onto the resin which is then washed, and antigens of interest are eluted using an excess of a five amino acid peptide (SEPEA). Peptide is removed in subsequent concentration steps. Resins can be regenerated and reused by washing under acidic conditions to remove excess peptide.

Experimental Procedures

Antigen selection. The *P. falciparum* and *P. vivax* proteins shown in Table 2.1 were selected due to prior implication in merozoite stage invasion of red blood cells[96]. Merozoite surface protein 1-42 (MSP1-42) is a GPI-anchored protein that is presented on the merozoite surface while apical membrane antigen 1 (AMA1) is located in the microneme organelle of the parasite

and is relocated to the parasite surface during schizont rupture[97-99]. In recent years reticulocyte-binding protein homolog 5 (RH5) has emerged as a promising blood stage antigen candidate. All three antigens are relatively large and contain a high cysteine composition. Sequence information was derived from the *Plasmodium* database, PlasmoDB.

HaloTag Constructs. The HaloTag gene, His6X and tobacco etch protease (TEV) site were sub cloned from the His6HaloTag T7 parent vector (Promega, USA) and into the N-terminus of the destination pEU-E01 multicloning site (MCS) vector giving the pEU-HaloTag vector. The pEU-E01 expression plasmid contains a SP6 bacteriophage transcription promoter site and a plant-like omega sequence for initiation of translation, schematic shown in Figure 2.1[100]. Codons were optimized for *Tritcum aestivum* genes and regions of high or low GC content were limited when possible, to prevent truncation of protein.

To the pEU-HaloTag plasmid a newly designed MCS was inserted using primers to create a pEU-HaloTag-MCS vector. *Pf* MSP1-42 protein (Life Sciences) was sub cloned into the multi cloning site of the constructed pEU-HaloTag-MCS vector. Primers were designed specifically for *Pf* MSP1-42 using restrictions sites for cloning. KpnI and BamHI restriction enzyme sites were added to the forward and reverse primers, respectively (Table 2.2).

After initial pEU-HaloTag-*Pf* MSP1-42 plasmid construction a longer linker between the HaloTag and antigen of interest was required. Due to the observation of limited cleavage after capture onto a HaloTag capture resin a 18 amino acid (AA) linker was added to allow for more space between the HaloTag and antigens of interest. The main advantage being that the TEV protease will gain better access to its cleavage site. First, a modified pEU-HaloTag-*Pf* MSP1-42 plasmid, with an 18 AA spacer, was designed (spacer sequence with original spacer AA in bold: GSGGGGSGGGSGGG**EPTT**). Primers were constructed for the extended spacer insertion

between the C-terminus of the HaloTag and the N-terminus of *Pf* MSP1-42 (Table 2.2) The blunt end PCR product was ligated using Phusion Polymerase with pre-heated block conditions giving the final pEU-HaloTag18AASpacer-*Pf* MSP1-42.

For universal construct design an MCS was incorporated in the pEU-HaloTag18AASpacer *Pf* MSP1-42 plasmid. Primers were designed to replace the *Pf* MSP1-42 sequence with a MCS (Table 2.2). The blunt end PCR product was ligated using Phusion Polymerase with pre-heated block conditions giving the final pEU-HaloTag18AASpacer-MCS plasmid (Figure 2.4). Subsequent HaloTag 18AA spacer constructs were subcloned from synthesized genes (Life Sciences) into the pEU-HaloTag18AASpacerMCS using specific primers with restriction digests (primers and restriction digests used shown in Table 2.2).

C-tag Constructs. Only constructs of *Pf* MSP1-42, *Pf* AMA1, and *Pf* RH5 were designed with a C-tag. Codon optimized genes were subcloned from supplied vectors (Life Science) into the empty pEU-E01 MCS using primers designed with specific restriction digestion sites. Primers and restriction enzymes used are shown in Table 2.2. Subsequently, antigens were cloned into a pEU vector that encoded the four amino acid C-tag epitope E-P-E-A.

Plasmid Isolation. All cloned plasmids were transformed into competent *E. coli* DH5α cells (Invitrogen Life Technologies) and colony PCR was performed on select colonies using primers to the pEU vector. Target colonies were selected for plasmid preparation using the Qiagen Midi Plus plasmid extraction system. High purity DNA was dissolved in sterilized deionized water (SDW) and concentrations determined by spectrophotometry at 260nm (Thermo Scientific Nano Drop 1000). All purified plasmids were sent for sequencing (Eurofins MWG Operon) and return sequences were verified with Geneious analysis software.

Cell-free Continuous Exchange Transcription & Translation. Cell free transcriptions were

carried out as previously reported in the literature[86, 100]. In a 100 µL translation, 10 µg of plasmid-carrying target gene was added to 80 mM HEPES-KOH, pH 7.8, 16 mM magnesium acetate, 2 mM spermidine, 50 mM β-mercaptoethanol, 40 units of RNase inhibitor (NEB), 130 units of SP6 RNA polymerase (NEB), and 3 mM each of GTP, ATP, CTP, and UTP. The mixture was incubated at 37 °C for four hours. mRNA was precipitated with 7.5 M ammonium acetate and three volumes of ethanol. The mixture was set on ice for 10 minutes followed by spinning at 21,000Xg for 20 minutes, followed by a 70% ethanol wash for 2 minutes. The pellet was dried for 10 minutes and solubilized in 30 µL of SDW.

All proteins were expressed in the wheat germ cell free translation system using the dialysis method.[86-87, 101] For 100 µL translation, the reaction mixture contained 30 µL of mRNA (1-1.5 mµ), 4 units of wheat germ lysate, 20 µg of creatine kinase, 40 units of RNase inhibitor, and 20 µL of 5X protein expression buffer (PEB) (1X PEB is 30 mM HEPES-KOH, pH 7.8, 100 mM potassium acetate, 2.7 mM magnesium acetate, 5 mM DTT, 0.4 mM spermidine, 0.3 mM concentrations of 20 amino acids, 1.2 mM ATP, 0.25 mM GTP, 16 mM creatine phosphate). The translation mixture was added to a Slide-A-Lyzer Mini 10kDA dialysis unit (Thermo Scientific) and immersed in a 1.5 mL micro centrifuge tube containing 1.2 mL of 1X PEB. Dialysis cup reactions were incubated for 36 hours at 26 °C.

Radiolabeled experiments. For verification of protein expression, the batch translation method was used. Microspin G25 columns (GE Healthcare) were used in purifying transcripts. 50 µL reactions contained (-)leucine translation buffer with 400n Ci ^{14}C leucine. Translations were placed in a 26 °C incubator for 4 hours. Total translations were collected and soluble fractions separated by spinning at 15,000 X *g* at 4 °C. 5 µL of soluble fraction were treated with 2 units of Precision Protease (PP) enzyme in 10 mL of 50 mM Tris pH 8.0 2 mM DTT and incubated 12

hours at 4 °C. Samples were boiled in equal parts 2X Laemmli Sample buffer with 2% β-mercaptoethanol (βme) and resolved by sodium dodecyl sulfate-polyacrylamide gel electrophoresis (SDS-PAGE). Gels were dried for two hours on a gel dryer and then exposed to a phosphor imager screen overnight (GE Healthcare Biosciences). The phosphorescent image was scanned on a GE Typhoon FLA 9000 Gel Imaging Scanner to visualize radiolabeled protein translations.

Bilayer Translation. The WGCF bilayer method was used for large scale production of antigens. The open bilayer system allows for addition of detergent directly to translation.[89] Briefly, a 6 mL transcription mixture contained 900 µg of plasmid DNA, 1.8 mL of 5X transcription buffer (400 mM HEPES-KOH, pH 7.8, 80 mM magnesium acetate, 10 mM spermidine), 75 mM β-mercaptoethanol), 1,500 units of RNase inhibitor (Promega), 7,500 units of SP6 RNA polymerase (NEB), and 25mM each of GTP, ATP, CTP, and UTP. The mixture was incubated at 37 °C for four hours and then spun at 23 °C at 4000Xg for 5 minutes. The soluble fraction containing transcribed mRNA was mixed with wheat germ extract to give a final OD 100 A_{260} units, 120µl creatine kinase (10 mg/mL), 800 units of RNase inhibitor (Promega), and 0.1% TritonX-100 to a final volume of 12 mL. To each well of a six well flat bottom culture plate (Falcon), 10 mL of 1X translation buffer with 0.1% TritonX-100 was added. Carefully, to the bottom of each well 1mL of translation mixture was pipetted creating two separate layers. Plates were incubated at 26 °C for 20 hours.

HaloTag protein purification. Wheat germ translation lysates containing synthesized HaloTag antigens were purified using Magne HaloTag beads (Promega, USA). For every 1 mL bilayer translation, 125 µL of bead slurry was used. Beads were washed three times with binding buffer (PBS pH 7.4, 0.005% Igepal). Translation was diluted by half with binding buffer and incubated

with beads using end to end rotation at 26 °C for 5 hours. Beads were washed three times with 50 mL binding buffer. Cleavage was carried out with 100 units of TurboTEV protease (Eton BioScience) in 500 µL cutting buffer (25 mM HEPES pH 8.0, 300 mM NaCl, 2 mM DTT, 0.05% TritonX-100) overnight at 4 °C. Cleavage solution was incubated with GSH coated beads for TEV protease capture. Incubation buffer was PBS pH 8.0, 0.005% IGEPAL. After removal of TEV protease protein fractions were concentrated 5-7X with Amicon Ultra 0.5 mL centrifugal filter (EMD Millipore, USA) and protein concentration was determined using standard Bradford assay.

C-Tag protein purification. Wheat germ translation lysates containing synthesized C-Tag antigens were purified using pre packed 1mL columns of CaptureSelect C-Tag Affinity Matrix (ThermoFisher). A 12 mL wheat germ bilayer translation of C-Tag protein could be purified on a 1mL CaptureSelect column. All steps were carried out at room temperature using a BioRad Econo desk top pump at 1mL/min (unless otherwise noted). Columns were equilibrated with 20 mM Tris pH7.5, 100 mM NaCl. Translation lysate was loaded onto column at 0.5 mL/min. Columns were washed with 20 column volumes of 20 mM Tris pH 7.5, 100 mM NaCl, 2 mM DTT. Purified C-Tag proteins were eluted using a peptide elution buffer. Synthetic peptide, SEPEA, was ordered at greater than 90% purity in the presence of TFA (GenScript). Proteins were eluted with 10 mL of elution buffer (20 mM Tris pH 8.0, 100 mM NaCl, 3 mM SEPEA peptide and final pH was adjusted to 7.4). Eluted fractions were pooled and buffer exchanged five times (20 mM Tris pH 7.5, 200 mM NaCl, 0.05% TritonX-100, 2 mM DTT) to a final volume of 1.5 mL using 10K Amicon Ultra 15 mL centrifugal filter (EMD Millipore, USA). Protein concentration was determined using standard Bradford assay.

Mass Spectrometry of Trypsin Digested Proteins. Protein bands resolved by SDS-PAGE were excised from the acrylamide gel, subjected to in-gel digestion, and peptide products were detected via linear trap quadrupole (LTQ) ion trap mass spectrometry. In addition, non-protein staining control region of the polyacrylamide gel was processed and analyzed in parallel to bands of interest. In-gel digestion were performed as described in Shevchenko et. al[102]. Dried peptide products were re-solubilized in 10 µL 5% acetonitrile for HPLC-MS analysis. Injection volumes of 4 µL were processed via HP 110 capillary LC, with a C18 column for peptide separation. The mass spectrometer used was a Finnigan LTQ ion trap, nano spray source. Spectra were collected in positive mode from 100 to 2500 *m/z*. Peak lists obtained from MS/MS spectra were identified using Proteome Discover (Thermo Scientific) version 1.4. The search was conducted using Sequest HT Search Wizard. Protein identification was conducted against suitable databases, usually of whole *Plasmodium falciparum* proteome (3D7) or whole wheat germ proteome.

Antibody Production. Rabbit immunizations were carried out by GenScript. Rabbits (n=2) were immunized intramuscularly with 200 µg of C-Tag purified *Pf* MSP1-42 protein formulated in Freund's complete adjuvant on day 0. Three booster immunization of 200 µg, 400 µg and 200 µg were carried out at days 14, 28 and 72. Booster immunizations were mixed with Freund's incomplete adjuvant. Animals were sacrificed and sera was collected. Total IgG was purified from rabbit sera using protein A column purification. Protein A purified antibodies were shipped frozen.

Western Blots. Protein samples were loaded onto a 12-4% gradient SDS-PAGE gel, then electrophoretically transferred to Immobilon PVDF membrane at 35V for two hours at 4 °C (Millipore, pore size 0.45 µM). Translated GFP was used as a control. Transfer buffer comprised of 0.025 M Tris base, 0.2 M glycine, 0.002M SDS. After blocking with 5% milk in wash buffer

(wash buffer: 0.15 M NaCl, 0.02 M Tris HCl, 0.005 M Tris base, 0.9 mM Tween20), the membrane was blotted with either mouse anti-HaloTag antibody (Promega, 1:1000), camelid anti-C-Tag biotin antibody (ThermoFisher, 1:1000), or raised rabbit anti-*Pf*MSP1-42 antibody (1:20,000). Infrared fluorescent secondary antibodies were used for western blot visualization. LiCor IRDye800CW goat anti-mouse, streptavidin, and goat anti-rabbit were used in 1:10,000 ,1:2000, 1:5000 titers respectively. PVDF membrane was directly scanned on a LiCor Odyssey gel imaging scanner. Blots were scanned at both 680 and 780nm.

Parasite Whole Culture Lysis. The *P. falciparum* 3D7 line was maintained in continuous culture using fresh erythrocytes at 2% hematocrit. A parasitemia of 5% was reached and cultures were synchronized by two incubations in 5% sorbitol three hours apart. Cultures were maintained to schizont stage, spun down and pellets were frozen at -80 °C. For culture lysate preparation pellets were thawed and washed twice with PBS (containing protease inhibitor cocktail, Roche). Saponin was added to a final concentration of 0.15% and incubated for two minutes at room temperature with gentle periodic tapping. Sample was spun at 5000rpm for ten minutes followed by three washes with PBS. A black pellet consisting of intact parasites minus RBC membrane was observed. To remove the parasite membrane lysis buffer (0.05 M Tris pH 8.0, 5 mM EDTA, 0.5% TritonX-100, 0.2X Roche Protease Inhibitor) was added to the pellet and incubated on ice for two hours. Tube was vortexed every 15 minutes. Final lysed sample was a light brown color. Lysed samples were aliquoted and stored at -20°C.

Growth Inhibition Assays. The *P. falciparum* 3D7 line was maintained in continuous culture using fresh erythrocytes at 0.5% hematocrit and synchronized by two incubations in 5% sorbitol three hours apart. Synchronized early/mid trophozoites were adjusted to 0.5% parasitemia and then incubated with various IgG concentrations using raised anti-*Pf* MSP1-4 in 96 well plate

(tested in triplicate). Final parasitemia was determined by SYBR Green I staining. Briefly, an equal volume of parasite culture was incubated with an equal volume of 2X SYBR Green I stain (in PBS) for 20 minutes in the dark. After incubation, total volume in wells was brought to 200 µL. A replicate plate was made with 1/5 dilution of original plate. 30,000 events per samples were read by flow cytometry (Accuri BD C6). Events were converted to percent parasitemia and then percent proliferation was determined by dividing the percent parasitemia of trend/percent parasitemia of control.

Results

HaloTag Protein Work. Due to the covalent nature of the HaloTag capture system, it is well suited to be used for protein purification with the wheat germ cell free system. Here we see the successful soluble expression and high-level purification of multiple malaria antigens. We chose to work with a small set of well-studied antigen targets (Table2.1).

The HaloTag constructs were designed with a N-terminal HaloTag-Spacer-Tabaco Etch Protease site (TEV)-a multi cloning site for gene insertion (see Table 2.2 for all primer designs). However, after expression and purification attempts with these constructs a desire to insert an extended spacer between the HaloTag and gene arose. The final cloning map is shown in Figure 2.1 where the N-terminal HaloTag is followed by an 18 amino acid spacer, instead of the original four amino acid spacer. Further, a new multicloning site was designed to make a universal vector that included the 18 amino acid linker. This multicloning site is shown in Figure 2.2. After insertion of all the antigen candidates into this newly designed vector autoradiograph experiments were carried out to verify expression and solubility. All HaloTag constructs showed successful protein expression at the expected molecular weights in the total translation (*Pf* MSP1-42 78 kDa, *Pv* MSP1-42 86 kDa, *Pf* AMA1 109 kDa, *Pv* AMA1 101 kDa, *Pf* MSP1-19

48.7 kDa, *Pv* MSP1-19 48.8 kDa Figure 2.3). Total translation lysates were then subjected to high speed centrifugation to observe if desired antigens would crash out into the pellet fraction. Pelleted fraction and soluble fraction were separated, and both were loaded at equal concentrations. From Figure 2.3 it is observed that none of the six antigens expressed displayed any major protein precipitation. Instead there is a clear band at the expected size in the soluble fraction sample for all antigens. The last lane in each autoradiograph experiment in Figure 2.3 shows the products after the total translation is treated with TEV protease. The disappearance of the expected molecular weight band confirms the presence of the correct TEV cut site (ENLYFQ). In all antigens expressed we see the disappearance of the HaloTag-antigen band and instead see the appearance of new bands. The band at 37 kDa that appears in all six TEV treated samples is the HaloTag protein fragments. The antigen fragment bands vary in size based on their molecular weights after cleavage (*Pf* MSP1-42 41kDa, *Pv* MSP1-42 49kDa, *Pf* AMA1 72kDa, *Pv* AMA1 64kDa, *Pf* MSP1-42 11.7 kDa, *Pv* MSP1-42 11.9kDa). The *Pf* and *Pv* MSP1-19 treated samples often did not show the protein band after treatment. This is likely because the cleaved protein fragments are only around 11kDa and often run off the gels. GFP is used as a control to show expression. GFP is highly soluble and that is shown in the pellet and soluble fractions. Furthermore, GFP which does not have a HaloTag or TEV cut is not altered under the TEV protease cleavage conditions.

After HaloTag constructs were verified to be soluble and contain a correct TEV protease site large scale translations were initiated. HaloTag expression was done using the bilayer method of protein translation. This method was chosen so that TritonX-100 could be freely added to the translation reaction without the worry of reaching the critical micelle concentration and blocking exchange of buffer and reagents in the standard membrane exchange method.

HaloTag proteins were purified using HaloTag capture beads followed by cleavage from the matrix using TEV protease as shown in the scheme of Figure 2.2. Purity of the cleaved and concentrated fractions varied antigen to antigen. The antigens that were isolated in highest purity were all the MSP1 antigen variants as see in Figure 2.5 A and B. The AMA1 antigens that were isolated showed significantly less purity (Figure 2.5 C). For further identification of the purified proteins, in gel trypsin digestion of protein bands was carried out. The digested products were analyzed by LCMS-LTQ mass spectrometry and then compared against the whole *Plasmodium* genome. Out of a genome of over 2000 genes each purified protein sample gave a high correlation "hit" of the expected antigen (Figure 2.5 D).

Literature reports suggest the wheat germ expression levels of malaria proteins to range from 5-45 µg/mL of translation lysate.[86, 103] *Pf* MSP1-42 was the most pure antigen recovered from the HaloTag schemes. From a 1mL bilayer translation roughly 10µg protein was recovered. The protein concentration of isolated samples was estimated using standard Bradford methods.

C-Tag Protein Work

A second purification tag was used in hopes of developing a more universally applicable purification scheme. The C-Tag is a epitope tagging system where the four amino acid tag, EPEA, is selectively recognized by camelid antibodies. Here we showed the purification of three different *Plasmodium falciparum* antigens using this one step tag.

C-Tag constructs were made using gene specific primers. Synthetic *Plasmodium falciparum* genes were amplified using forward and reverse primers which had specific restriction digest sites. Reverse primers also contained an additional three AA linker and the C-Tag amino acids. Using this extended reverse primer the amplified gene could be treated with restriction enzymes and ligated into the empty pEU wheat germ vector giving a gene insert along

with the C-terminal tag. All primer and restriction digestion enzymes used are listed in Table 2.2. To confirm correct construct design and protein expression autoradiograph experiments were carried out. All C-Tag constructs expressed at the expected molecular weight on SDS-PAGE gels (*Pf* MSP1-42 40kDa, *Pf* RH5 59kDa, *Pf* AMA1 kDa 69kDa Figure 2.3). As seen with the HaloTag expression, C-Tag protein expression yielded highly soluble malaria antigens after centrifugation. Little protein is observed in the pellet fractions on the autoradiograph and a majority is seen in the soluble fraction.

A one step purification was applied to all C-Tag antigens. Figure 2.5 shows the purified product of Plasmodium falciparum antigens MSP1-42, AMA1, and RH5. All antigens were purified, but with differing degrees of purity. The purest antigen observed was *Pf* MSP1-42 where a single band is observed after elution from the capture matrix with peptide SEPEA (Figure 2.8A). *Pf* Rh5 showed two distinct bands after purification while *Pf* AMA1 proved to again be the most impure antigen (figure 2.8B and C). In comparison to HaloTag purification the C-Tag was better able to purify challenging antigens like *Pf* AMA1. LC LTQ MS was carried out on in gel trypsin digested products from the antigen purifications. After separation, trypsin digested products are analyzed on a LTQ MS and peptides are analyzed against the Plasmodium falciparum genome. For all three C-Tag purified antigens, the top hit was the expected purified protein. Many high confidence peptides and large percent coverage gave a high confidence of correct identification (Figure 2.8 D).

Based on recovery of C-Tag GFP, which was monitored by western blot and fluorescent quantification, total recovery of C-Tag proteins was estimated around 90%. A 1mL bilayer translation of *Pf* MSP1-41 yielded 35µg of purified protein. This is roughly 3.5X more protein isolation in comparison to the HaloTag purification of *Pf* MSP1-42. With better purity observed

across all antigens and higher yields the C-Tag purification scheme is a highly valuable tool for malaria protein isolation.

The ability to recover large microgram quantities of highly pure antigens using the C-Tag led to the production of antibodies. *Pf* MSP1-42 was purified from multiple bilayer translation reactions and sent for antibody production. Rabbit were immunized with the purified antigens and sacrificed for serum collection. Total IgGs were purified using a protein A column. These purified rabbit anti-*Pf* MSP1 42 antibodies were tested first for sensitivity to the purified *Pf* MSP1-42 antigen. Western blot data shows signal against even 50ng of purified antigen using a titer of 1:20,000 (Figure 2.9A). The low titer concentration and detection of ng levels of antigen shows the antibodies are highly sensitive to their raised antigen. When probed against the total wheat germ cell lysate in the total and flow through fractions (Figure 2.9A) some nonspecific signal is observed. As the antigens are expressed in the wheat germ lysate and then purified, observation of such bands suggests some residual background impurities were present in the purified antigen samples sent to GenScript for antibody production. Although activity against the wheat germ background is not ideal it was more important to test the anti-*Pf* MSP1-42 background signal against the whole parasite lysate. For this parasite lysates were prepared from 3D7 cultures. Figure 2.9B shows two replicate gels. The left gel image is a western blot while the right is the Coomassie stain of the gel. Out of the total lysate loaded only a single intense band is observed near 190kD. This band represents the full-length *Pf* MSP1-42 before proteolytic cleavage which occurs within the cell, just before sporozoites are preparing to rupture and transform into merozoites. As mature merozoites, the protolyzed *Pf* MSP1-42 is displayed on the infected red blood cell surface. Thus, capturing this stage of the protein's life span is challenging and western blot using anti-*Pf* MSP1-42 antibodies detects only the full-length native antigen.

The Coomassie gel in Figure 2.9B shows the tremendous amount of malaria proteins present in the total cell lysis. Yet, the raised anti *Pf* MSP1-42 antibodies only bind a single protein. This shows the high level of selectivity the raised antibodies display.

Malaria antigens do not possess a trackable function like many enzymes would, thus identifying if antigens are correctly folded can be challenging. To show that expressed antigens are correctly folded the antibodies raised against the purified C-Tag *Pf* MSP1-42 were tested for the ability to block parasite invasion. Growth inhibition assays were conducted with varying levels of IgG (figure 2.9 C). With increasing concentration of raised anti *Pf* MSP1-42 parasite proliferation decreases. At close to 0.9 mg/mL antibody concentration parasite proliferation dropped below 50% after one invasion cycle. Literature values of similar experiments show proliferation at 40% at identical concentrations of anti *Pf* MSP1-42 antibodies.[104]

Discussion

Previous literature and work in the Rathod lab has shown the usefulness of the wheat germ cell free translation system in expression of high-quality malaria proteins.[86-87, 105] The number of malaria proteins that have been shown to express in full length and functional form in the wheat germ system greatly outnumbers those successfully expressed in other popular expression systems like the cell free *E. coli* system. A major bottleneck in malaria antigen prioritization has been the production of full length, soluble, and correctly folded proteins. Not only is expression a challenge but producing highly pure antigens is also a major obstacle. Purification of malaria antigens is hindered by the large number of disulfide bridges, and the "sticky" nature of the antigens that leads to strong nonspecific interactions with translation system proteins. The unique nature of each malaria antigen makes it difficult to find a universal expression and purification scheme. Here we have shown the wheat germ cell free system is

ideal for malaria antigen expression and have shown two promising single step purification systems that give high purity antigens for further studies.

The autoradiograph images illustrate that the wheat germ system can express full length malaria antigens. Even after subjection to high levels of centrifugation we see the antigens remain in their soluble form. This is a simple, yet critical point that should be noted. If proteins cannot be expressed insoluble form, they are rendered useless. Even in situations where proteins can be refolded and solubilized many more steps are added to the expression workflow. It shows that characteristics like antigen size, number of disulfide bonds, or origin of antigen in the parasite (membrane bound or organelle localized) do not affect the soluble nature of the wheat germ system products. The library of malaria antigens that are studied and worked with can be vastly expanded if expression is carried out in the wheat germ system. This can greatly help the malaria community in the prioritization of malaria antigens.

Other groups have shown the use of the wheat germ cell free system paired with affinity tags can lead to successful malaria antigen isolation. It is observed that one must determine the best affinity tag for purification on an antigen by antigen basis. Even then, level of protein purity can greatly vary among antigens and purity levels may only reach 80%. Although not ideal these antigens are still considered "pure."[106-107] Here we wanted to develop a single step purification scheme that worked well in collaboration with the wheat germ system and produced highly pure antigens. The ability to have a single scheme that can be applied to all antigens of interest is highly valuable. I have worked with four different tagging systems to find the most well-suited tag for purification from the wheat germ system. The GST tag and the HIS tag are both tagging systems that have been reportedly used in the literature for malaria antigen purification. Although they have been used to purify malaria antigens, the level of purity is rarely over 80%.

Even with this low purity these antigens are considered pure enough for further studies like raising antibodies to these antigens. There has been little progress in the development of new tagging systems implemented in wheat germ protein purification. The results here show that both the covalent HaloTag capture system and the epitope C-Tag system are both well suited for antigen purification.

This is the first work showing the use of HaloTag for malaria antigen purification. The HaloTag showed good purity in select antigens such as MSP1-42 and MSP1-19 but less so in AMA1. The degree of impurity is surprising as the purification scheme is designed to release only those proteins that contain the specific TEV protease site. Unlike affinity tag purification the HaloTag is a covalent capture and should therefor lead to more specific protein isolation. The variabilities make it still a challenging tag to be used universally and degree of purity will vary depending on antigen of interest.

The C-Tag has previously been shown to purify *Pf* RH5 from the *Drosophila melanogaster* expression system but not using the wheat germ system.[108] This was the first work that showed multiple malaria antigens can be purified from wheat germ expression using a simple streamline C-Tag purification scheme. The work here suggests that C-Tag is a better suited tagging system for malaria antigens that can be more uniformly applied to different proteins. Levels of purity in all the antigens tested here were at least 90% or higher. The specificity of the epitope tag results in less collection of nonspecific bound proteins in the final sample. This makes it a very useful tag in protein isolation. Furthermore, the nature of release from the capture resin is use of a competitor peptide. This allows purified proteins to be released from the capture resins at physiological pH ranges that are best suited for the protein of interest. This avoids any protein unfolding or degradation during the purification process. The ability to

raise rabbit antibodies against the purified *Pf* MSP1-42 C-Tag antigen and show their ability to block parasite invasion in a concentration dependent manner indicated the *Pf* MSP1-42 antigen was not only highly pure but also in its native folded and functional form. The working library of malaria antigens in the Rathod lab can easily be expanded and we are confident the C-Tag system can be applied for successful purification. Within the malaria community, the C-Tag can be adopted as another essential tool in protein purification and downstream assays.

Chapter 2 Figures

Table 2.1 Antigen candidate table.

Gene Identifier	Name (Abbreviation)	Total Antigen Size bp	Expressed Fragment bp (kDa)	Amino Acids	pI	Cysteine Composition
P.falciparum						
PF3D7_0930300	Merozoite Surface Protein 1 (MSP1-42)	5163	1095 (41)	1362-1721	5.41	13 (3.6%)
PF3D7_1133400	Apical Membrane Antigen 1 (AMA1)	1869	1881 (72)	2-623	5.23	17 (2.7%)
PF3D7_0930300	Merozoite Surface Protein 1-19 (MSP1-19)	5163	321 (11.7)	1597-1704	4.48	12 (11.1%)
PF3D7_0424100	Reticulocyte binding protein homologue 5 (Rh5)	1578	1578 (62.8)	1-526	8.81	6 (1.1%)
P. vivax						
PVX_099980	Merozoite Surface Protein 1 (MSP1-42)	5256	1299 (49)	1325-1752	4.79	12 (2.8%)
PVX_092275	Apical Membrane Antigen 1 (AMA1)	1689	1702 (64)	2-623	7.48	19 (3.4%)
PVX_099980	Merozoite Surface Protein 1-19 (MSP1-19)	5256	327 (11.9)	1590-1704	5.02	7 (6.1%)

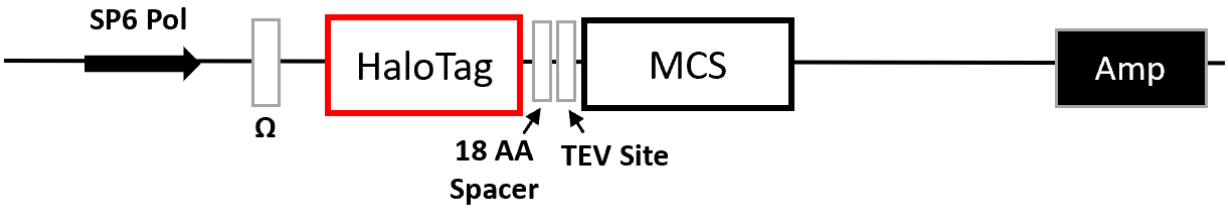

Figure 2.1 HaloTag cloning map. From left to right is the SP6 RNA polymerase binding site, the omega ribosomal biding site, HaloTag sequence, 18 amino acid spacer, TEV protease cleavage site, multicloning site for insertion of antigens of interest and a ampicillin resistance marker.

Figure 2.2 HaloTag multicloning site map. Constructed multi-cloning site for HaloTag constructs with 18AA spacer between HaloTag and antigen of interest.

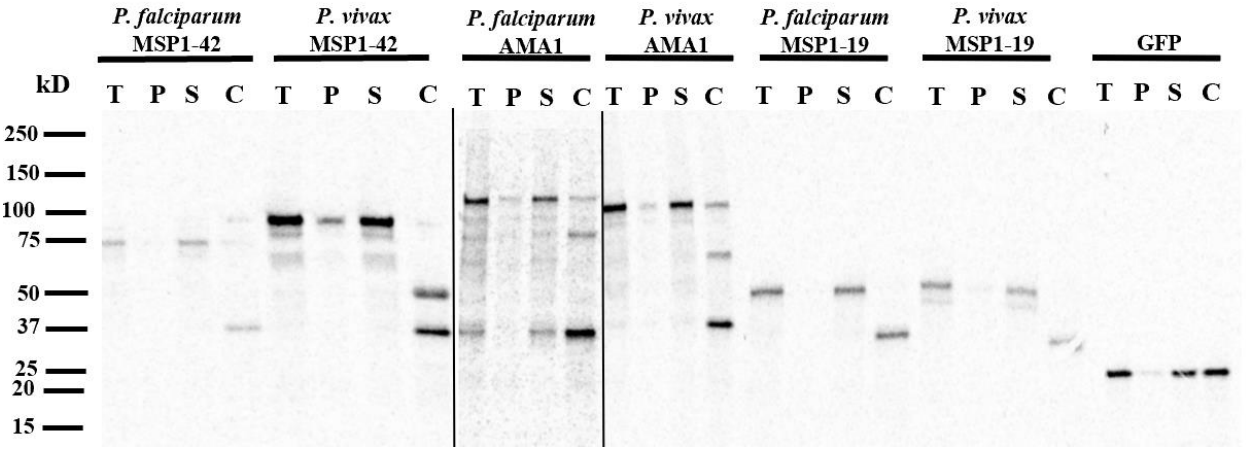

Figure 2.3 HaloTag 18AA spacer construct autoradiographs. Each antigen was expressed with ^{14}C leucine in the translation mixture. Translations were processed and loaded onto a SDS-PAGE gels followed by image transfer and scanning on a phosphorescent screen. T: total translation, P: pelleted sample after high speed centrifugation, S: soluble fraction after high speed centrifugation, FC: soluble fractions treated with TEV protease to visualize cleavage of the HaloTag from antigen. GFP was used as a control. Image between the two vertical solid black lines is from separately run gels.

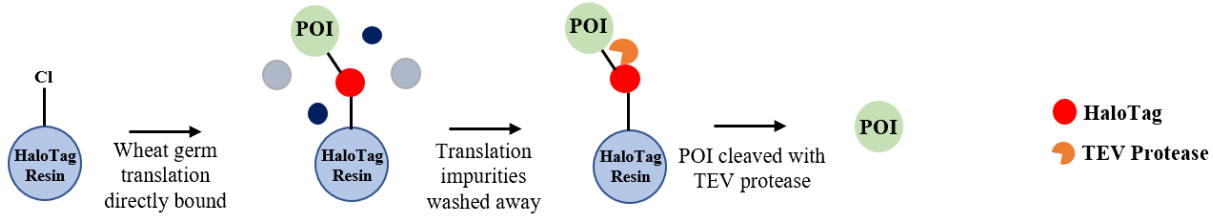

Figure 2.4 HaloTag Purification Scheme. Magnetic HaloTag bead resins marketed to capture HaloTag proteins are incubated with wheat germ translations of HaloTag fused proteins. Beads are washed and proteins of interest (POI) are isolated by cleavage from the HaloTag resin using TEV protease.

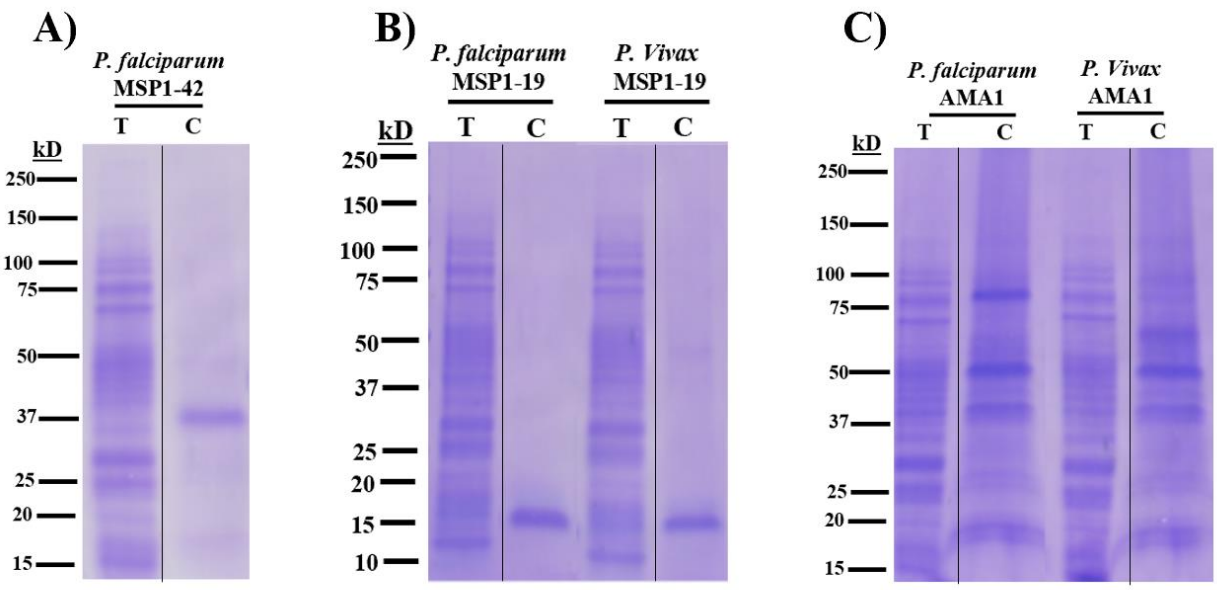

D)

Band	POI	*Pf* or *Pv* Proteome Hit	Peptides with high xCorr	Coverage
A 37kD	Pf MSP1-42	Merozoite surface protein 1	10/36	17.20%
B 15kD	Pf MSP1-19	Merozoite surface protein 1	11/134	78.54%
B 15kD	Pv MSP1-19	Merozoite surface protein 1	8/133	78.70%
C 75kD	Pf AMA1	Apical Antigen 1	20/44	56.70%
C 64kD	Pv AMA1	Apical Antigen 1	22/55	75.98%
C 50kD	TEV protease	***	***	***

Figure 2.5 HaloTag purified antigens. SDS-PAGE gels of the purified HaloTag antigens. Gels were stained with Coomassie blue. Solid vertical lines indicate deleted lanes for simplicity. A) Purification of HaloTag *Pf* MSP1-42 B) Purification of HaloTag *Pf* and *Pv* MSP1-19 C) Purification of HaloTag *Pf* and *Pv* AMA1 D) LTQ data analysis of trypsin digested proteins. Trypsin digested products from gel bands are listed by size and the purified protein of interest (POI). Highest aligned hit is listed along with number of peptide fragments that gave a highly positive correlation to the protein hit. TEV protease is listed for reference when it was not completely removed from the purified protein fractions.

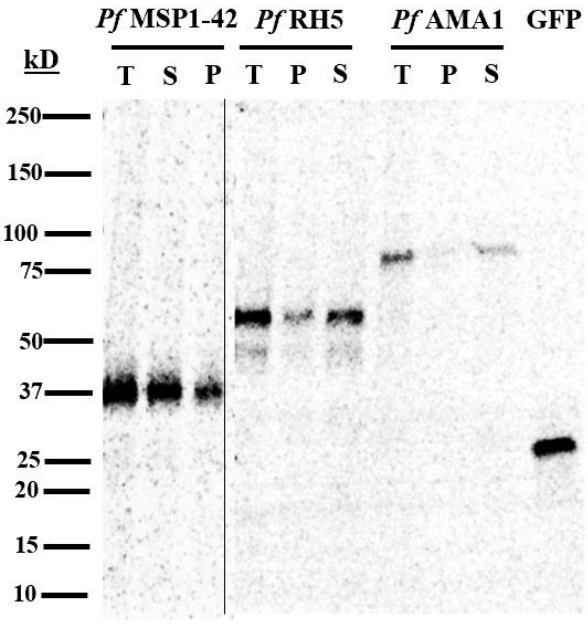

Figure 2.6 C-Tag antigen autoradiographs. Each antigen was expressed with ^{14}C leucine in the translation mixture. Translations were processed and loaded onto SDS-PAGE gels followed by image transfer and scanning on a phosphorescent screen. T: total translation, P: pelleted sample after high speed centrifugation, S: soluble fraction after high speed centrifugation. C-Tag GFP was used as a control. Image between the two vertical solid black lines is from separately run gels.

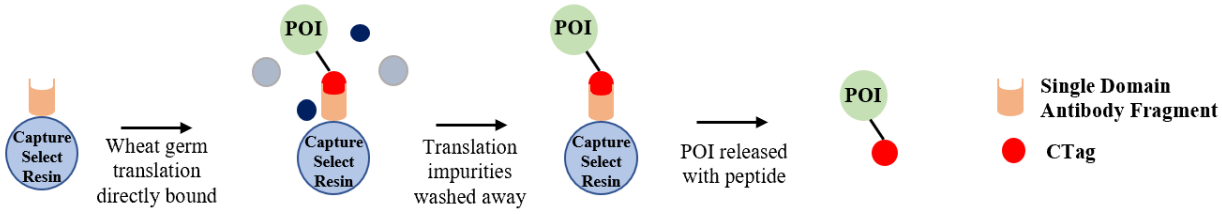

Figure 2.7 C-Tag Purification Scheme. Capture select matrix is coated with single domain antibody fragments specific for the C-tag (tan U shape). C-Tag (EPEA, shown in red) binds to matrix and is subsequently washed and eluted with peptide SEPEA to afford the isolated protein of interest (POI).

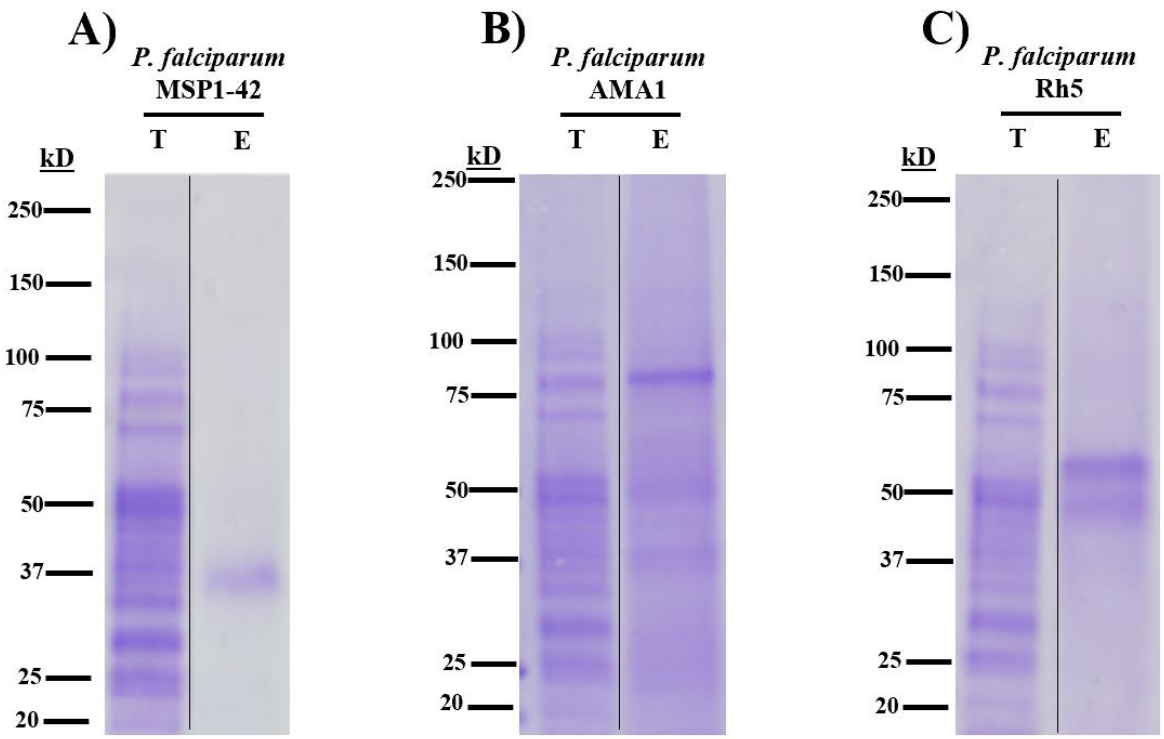

D)

Band	POI	*Pf* Proteome Hit	Peptides with high xCorr	Coverage
A 37kD	Pf MSP2-42	Merozoite surface protein 1	18/43	18.02%
B 75kD	Pf AMA1	Apical Antigen 1	12/28	45.34%
C 62kD	Pf RH5	Reticulocyte binding homologue 5	23/41	71.1

Figure 2.8 C-Tag purified antigens. SDS-PAGE gels of the purified C-Tag antigens. Gels were stained with Coomassie blue. Solid vertical lines indicate deleted lanes for simplicity. A) Purification of C-Tag *Pf* MSP1-42 B) Purification of C-Tag *Pf* AMA1 C) Purification of C-Tag *Pf* RH5. D) Trypsin digested products from gel bands are listed by size and the purified protein of interest (POI). Highest aligned hit is listed along with number of peptide fragments that gave a highly positive correlation to the protein hit. TEV protease is listed for reference when it was not completely removed from the purified protein fraction.

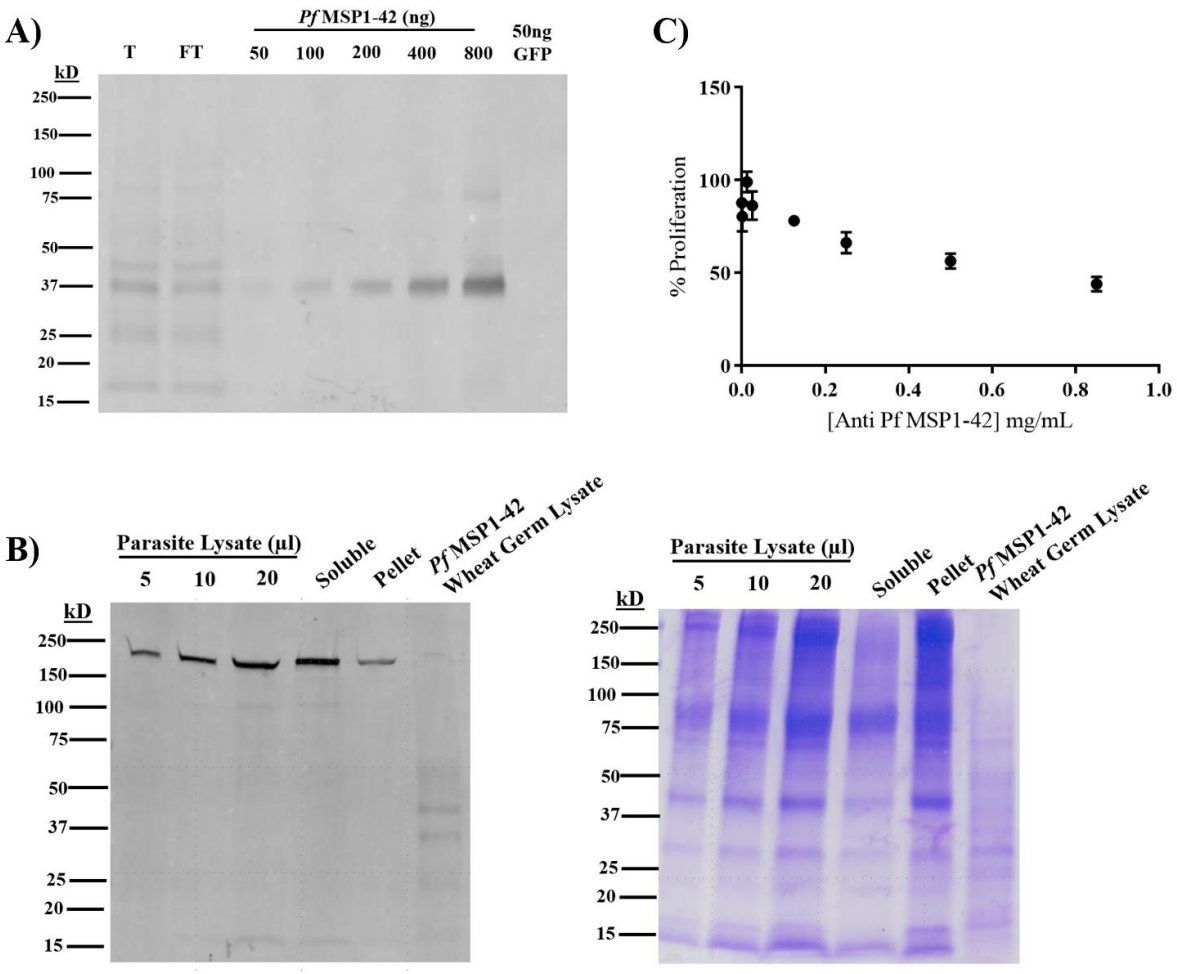

Figure 2.9 Analysis of raised antibodies against C-Tag purified *Pf* MSP1-42. Antibodies were raised in rabbits against the purified C-Tag MSP1-42. A) Antibody titer against the total and flow through fractions of wheat germ translation, C-Tag purified *Pf* MSP1-42, and C-Tag purified GFP. B) Left image is a western blot using raised Anti C-Tag *Pf* MSP1-42 antibodies. Western blot shows antibody selectivity against *Pf* parasite culture lysate, the soluble and pelleted fraction of lysis, and the *Pf* MSP1-42 wheat germ translation. Right image is a replication of the western blot (left) but using Coomassie stain to visualize proteins. C) Effects of parasite culture growth (3D7) with increasing concentration of Anti *Pf* MSP1-42 antibodies.

Table 2.2 Primer design for HaloTag and C-Tag vectors. Primer sequences used for vector designs.

Construct	Forward Primer	Reverse Primer	Restriction Sites Used (Forward and Reverse)
pEU-HaloTag Pf MSP1-42	ATCAGGTACCATCGAGAAGAACATCTTCACCTTCAAC	GATGCTCATCCTCTACAGCTTCATCTGATGAGGATCCATCT	KpnI/BamHI
pEU-HaloTag18AASpacer Pf MSP1-42	GGAGGTGGAGGCAGCGGCGGTGGAGAGCCAACCACTGAGGATCTGTAC	GACGCTCGAGATTTCCGGCGGGTCCGGTGGAGGCGGTAGT	Blunt End Ligation
pEU-HaloTag18AASpacer-MCS	ATACTAGGATCCACCGGTGGCCGGCCACTAGTCCATGGTTTTGTATAGAATTTACGGC	CTGTACTTTCAGAGCGATAACACTAGTTCTAGAGAGCTCGGTACCCTTAAGGCGTCG	Blunt End Ligation
pEU-HaloTag18AASpacer Pf MSP1-19	ATCATCTAGACTCATCGAGGGCAAGTTCCAA	GCTCCTCCAGCAACTTCCTCTGATGACCATGGATCT	XbaI/NcoI
pEU-HaloTag18AASpacer Pf AMA1	ATCATCTAGACGCAAGCTCTACTGCGTTCT	TGCTCATGGAAAAGCCGTACTATTGATGAGGCCGGCCATCT	XbaI/NcoI
pEU-HaloTag18AASpacer Pf RH5	ATCATCTAGAATCAGGATCAAGAAGAAGCTCATCC	AAGAAGAACAAGCCACTCACTCAATGATGACCATGGATCT	XbaI/FseI
pEU-HaloTag18AASpacer Pv MSP1-42	ATCATCTAGACAAGACTACGCCGAGGACTAC	TTCCTGCTCTGCATGGAACTGTGATGACCATGGATCT	XbaI/NcoI
pEU-HaloTag18AASpacer Pv MSP1-19	ATCATCTAGAGAGAAGCTTGAAGAGTACAAGAAGTC	AGAGGCCGAGTGCAAGATGTGATGACCATGGATCT	XbaI/NcoI
pEU-HaloTag18AASpacer Pv AMA1	ATCATCTAGAAACAAGATCTACTACATCATCTTTCTCTCC	TGCTCATGGAAAAGCCGTACTATTGATGAGGCCGGCCATCT	
C-Tag Pf MSP1-42	GGATCCATGATCGAGAAGAAC	TGATGCTCATCCTCTACAGCTTCATCGGCGCCGCCGAGCCAGAGGCCTGACGGCCG	XhoI/EagI
C-Tag Pf MSP1-19	CTCGAGATGCTCATCGAGGGCAAGTTCCAAG	TGCTCCTCCAGCAACTTCCTCGGCGCCGCCGAGCCAGAGGCCTGACGGCCG	XhoI/EagI
C-Tag Pf AMA1	CTCGAGATGCGCAAGCTCTACTGCGTTCTC	GTGCTCATGGAAAAGCCGTACTATGGCGCCGCCGAGCCAGAGGCCTGACGGCCG	XhoI/EagI
C-Tag Pf RH5	GGATCCATGATCAGGATC	CAAGCCACTCACTCAAGGCGCCGCCGAGCCAGAGGCCTGACGGCCG	BamHI/EagI

Chapter 3: Novel periodate cleavable HaloTag linker synthesis

HaloTag Ligands

Current commercially available HaloTag linkers

The proprietor company of HaloTag is Promega. Promega offers a wide range of HaloTag ligands for use in a variety of assays. A basic HaloTag capture moiety includes a polyglycol chain that can vary in length and a six carbon chloroalkane chain where the HaloTag binds specifically and covalently. This backbone HaloTag capture structure is usually coupled to fluorescent, or affinity labels and tags. These HaloTag capture derivatives can be used in a variety of applications including cell surface tagging, intracellular membrane or protein labeling and imaging, and pull down assays.[109] Ligands on the market have been developed to contain a variety of functionalities including fluorescent labels, affinity tags, and solid phase attachment abilities. Additionally, some are cell impermeable like Alexa Fluor 488 Ligand and others are permeable like the TMR ligand or Oregon Green ligand. HaloTag ligands derivatized with Biotin or PEG-Biotin are also available and allow for assay development on solid phases such as bead based pull down assays.

The wide array of HaloTag capture ligands available for purchase allows for creative assay design. However, one major drawback of the available ligands is that none are marketed as chemically cleavable. The ability to cleave a chemical linker is a valuable tool in many different biochemical assays. First a cleavable linker can serve as a very important control. Showing the presence of a signal with HaloTag captured to a linker followed by loss of that same signal after a chemical treatment would be a useful tool. This observed loss of signal is a way to track how well the ligand's target was modified and how much of the observed signal was from the specific ligand HaloTag interaction and how much was from background noise. Second, a HaloTag

capture ligand which is cleavable would allow for the complete HaloTag fusion protein to be released. Currently Promega sells the HaloTag plasmid with a TEV protease site between the HaloTag and the fusion protein of interest. Thus, using TEV protease it is possible to remove the fusion proteins from the capture scheme, but not the HaloTag protein itself. There is no way to remove the covalently bound HaloTag protein from the capture targets. Last, synthesis of a cleavable linker can increase availability of capture linker at a fraction of the cost. The average cost of the marketed linkers Promega sells is roughly $600 for 90µg of ligand. The high price of these linkers make the self-synthesis of them highly appealing.

Advantage of an oriented linker

Reproducible immobilization of antigens on microarrays is a critical component of assay development, yet rarely is addressed. The current method of immobilization, whether on plate-based arrays or bead-based assays, uses nitrocellulose adsorption or standard carbodiimide coupling. In these situations, the proteins get coupled to the array matrix in a non-oriented manner. This results in proteins being presented on the array surface in a variety of orientations. With the infinite possibilities of protein presentation, assay sensitivity and selectivity suffer. Furthermore, proteins that contain a large number of lysines may be particularly challenging to use in bead-based assays as multipoint attachment and incorrect presentation can effect assay results.[110]

Only a limited number of attachment strategies of proteins or peptides to bead based arrays have been described. Luminex xMap technology is relatively new to many fields and most of the work done with these beads utilizes carbodiimide chemistry. One of the more successful oriented assays uses the high affinity partners avidin-biotin. Peptides that are modified to have a biotin tag can non-covalently link to avidin-coated microspheres.[111] The downside of using the

biotin-avidin interaction for coupling is it then prohibits the use of the same avidin-biotin interaction for downstream assay detection. Another group utilized a heterobifunctional cross-linker (SMPB) which contains an amine reactive ester at both sides. Using this cross linker, they were able to link bovine serum albumin coated microspheres with peptides through the N-terminal of cysteine residues.[112] Although peptides were oriented correctly, epitope presentation was poor.

Of the bead-based assay work that has applied uniform attachment strategies, whole proteins have rarely been used. More often this kind of work is done using peptide or protein fragments. There is need of bead-based assays that can uniformly present proteins and antigens of interest as tools for antigen discovery.

Synthesis of novel periodate cleavable linker

The importance of reproducible antigen presentation in bead based assays lead to the synthesis of a novel periodate linker. The linker was designed with the needs of downstream application in mind. The use of the linker would be for capture of HaloTag fused malaria antigen candidates. The capture of these antigens would ideally be on the assay developed to characterize the immuno-responsiveness of patient serums against these recombinant antigens. Most assays that look at immuno-responsiveness immobilize antigens on a solid surface without the ability to recover the antigens. Thus, once captured there is no possibility of antigen recovery or later assessment of antigen integrity. With this in mind we set out to develop a chemically cleavable linker with the ability to be immobilized on a solid surface in an oriented manner and also be able to capture HaloTag recombinant proteins.

The linker (**11** in scheme 3) was designed with three main chemical features. The final application of the linker is to be used on the carboxylated polystyrene beads designed for use in

the BioPlex200 multiplexing instrument. The free amine gives the ability to immobilize the linker on a solid surface in a reproducible orientational manner. Using carbodiimide chemistry the carboxylated bead surfaces are activated and the free amine of the linker can form a stable amide bond with the beads. The next feature of the linker was designed to capture HaloTag proteins. HaloTag is known to selectively bind in an irreversible manner to chloroalkane derivatives. Specifically, it is known that a six-carbon chloroalkane chain gives optimal capture ability. With this in mind, the linker was designed based of the structure of a commercially available HaloTag capture linker sold by Promega.[109] The final feature that makes this linker novel is the addition of a free diol near the amine. When treated with periodate this vicinal diol undergoes oxidative cleavage to form two new products via the Malaprade reaction. The 1,2-diol forms a cyclic periodate ester which undergoes a rearrangement which breaks down the cyclic iodate and forms two new carbonyl groups.[113] The selective yet fast Malaprade mechanism made it appealing for the application of linker-antigen complex removal from a bead based surface. Additionally, sodium periodate is a mild oxidant that has been shown to be compatible with protein functionalities. With these three structural features within a single chemical linker the development of a novel multiplexing platform would be possible.

Experimental Methods

Chemicals used for synthesis were obtained from Sigma-Aldrich unless otherwise noted. Dry and air free solvents were obtained from a solvent purification system. 1H-NMR spectra were obtained on a Bruker NMR spectrometer (PABBI, BBI, or TXD probes used on 300 MHz).

Synthesis of 4-Phthalimido-4-deoxy-2,3-O-isopropylidene-D-erythronic acid (2)

Synthesis was carried out as described in Seki H. et. al.[114] Briefly, 2,3-O-Isopropylidene-D-erythronolactone (**1** 1g, 6.32 mmol Alfa Aesar) and potassium phthalimide salt (1.17 g, 6.32 mmol) were added to round bottom flask. Dry DMF was added (10 mL). Reaction was stirred at room temperature under inert atmosphere, solution was a mint green color. Reaction was heated to 160 °C and refluxed for four hours, reaction turned dark brown and the presence of a light brown precipitate observed. The reaction was cooled to room temperature and solvent was dried on a rotary evaporator. Product was dissolved in 25 mL H_2O and 1 M HCL to pH 2.0. A tan precipitate was observed. Product was vacuum filtered and washed three times with 20 mL H_2O. The crude product was purified by C18 reverse phase combi flash chromatography (H_2O/Acetonitrile) to afford 4-Phthalimido-4-deoxy-2,3-O-isopropylidene-D-erythronic acid as a tan powder.

Yield 26% MS (ESI): M-H calcd 304.09; found 304.0 1HNMR 3.83 (m, 2H), 7.03 (m, 2H), 4.92 (m, 1H), 4.76 (d, 1H), 3.85 (d, 2H), 1.62 (s, 3H), 1.34 (s, 3H)

Synthesis of 4-deoxy-2,3-O-isopropylidene-D-erythronic acid (3)

Synthesis was carried out as previously described in Seki H. et. al.[114] Here, **2** (815 mg, 2.67 mmol) was mixed with 30 mL of 50% EtOH. After stirring on ice for five minutes, excess anhydrous hydrazine was added (857 mg, 26.7 mmol) to the solution. Reaction was carried out for three hours and was allowed to come to room temperature. Once reaction went to completion,

300 mL of 20% aqueous acetic acid was added (roughly pH 3.0) and a tan precipitate formed. After filtration, filtrate was concentrated to one-sixth of the original volume. Additional precipitate formed and was filtered away. Finally, filtrate was chilled and cold acetone was added (six times volume of filtrate). Viscous solution is placed at -20°C and following day a white precipitate is collected.

Yield 60% MS (ESI): calcd 175.08; found 175.0 (not shown) ^{1}H NMR (300MHz, D_2O) 4.50-4.72 (m, 2H), 2.82-3.07 (ddd, 2H), 1.47 (s, 3H), 1.33 (s, 3H)

Synthesis of Fmoc-4-amino-4-deoxy-2,3-Oisopropylidene-D-erythronic acid (4)

Synthesis was carried out as previously described in Seki H. et. al.[114] White solid **(3)** (610 mg, 3.48mmol) was dissolved in 5 mL dioxane. The reaction was chilled on ice and 8 mL of 10% Na_2CO_3 was added. Separately, 9-Fluorenylmethoxycarbonyl chloride (Fmoc) was dissolved in 7 mL dioxane and chilled. The Fmoc solution was added dropwise at a rate of 0.2 mL/30 seconds. Reaction was allowed to come to room temperature overnight. Reaction was dried down and crude product was purified by C18 reverse phase combi flash chromatography (H_2O/Acetonitrile).

Yield 82% MS (ESI): calcd 397.15; found 397.6 M+1 and 420 M+Na. ^{1}H NMR (300MHz, DMSO-d_6) 7.89 (d, *J*=7.5 Hz, 2H), 7.67 (d, *J*=7.4 Hz, 2H), 7.42 (t, *J*=7.4 Hz, 2H), 7.33 (t, *J*=7.4 Hz, 2H), 7.25 (t, *J*=5.7 Hz, 1H), 4.26 (m, 5H), 3.09 (t, *J*=5.7 Hz, 2H), 1.37 (s, 3H), 1.21 (s, 3H).

Synthesis was carried out as previously described in Los et. al. [115]

Synthesis of Boc protected 1-Amino-3,6,9-trioxaundecanyl-11-ol (6)

1-Amino-3,6,9-trioxaundecanyl-11-ol (Combi Blocks) was added to 7 mL ethanol. Di-tert-butyl dicarbonate was added to the reaction and let stir two hours at room temperature. The reaction was dried on a rotovap to a clear colorless oil. The crude mixture was washed twice with 15 mL

1N HCl and 10 mL H_2O. Organic layers were combined and washed twice with saturated sodium bicarbonate. Resulting product was dried over sodium sulfate and concentrated to a yellow tinted oil.

Yield 90% MS (ESI): calcd 293.3 found 316.0 M+Na and 415.2 Di-Boc M+Na ^{1}H NMR (CDCl3) δ=5.64 (bs, 1H exchangeable), 3.56-3.74 (m, 14H), 3.33 (s, 2H), 1.47 (s, 9H).

Synthesis of Boc protected 18-Chloro- 3,6,9,12-tetraoxaoctadecan-1-amine (not shown in scheme) Synthesis is previously described in Los G. et. al.[115] Briefly, sodium hydride (60 mg, 2.02 mmol) was added to a dry round bottom flask. Reaction was chilled on ice and kept under inert atmosphere. Boc protected 1-Amino-3,6,9-trioxaundecanyl-11-ol (397 mg, 1.35 mmol) was taken up in 1.0 ml dry DMF. The resulting mixture was added to the reaction flask dropwise via syringe. Another three mL of dry DMF was added to the reaction flask. The reaction was kept at 0° C for one hour. To the resulting mixture 1-chloro-6-iodohexane (336 mg, 1.36 mmol) was added dropwise via syringe. Reaction was stirred overnight at 4°C. Reaction was quenched with ice cold water and solvent was stripped. A white slurry with precipitate was formed. The crude product was purified by silica combi flash chromatography (Hexane/Ethyl Acetate) to afford a pale yellow oil.

Yield 43% MS (ESI): calcd 411.98 found 434.3 M+Na ^{1}H NMR (CDCl3) δ=5.08 (bs, 1H exchangeable), 3.53 & 3.37 (m, 20H), 1.71 (m, 2H), 1.49 (m, 2H), 1.43 (m, 4H & Boc 9H) .

Synthesis of 18-Chloro- 3,6,9,12-tetraoxaoctadecan-1-amine (8)

Boc protected 18-Chloror- 3,6,9,12-tetraoxactadecan-1-amine (293 mg, 0.71 mmol) was added to round bottom flask with 15 mL of dry methylene chloride. To the reaction excess trifluoroacetic acid (810 mg, 7.11 mmol) was added. Reaction was stirred at room temperature for two hours. Solvent was evaporated off on rotovap. Methylene chloride was added twice (20

ml each) and rotovaped off. Crude product was purified with C18 combi flash chromatography (H_2O/Acetonitrile). Fractions with desired product were determined using thin layered chromatography and ninhydrin staining (0.2 g ninhydrin solid in 100 mL ethanol).
Yield 40% MS (ESI): calcd 311.84 found 312.1 M+H ^{1}H NMR (DMSO-d_6) δ=7.83 (bs, 3H exchangeable), 3.53 & 3.37 (m, 20H), 1.71 (m, 2H *J*=14.2), 1.49 (m, 2H *J*=6.8), 1.34 (m, 4H)

Synthesis of fmoc-diol protected HaloTag capture linker (9)

Reaction flask was chilled on ice and kept under nitrogen. 4-Phthalimido-4-deoxy-2,3-O-isopropylidene-D-erythronic acid **(4)** was added (137 mg, 0.449 mmol) with 4.5 mL dry DMF. 1-Ethyl-3-(3-dimethylaminopropyl) carbodiimide (92 mg, 0.481 mmol), 1-Hydroxybenzotriazole hydrate (65mg, 0.481mmol), and triethylamine (81 mg, 0.802 mmol) were added to the reaction flask. The solution was mixed for twenty minutes on ice. 18-Chloro- 3,6,9,12-tetraoxaoctadecan-1-amine (100 mg, 0.321 mmol) was taken up in 0.5 mL dry DMF and added to reaction mixture dropwise via syringe. Reaction was allowed to come to room temperature and stirred for 19 hours. Solvent was stripped off and crude product was taken up in methylene chloride. Mixture was extracted two times with methylene chloride and ice-cold water. Organic layers were combined and dried over sodium sulfate. Solution was decanted, and solvent stripped to afford **9**. Crude product was purified with silica combi flash chromatography (methylene chloride/ethyl acetate).
Yield 54% ^{1}H NMR (300MHz, MeOD) 7.30-7.89 (m, 8H), 4.22-4.59 (m, 5H), 3.14-3.61 (m, 20H), 1.98 (s, 2H), 1.75 (m, 2H), 1.39-1.57 (m, 6H and 1.39s, 3H; 1.57s, 3H).

Synthesis of fmoc protected HaloTag capture linker (10)

Fmoc-diol protected HaloTag capture linker **(9)** (65 mg, 0.094 mmol) was treated with 15 mL 1N HCl (0.015 mol) in 20 mL methanol. Reaction was stirred at 80 °C for one hour. Mixture was

rotovaped and crude mass spectra was taken to monitor reaction completion. Crude product was directly used in synthesis of **(11)**.

Synthesis of HaloTag capture cleavable linker (11)

Piperidine (3.44 g, 0.040 mol) was added to crude product **(10)** (62 mg, 0.095 mmol) in 20 mL dimethylformamide. Reaction was stirred for 30 minutes at room temperature. Solvent was removed and crude product was purified by C18 reverse phase combi flash chromatography (H_2O/Acetonitrile with 1% acetic acid in mobile phase). Fractions were tested for purity using LC-MS. Only greater than 95% pure fractions were combined.

Yield 17.2% MS (ESI): calcd 429.1 found 429.9 M+H

Treatment of HaloTag capture cleavable linker (11) with periodate

Ability to cleave the final HaloTag capture linker **(11)** was assessed on a microscale. The cleavable HaloTag capture linker (1mg, 0.023 mmol) was taken up in 0.23 mL water. Separately, excess sodium periodate (5.3mg, 0.025 mmol) was taken up in 0.16 mL and added dropwise to the link **11**. Reaction was monitored using LCMS with a C18 reverse phase column. Time points of the reaction were taken before the addition of periodate, time 0, and time 2 hours. Samples from the reaction mixture were diluted 25 times and 4 µL of sample were injected (equivalent to 0.1 mg of **11**).

Results

Scheme 1: First building block for Cleavable HaloTag Capture Linker

Scheme 1 was designed to provide one of two building blocks for the final cleavable HaloTag capture linker. In the design we took advantage of the vicinal diol moiety, which can be cleaved with the mild oxidant, sodium periodate. Synthesis of the first building block for the final HaloTag capture linker **(11)** was a three-step process. We synthesized the isopropylidene-

protected diol **2** by the method of Kamiya et al.[114] Starting from commercially available (-)-2,3-*O*-isopropylidenne-D-erythronolactone **1**. Our yield was 26% which was less then previously reported but this may be a result of the addition of a C18 reverse phase purification. The original literature reports only carry out recrystallization. The second step of Scheme 1 was the treatment of the phthalimide protected amine with hydrazine to afford **3**. Yield was 60% and provided highly pure product as seen by NMR (Figure 3.2). The most distinct proton peaks in the NMR of the desired product are the 3H singlets at 1.30 ppm and 1.47 ppm. These correspond to the methyl protection group on the diol and were a good indication of product present throughout Scheme 1. The final step of Scheme 1 was the fluorenylmethyloxycarbonyl (Fmoc) protection of the free amine of **3**. Although various reaction conditions were attempted standard dioxane with 10% sodium carbonate added gave the best synthesis of **4**. Final C18 reverse phase purifications gave 82% yield with high purity as seen by NMR and MS (Figure 3.3). Through this multistep synthesis the original vicinal diol group from the (-)-2,3-*O*-isopropylidenne-D-erythronolactone is not altered. This is important as the vicinal diol group hydroxyl groups must be oriented in a fashion that the formation of the cyclic periodate ester intermediate is not sterically hindered. This synthesis scheme resulted in the first building block for the synthesis of the HaloTag linker. Building block **4** contains a Fmoc protected amine and a free carboxyl group making it suitable for downstream carbodiimide chemistry. Building block **4** also contains a protected vicinal diol which is useful for linker cleavage as observed in following sections.

Scheme 2: Second building block for Cleavable HaloTag Capture Linker

Scheme 2 reaction development was designed to produce a HaloTag capture moiety with optimal capture ability as well as contain a free amine so the structure could serve as the second building block for the final linker synthesis. Using standard tert-Butyl amine protection the

primary amine of commercially available 1-Amino-3,6,9-trioxaundecanyl-11-ol **(5)** was protected for subsequent reactions **(8)**. The remaining alcohol group underwent a Williamson etherifacation. The hydrogen of the primary alcohol group is removed with sodium hydride followed by a S_n2 substitution. The chlorine of the commercially available 1-chloro-6-iodohexane (**7)** acted as the leaving group. Yield of this reaction was close to 50% and gave a highly pure product (Figure 3.6). After standard boc deprotection the final product **8** was obtained at 40% yield. The NMR data of product **8** and the Boc protected **8** only differed by the loss of the nine-hydrogen singlet at 1.47 ppm. This confirmed the free amine was formed and could be used in subsequent carbodiimide couplings. Product **8** was the second building block for the final cleavable HaloTag capture linker.

Scheme 3: Cleavable HaloTag Capture linker

The cleavable HaloTag capture linker synthesis was designed to couple the two synthesized building blocks and forge the final linker product. Products from previous Scheme 1 and Scheme 2 gave the two building blocks that could be coupled with carbodiimide chemistry. Reaction optimization was required to afford the product at a reasonable yield of 54%. Reaction time was monitored by ninhydrin staining of TLC to watch for the disappearance of the limiting reagent, free primary amine **8**. It was observed that the reaction took more than twelve hours to run to completion. Further, solvent conditions were tested to find the best suited conditions. Again, reaction progress was monitored by watching for the disappearance of the free amine by ninhydrin staining TLC. Although acetonitrile did give some product, only under dry DMF conditions did the reaction run to completion. After isolation of **9** the product was carried through two sequential reactions without purification in between. This was in efforts to prevent loss of product as the reactions were run on microscales. The two sequential reactions were

simple HCL treatment for one hour at 80 °C to open the protected vicinal diol and the second was Fmoc deprotection with standard piperidine treatment for 20 minutes at room temperature. The final cleavable HaloTag linker was synthesized at a yield of roughly 20%. The mass spectral data of isolated **11** after reverse phase purification on C18 column shows a highly pure sample with only a single peak at 429.7 m/z as expected (Figure 3.8).

Cleavability of Linker

The ability to cleave the synthesized HaloTag linker **11** was a feature that was desired at the start of synthesis. The final product synthesis incorporated a free vicinal diol that when treated with periodate could be cleaved. This cleavability was tested in solution and cleavage progress was tracked using LC/MS (figure 3.10). Samples were analyzed on LC/MS before the addition of sodium periodate, at time 0, and at time 2 hours. Before sodium periodate a major peak is observed on the chromatograph at 8.1min, and a minor peak at 12.5min. With the addition of periodate, a new large peak on the chromatograph was observed at 1.5 min which was likely salts from the sodium periodate. The main linker peak of **11** was observed at 8.1min with 429.7 m/z. After two hours a sample was tested and there was no longer a peak at 8.1min present. A new peak at 10.8 min was formed. The m/z of this peak was identified as 370.5. This correlates with the expected cleavage product after periodate treatment. Periodate treatment of free diols produces two new aldehyde products. The aldehyde cleaved product has a molecular mass of 367.8 however the observed mass is 369.1 which correlates to the aldehyde product after reduction to an alcohol (figure 3.9). In just the two hours there is a complete loss of the starting linker **11** and only the formation of a single new product peak indicating no degradation of the cleaved products.

Discussion

The available HaloTag capture linkers on the market are limited in structural features that confer cleavability and often are extremely expensive. Here we aimed to develop a chemical linker that would capture HaloTag fusion proteins with the same selectivity as marketed linkers, however we added two important features. The HaloTag linker synthesized here (**11**) was developed to contain three main structural features: (1) the ability to capture HaloTag recombinant proteins with a chloroalkane chain (2) contain a free amine for carbodiimide coupling to carboxylated polystyrene beads for bead-based assay development and (3) include a chemically cleavable site providing the ability to remove and recover the HaloTag-fusion protein complex from bead-based surfaces. This linker is the first of its kind, and due to the specificity of the HaloTag capture and these unique structural properties, can be used in a wide variety of applications.

Synthesis of the linker was broken down into three schemes with a total of nine steps. Final linker yield obtained although low, is still sufficient for the application in bead-based assays. The amount of linker needed for bead-based applications is in the microgram level making recovery in the milligram level acceptable. The synthesis presented here was meant to limit the number of challenging or sensitive reaction steps. Many of the steps were based on traditional well-studied synthesis reactions such as Boc and Fmoc protections and deprotections as well as using solution-based carbodiimide chemistries. This makes it possible for scientists not heavily trained in organic chemistry synthesis skills to still be able to produce the desired product. For future work there is a scope to improve final yield of the cleavable linker **11.** Linker synthesis reactions were meant to be as simple and easy to reproduce as possible, this meant that at times reactions were conducted at suboptimal conditions. Reaction optimization may improve

yields and recovery in future synthesis attempts. Reaction scales, solvents, and temperatures should all be considered in efforts to improve yields and final recovery.

The total synthesis described in the previous scheme was designed to afford a chemical linker that could be used in bead-based assays along with HaloTagged fusion proteins. Together these two tools could lead to a novel tool of serum analysis using multiplexing technologies. The HaloTag fusion proteins can quickly and covalently capture to the synthesized HaloTag linker (**11**). With this linker coupled to multiplexing beads (Luminex) one could imagine the endless design of assays. Any protein of interest can be expressed with the HaloTag fusion and captured to the spectrally unique beads of Luminex. This makes multiplexing possible so that any protein, antigens or enzymes, can be studied for cellular or immune responses. Furthermore, the gentle cleavage of the linker makes recovering captured proteins from a solid surface possible. This allows for the determination of protein stability during an assay, specifically whether proteins are keeping their three-dimensional structure once adhered to a surface. The main application of the linker and HaloTag proteins here was to study human immune responses against malaria parasites. However, the methods and tools designed here can easily be adapted and applied for other fields and scientific studies.

Chapter 3 Figures

Scheme 1 Synthesis of free carboxylic building block. Synthesis of Fmoc-4-amino-4-deoxy-2,3-Oisopropylidene-D-erythronic acid **(4)** for use in final synthesis of HaloTag capture cleavable linker **11**

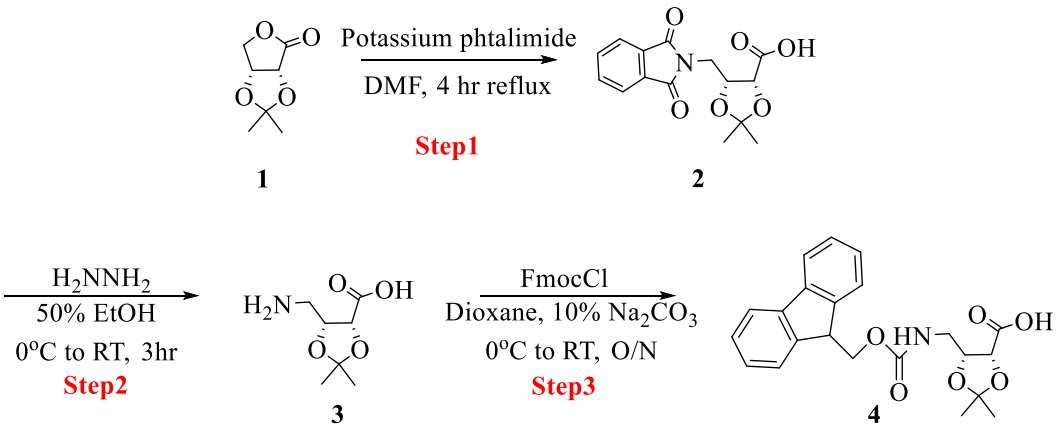

Scheme 2 Synthesis of free amine building block. Synthesis of 18-Chloro- 3,6,9,12-tetraoxaoctadecan-1-amine **(8)** for use in the final synthesis of HaloTag capture cleavable linker 11

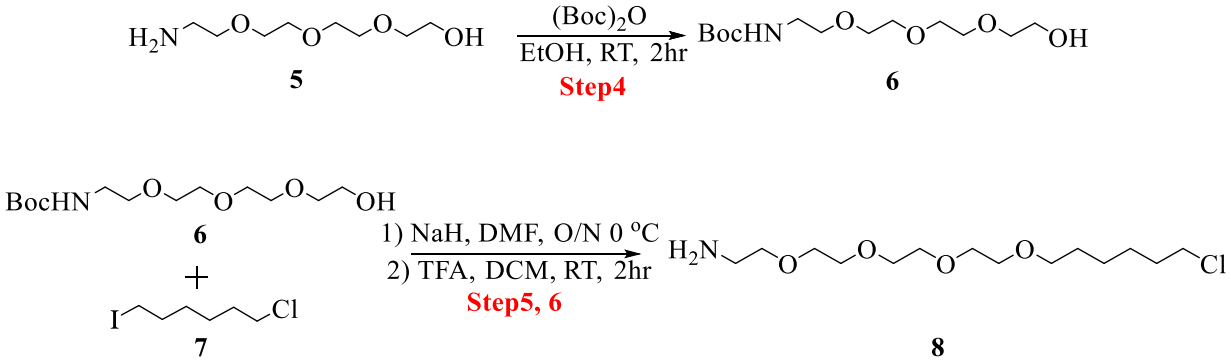

Scheme 3 Synthesis of HaloTag capture cleavable linker. Synthesis of **(11)** starting with building blocks 4 and 8

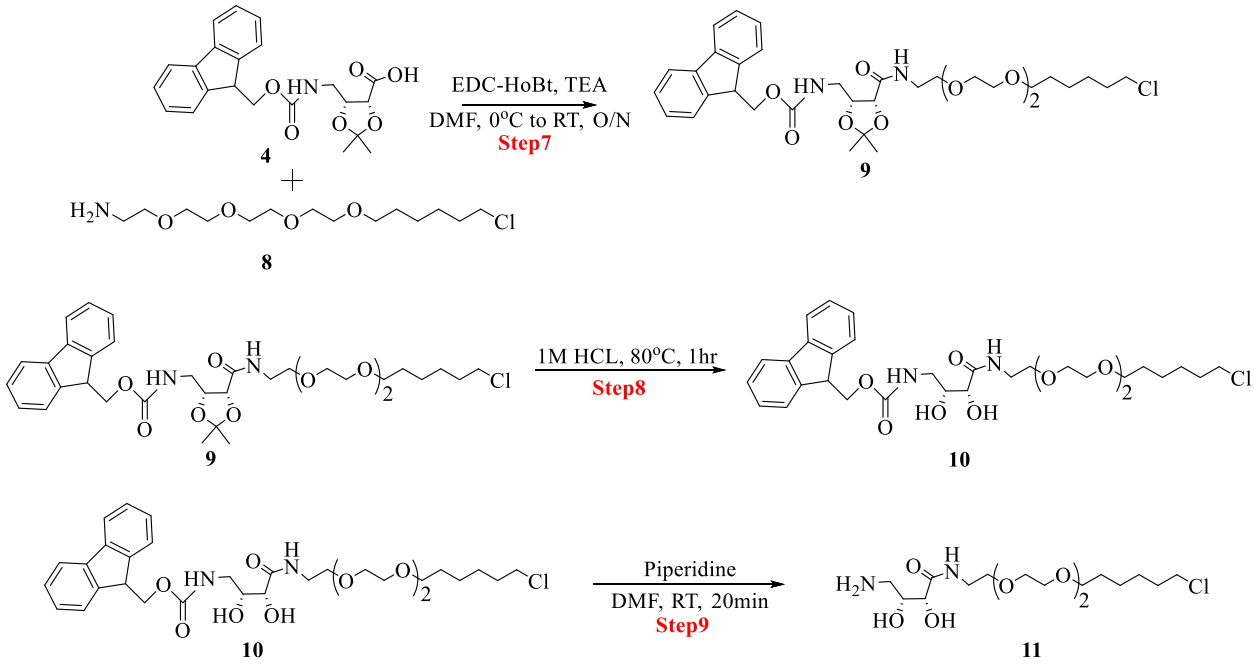

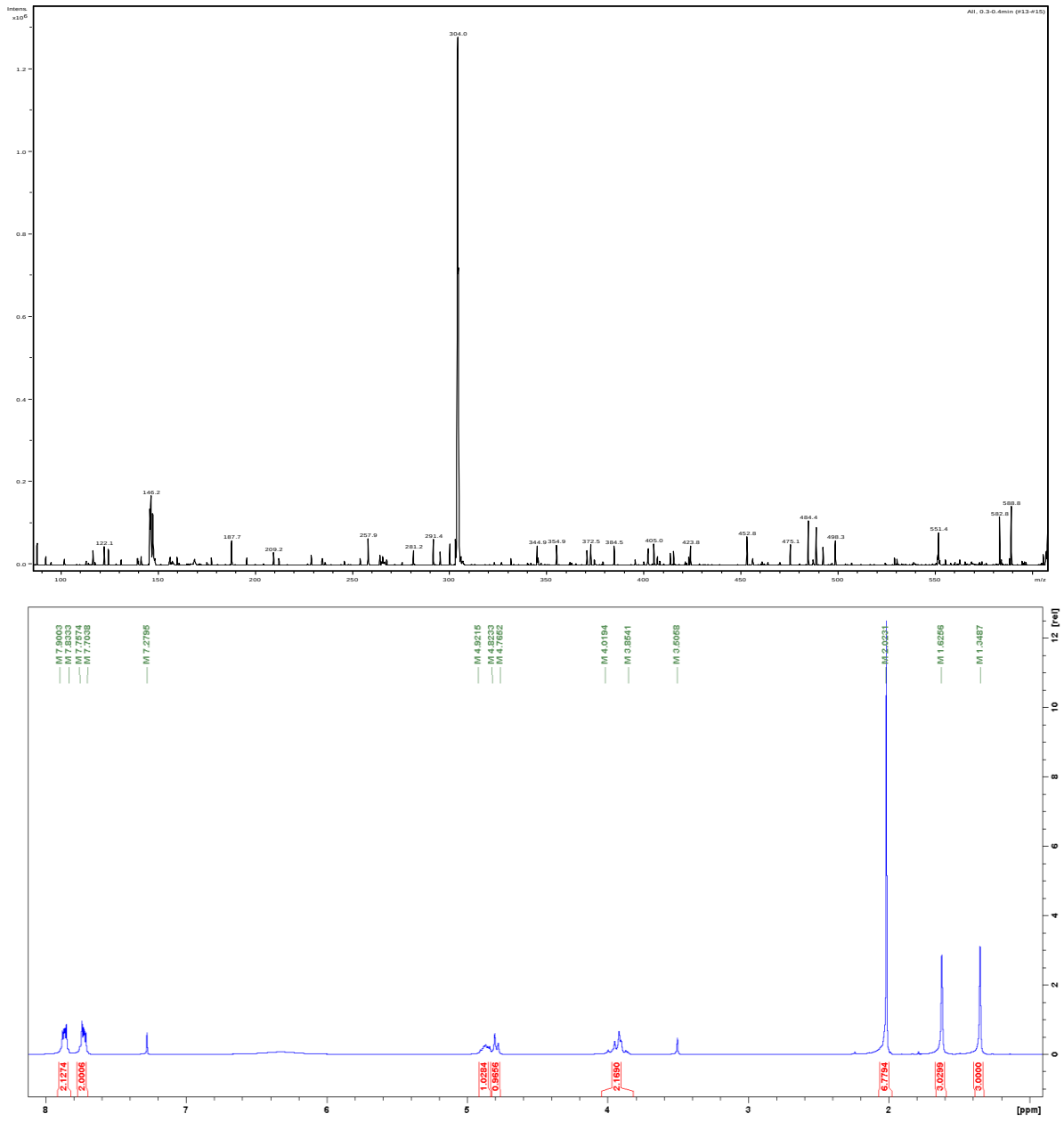

Figure 3.1 Mass spectrum and ^{1}H NMR spectrum of 2. Spectral analysis of 4-Phthalimido-4-deoxy-2,3-O-isopropylidene-D-erythronic acid (2)

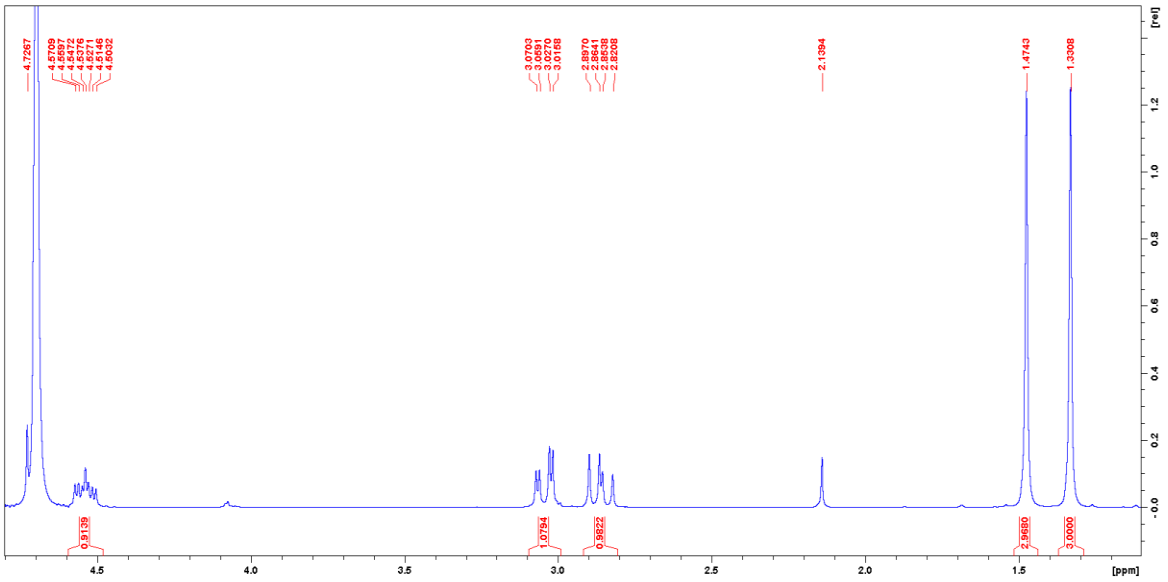

Figure 3.2 ^{1}H NMR spectrum of 3. Spectral analysis of 4-deoxy-2,3-O-isopropylidene-D-erythronic acid (3)

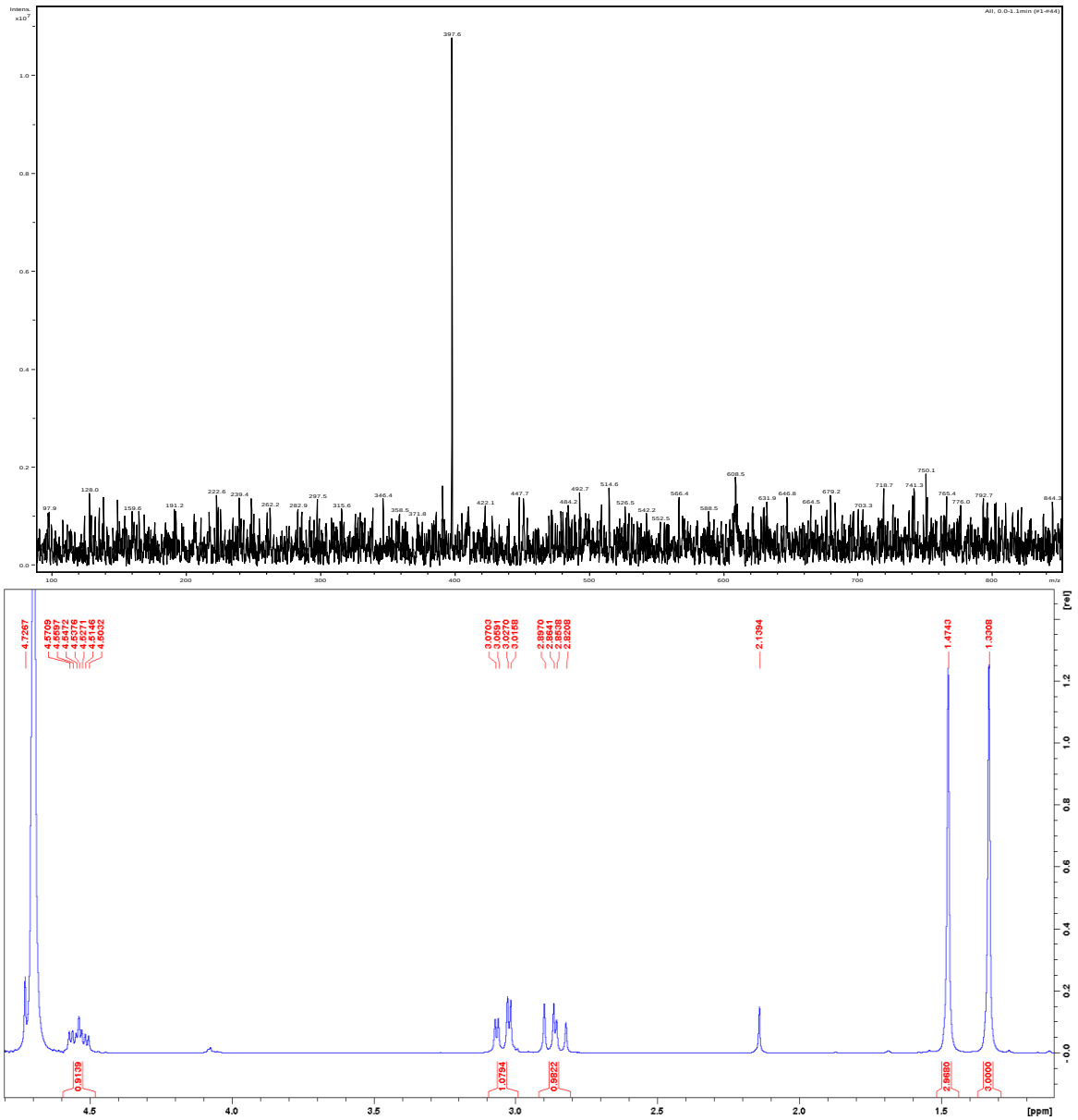

Figure 3.3 Mass spectrum and ^{1}H NMR spectrum of 4. Spectral analysis of Fmoc-4-amino-4-deoxy-2,3-Oisopropylidene-D-erythronic acid (4)

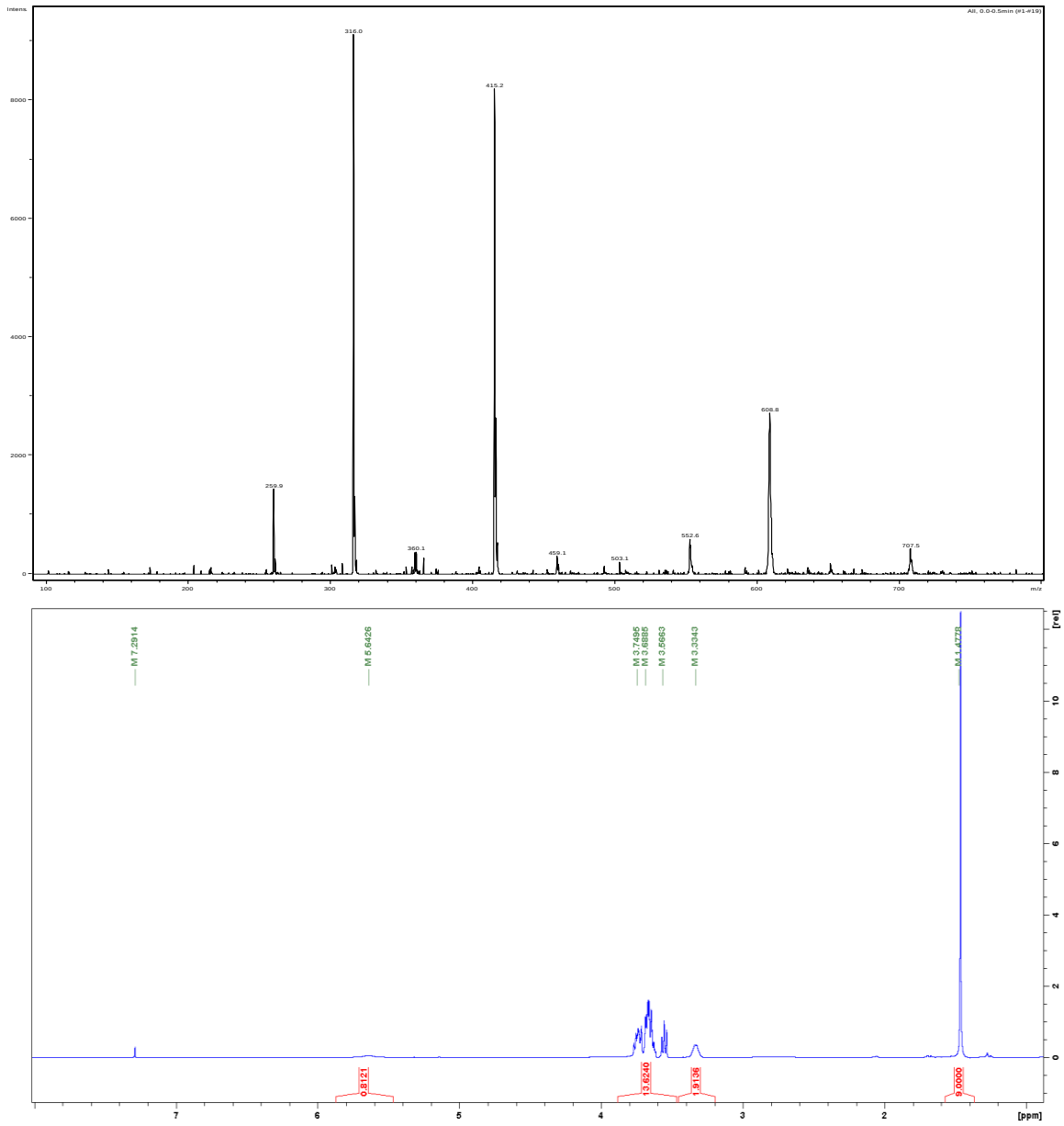

Figure 3.4 Mass spectrum and ^{1}H NMR spectrum of 6. Spectral analysis of Boc protected 1-Amino-3,6,9-trioxaundecanyl-11-ol (6)

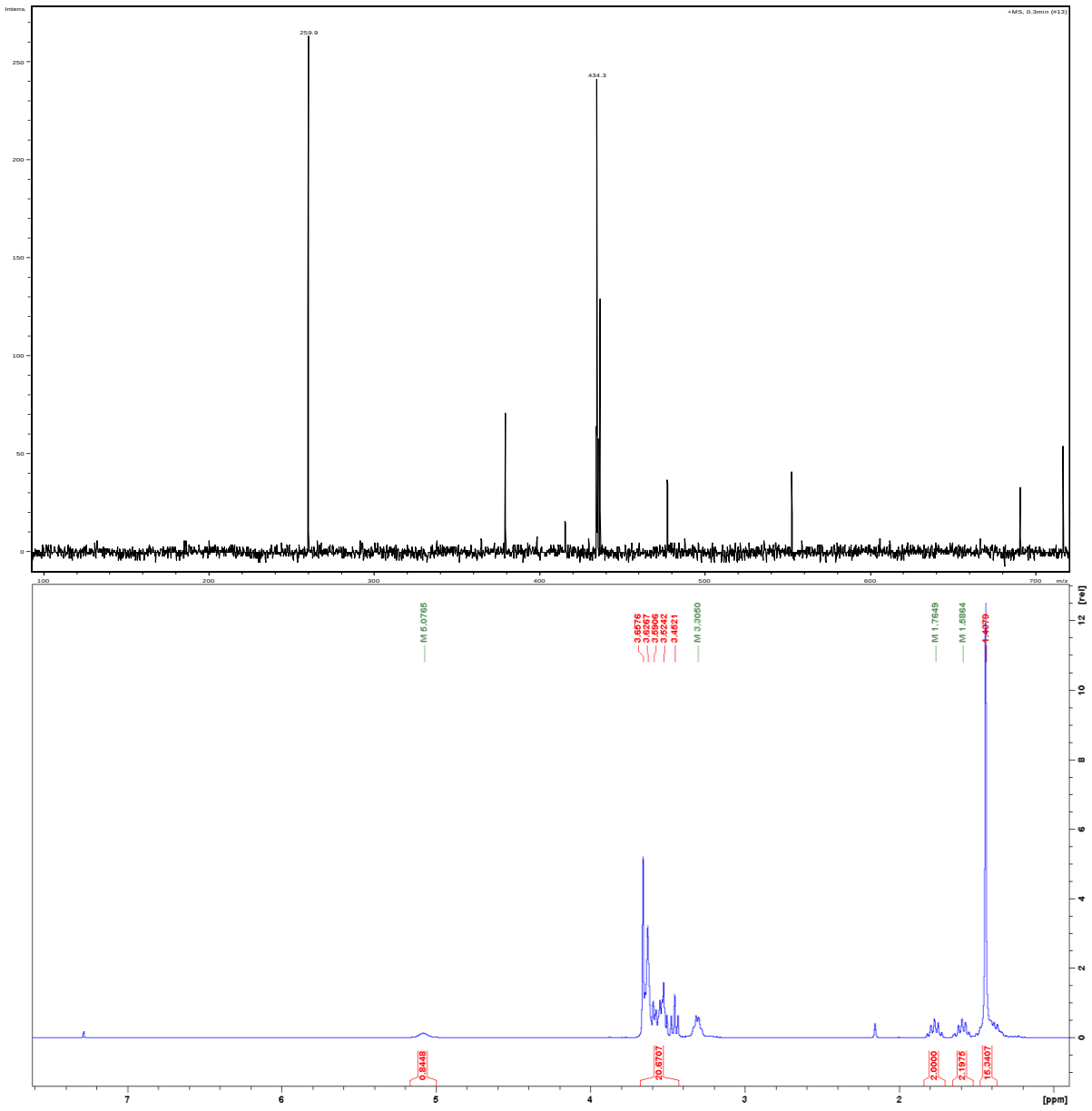

Figure 3.5 Mass spectrum and ^{1}H NMR spectrum of Boc protected 18-Chloro-3,6,9,12-tetraoxaoctadecan-1-amine. Intermediate was isolated but not shown in reaction scheme.

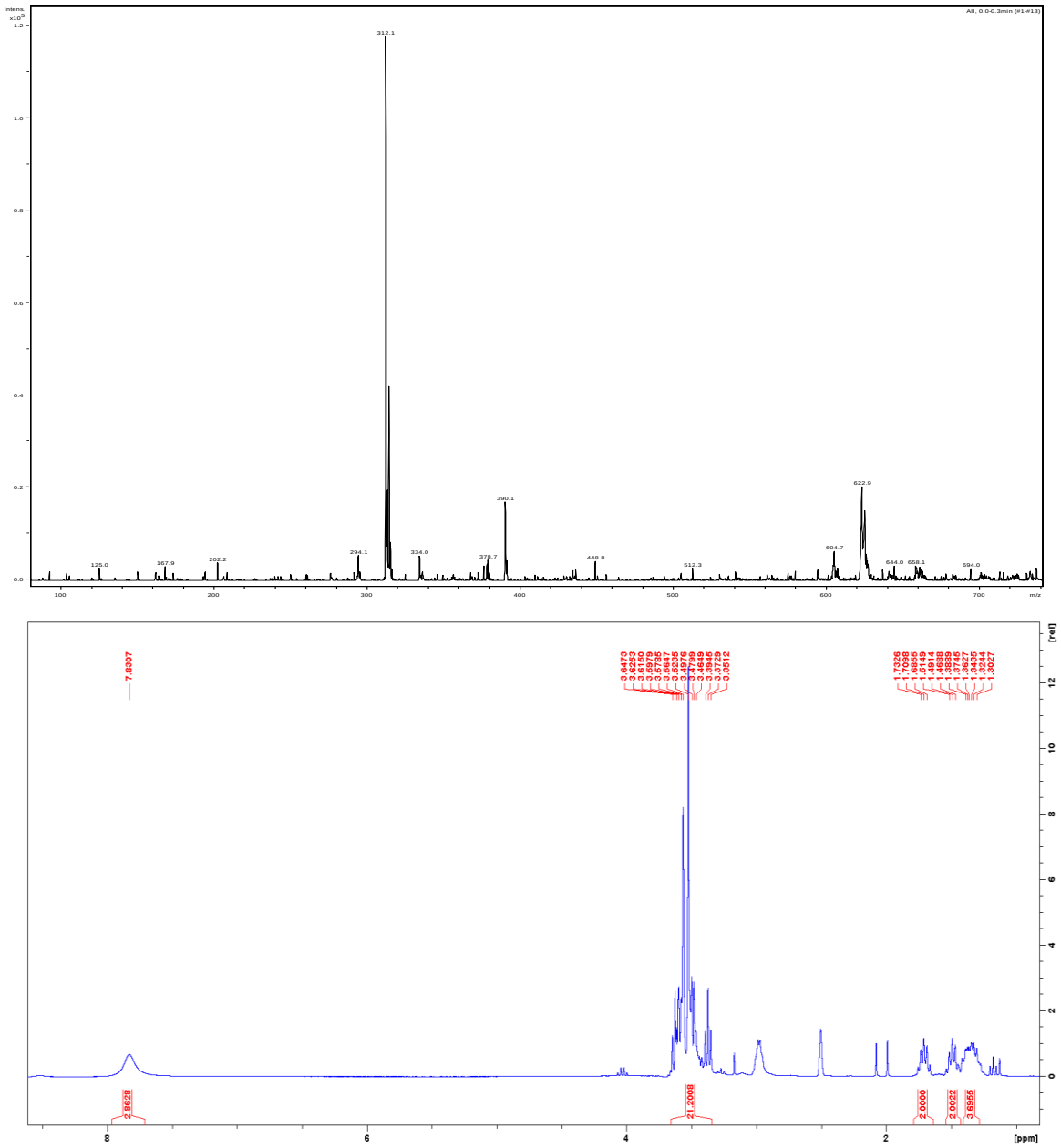

Figure 3.6 Mass spectrum and ^{1}H NMR spectrum of 8. Spectral analysis of 18-Chloro-3,6,9,12-tetraoxaoctadecan-1-amine (8)

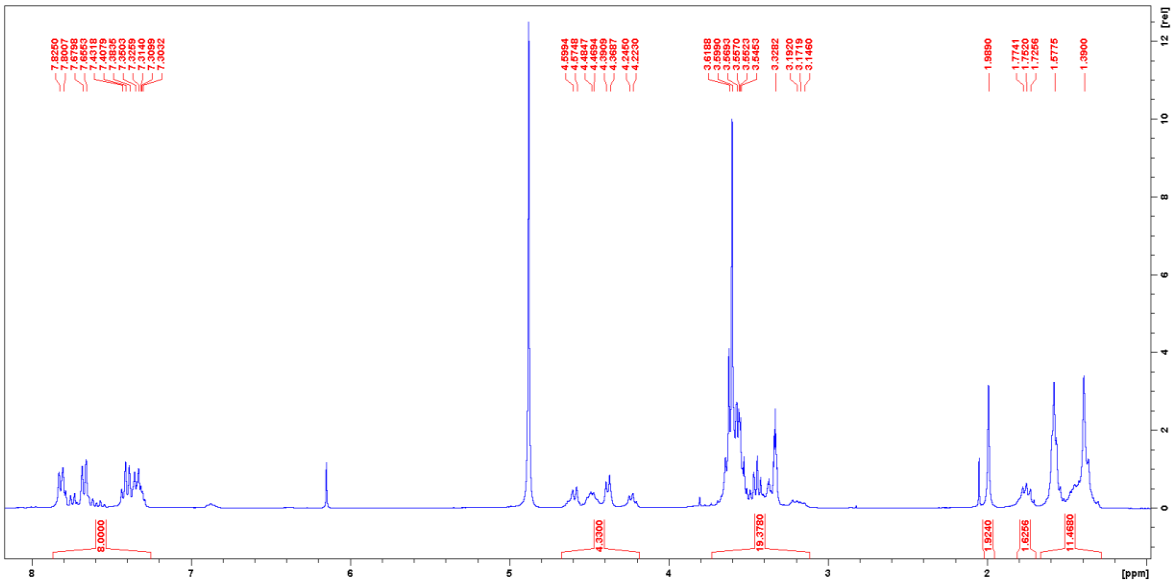

Figure 3.7 ^{1}H NMR spectrum of 9. Spectral analysis of Fmoc-diol protected HaloTag capture linker (9)

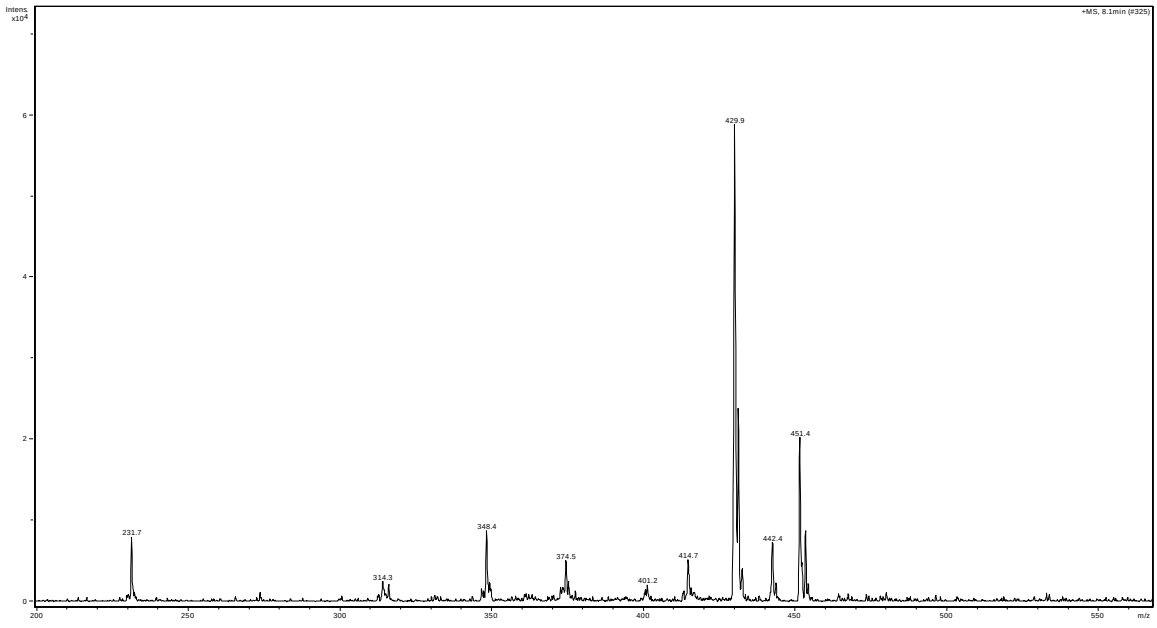

Figure 3.8 ^{1}H NMR spectrum of 11. Spectral analysis of HaloTag capture cleavable linker (11)

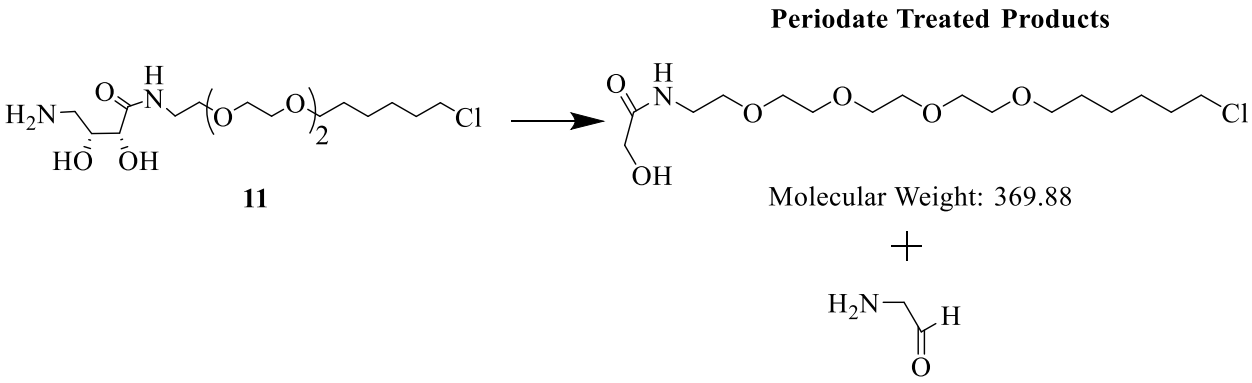

Figure 3.9 Periodate treatment of 11. Cleavage products after treatment of **11** with periodate are shown.

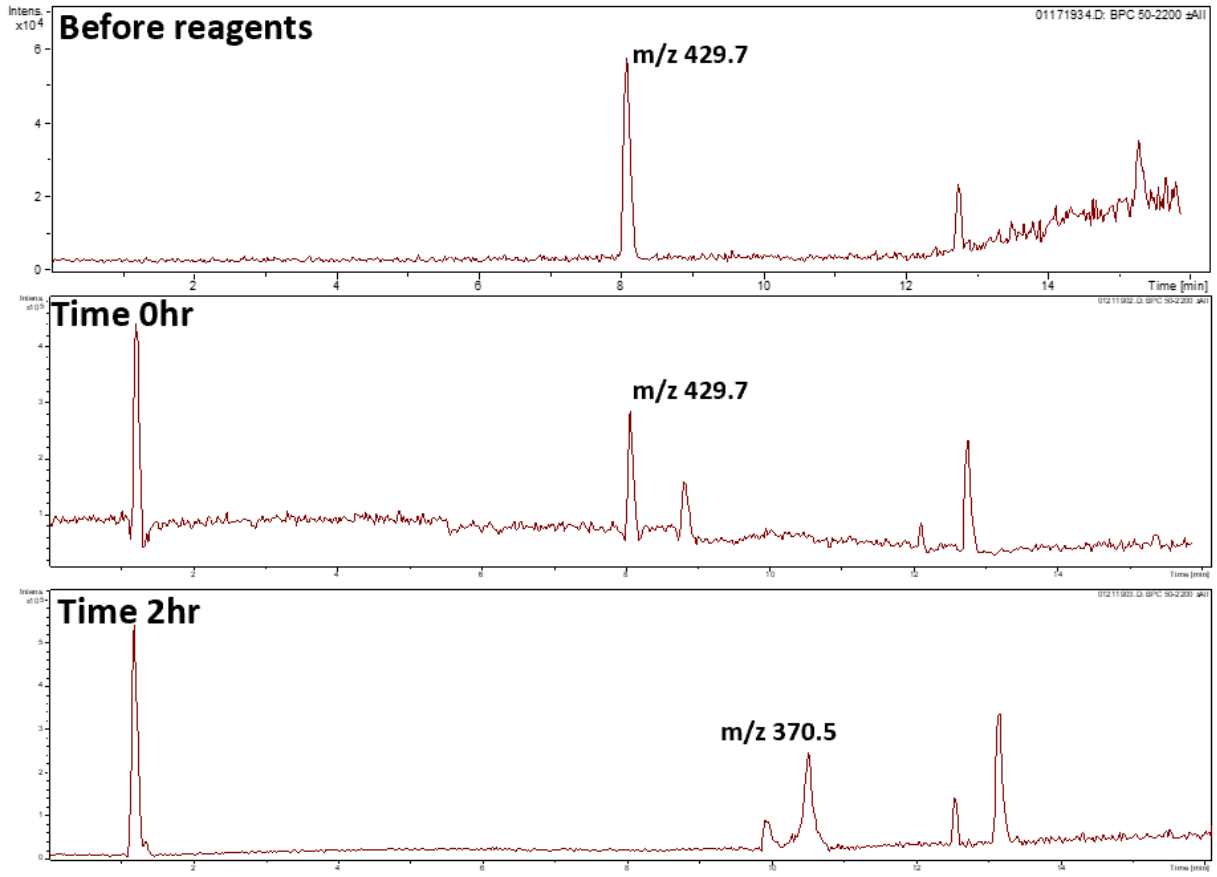

Figure 3.10 Time course of HaloTag capture cleavable linker (11) with periodate. Time points were analyzed by mass spectra for the disappearance of starting material (m/z 429.7) and formation of expected cleavage product (m/z 370.5).

Chapter 4: Multiplexing Assay Development and Application

Multiplexing Technology

Multiplexing capabilities

As described in previous chapters, multiplexing technology is a relatively new tool with the potential to be highly effective in sera analysis. The ability to multiplex using unique microspheres makes it possible to interrogate multiple antigens of interest simultaneously against a patient sample. The Luminex company has developed polystyrene microspheres that are internally dyed with precise amounts of two distinct fluorochromes. The dyes have unique emission profiles which produce spectral characteristics for the individual microsphere regions (or bead sets).[69] Using these bead sets and a specialized instrument (BioPlex200) it is possible to carryout simultaneous detection of multiple analytes in a single well of a 96-well plate, reducing time labor and cost of an assay.

Advantages of multiplexing technologies

A detailed comparison of traditional protein microarrays and novel multiplexing assays was made earlier in the Antigen Prioritization section of the introduction. With the goal of developing a technically advanced system for investigating antibody responses in malaria patient serum we find that the multiplexing system is best equipped. Some key advantages of using the multiplexing system are briefly reviewed here. The first advantage is that these technologies provide streamlined assay preparation. With the multiplexing system, a spectrally unique bead set of one million beads is coated with antigen in a single step which takes less than three hours. Once prepared, these beads can serve in over 300 single well reactions, or more specifically can be interrogated against over 300 different patient sera. The unique spectral properties of the bead

sets allow for multiplexing capabilities in which 100 different bead set-antigen pairs can be simultaneously analyzed in a single mixture while using minute amounts of patient sample. Furthermore, unlike protein microarrays multiplexing assays allow for antigen-antibody binding interactions to occur in a more native environment where multiple antigens are present during the binding event. The biggest drawback of traditional protein microarrays is the chemistries used to adhere antigens to the slide surfaces. Antigens are printed directly to nitrocellulose slides from translation lysates, raising possible nonspecific antibody reactivity. Direct printing on slides leads to the antigens being presented on the slide surface in a random orientation. Random printing can lead to proteins losing the ability to bind to antibodies, either because of epitope masking or loss of binding function.[56, 65-66, 79] For these reasons there has been a shift to investigate serum antibody profiles using bead-based fluidics systems.[76, 116] Lastly, the expansive bead chemistries of this platforms allow for custom assay development based on the needs of the study. Given these advantages we choose the BioPlex multiplexing platform to develop the highest quality array system possible.

Chemistries for Luminex bead modification

Many in the malaria field have applied multiplexing technologies to study naturally acquired immunity (NAI) in patient sera.[70, 76, 116-117] Designing multiplex assays for NAI investigation requires that antigens of interest be expressed and coated onto the spectrally unique bead sets. This entails chemically linking or capturing antigens onto the beads to form a stable bead-antigen complex. All reported methods of multiplex studies follow manufacturer protocols of bead modification, given by the bead manufacturers.[75-78] In these modifications, carboxylated bead sets are modified with purified antigens or peptide fragments of antigens. These antigens are coupled to the beads using standard carbodiimide chemistry utilizing 1-Ethyl-3-(3-

dimethylaminopropyl) carbodiimide (EDC) and N-hydroxysulfosuccinimide (Sulfo-NHS) as shown in Figure 4.1A. One major disadvantage of this method is antigens must be first purified and then coupled to the beads. This adds a tremendous amount of time to development of an assay. Malaria protein expression and purification has long been a bottleneck in antigen prioritization (discussed in detail in Chapter 2). Many of the malarial antigens which are targets of NAI are surface exposed and membrane bound proteins which makes them challenging to isolate in their pure forms. Further, from my reported results in Chapter 2 we see that a single purification scheme applied to several different proteins does not necessarily produce the same results. Using the optimized purification methodology, we see in one instance a clean and pure antigen can be isolated whereas under the same conditions for another antigen we observe lower purity of the isolated product (Figure 2.5 & 2.8). When the goal is to have a streamlined method for bead modification, optimizing purification for each antigen of interest would take a tremendous amount of time. Another major disadvantage of protein capture using the standard EDC/Sulfo-NHS chemistry is non-uniform presentation of the antigens. Not only does this non uniform presentation lead to variations in epitope recognition by patient serum antibodies, the carbodiimide chemistry coupling can also lead to antigens losing their ability to recognize epitopes completely. When activated amines are in nearby proximity on a protein there is the potential for both amines to couple to the bead surface. It has been reported that the coupling of a single protein at multiple locations can mask or loose the epitope binding capabilities through protein unfolding.[66] Based on the tremendous labor and potential variation or loss of antibody binding we found it necessary to identify additional bead modification chemistries that may be better suited for high-throughput multiplexing assay development.

Bead modification with HaloTag linker

The first alternative multiplexing bead chemistry considered was the HaloTag capture linker. As discussed in Chapter 2, HaloTag is a modified dehalogenase which can covalently capture chloroalkane derivatives. It had been previously reported that a Promega marketed HaloTag capture linker could be chemically modified onto carboxylated Luminex bead sets to form multiplexing beads which have the ability to capture HaloTagged fusion proteins.[118] One drawback described in the literature was that the marketed HaloTag capture linker did not have a feature which allowed for cleavage off the beads once proteins were captured. The ability to recover protein complexes once captured on the bead would serve as a control when designing multiplexing assays. With many of the current assays, once proteins are on the beads the scientist is "blind" to the chemistry occurring on the beads. Cleavability of the linker would allow use to understand how well the beads are being modified before we start detecting for downstream signals. Additionally, cleavability of a linker would allow for functional characterization of bound antigens after completion of an immune assay. This would ensure that antigens retain proper folded structure throughout the entirety of an assays. To address this, we developed and synthesized a HaloTag capture linker which could be chemically linked to the multiplexing beads but also can be cleaved from the beads with periodate treatment. The design and synthesis of this linker is discussed in detail in Chapter 3. A schematic representation of how this cleavable HaloTag linker could be used with the multiplexing beads is shown in Figure 4.2. The highly selective nature of the HaloTag capturing ability makes this a well-suited chemistry for recombinant protein capture directly from in vitro translation lysates. As discussed in Chapter 2, the Rathod lab utilizes the wheat germ cell free expression system for malaria protein expression. After translation using this system, we are left with a mixture of expressed protein of interest

along with a high level of background wheat germ proteins. Separating the single protein of interest usually means one must carry out an affinity purification step as discussed in Chapter 2. With the assay design shown in Figure 4.1B it is possible to capture the HaloTagged antigen of interest directly from the wheat germ lysate onto the multiplexing beads. This is a time saving step making high-throughput assay design more feasible. For this reason, we pursued the chemical modification of the multiplexing beads using HaloTag capture linkers.

Bead modification with anti-C-tag antibody

A second multiplexing bead chemistry that was considered was an epitope capturing antibody. As discussed in Chapter 2 the C-tag is a four amino acid epitope which is selectively recognized by a camelid antibody (NbSyn2). We have previously shown C-tagged antigens can be isolated in high purity using capture columns coated with these camelid antibodies. Based on these purification results it seemed probable that we could exploit the C-tag antibody capturing ability on the multiplexing bead surfaces. By chemical modification of the multiplexing beads with Anti-C-tag antibodies we developed an assay in which C-tagged proteins can be directly captured from the wheat germ lysate (Figure 4.3C), similar to the HaloTag linker scheme. Again, this type of chemical modification allows for a single step protein capture from lysates, onto the pre-modified beads. After this capture step beads can be directly used in the multiplexing assays. This greatly simplifies the assay development making high-throughput multiplexing a possibility.

All three of the discussed chemical modifications were attempted on the multiplexing beads. The aim of this work was to determine which chemical modification strategy resulted in the most reproducible, least laborious, and most high-throughput methodology for multiplexing. As such, a reliable multiplexing assay is critical for future studies of NAI in malaria patients.

Experimental Section

Direct coupling of antigens to beads. The covalent coupling of C-tag purified proteins to carboxylated magnetic Luminex microspheres by carbodiimide chemistry was done under standard Luminex Cookbook instructions with minor changes. All bead chemistry was done in LoBinding microcentrifuge tubes and magnetic beads were separated by using a MagneSphere magnetic separating stand (Promega). Briefly, $7.5x10^5$ beads from color region 21 were washed once with sterile deionized water followed by two washes with 0.1 M MES pH 4.5 activation buffer (50 µL wash volumes). After each wash beads were vortexed and sonicated for twenty seconds. After washing, 26.5 µL activation buffer was added to beads and they were again vortexed and sonicated for 20 seconds. Sulfo-NHS was added (3.3 µL 50 mg/mL) followed by a brief vortex of beads. Steps were repeated with EDC addition (3.3 µL 50 mg/mL). The microcentrifuge tube with beads was set in a drawer to protect from light. Every five minutes the tube was gently vortexed and then placed back in dark. After 25 minutes of activation the beads were washed two times with 0.1 M MES pH 4.5.

The nature of the direct coupling experiments allows for small scale bead modification to minimize reagent waste. Thus, activated beads were aliquoted into 96-well plate wells at a working concentration of 3000 beads/well with the activation buffer. Once beads were added to the wells they were washed once with 0.1 M MES 5.0. All washes in 96 well plates were done by using an IKA MS3 plate mixer at 800 rpm followed by BioRad magnetic plate separator. Plates were clipped in and placed in a dark drawer for 90 seconds followed by one forceful inversion of the plate to remove liquids from the wells. C-tag purified proteins were added at various concentrations (ranging from 0-15 µg/mL) with 0.1M MES pH5.0 coupling buffer. Working reaction volumes were 100 µL. Proteins were captured at a minimum of two hours.

CaptureSelect biotinylated anti-C-tag conjugate (ThermoFisher 7103252100) were used at a titer of 1:1000 and bound for one hour at a working volume of 100 µL. Following primary antibody binding, beads were washed three times for ten minutes each using PBS, 0.1% BSA. Secondary streptavidin phycoerythrin conjugate (SAPE) was incubated at a titer of 1:100 for 30 minutes followed by a single three-minute wash. Beads were resuspended in 100 µL wash buffer and read on a BioPlex 200, set to read 50 beads from each bead region.

Conjugation of HaloTag linkers to Luminex beads. Bead activation was done similarly to the methods described above. Briefly, $8.3x10^5$ beads were activated with 26.4 µL of 0.1M MES pH 4.5 and 3.3 µL of Sulfo-NHS and EDC (50 mg/mL). After a twenty-five-minute incubation in dark with periodic vortexing the beads were washed twice with the activation buffer at pH 4.5. Various coupling buffers were tested for optimal HaloTag linker coupling. Best results were obtained using coupling buffer of PBS pH 7.4 or 0.1M Boric Acid pH 8.5. All washes were done in 50 µL volumes with 20 seconds of vortexing and sonication. After washing beads were resuspended in the activation buffer and split evenly into two new microcentrifuge tubes. Buffer was removed and replaced with 100 µL of each coupling buffer. At this step the chemical HaloTag capture linker was added (0.165 mg in 10%DMSO). Two linkers were tested (1) purchased capture linker O4 (Promega) and (2) the synthesized capture linker from Chapter 3. After the HaloTag capture linker addition, the beads were gently vortexed and sonicated for ten seconds followed by a two-hour incubation in the dark with rotation. After incubation, beads were washed three times with PBS-TBN (PBS, 0.1% BSA, 0.02% Tween20, 0.05% Azide). Beads were placed in a final volume of 300 µL and stored in PBS TBN at 4 °C. Final bead number per microliter was determined using a hemocytometer.

Capture of purified HaloTag protein with linker modified beads. The Luminex microspheres coupled with HaloTag linkers were verified for bead modification using purified HaloTag protein. Purchased HaloTag standard protein (Promega) was incubated with the modified HaloTag capture beads at various concentrations. Briefly, 3000 beads were added to each well. Beads were washed once with PBS. HaloTag standard protein was added at 0, 0.25, 2.5, and 25 µg/mL with PBS buffer to a working volume of 100 µL. Plate was agitated on a plate shaker for two hours, allowing for HaloTag protein to capture to chemical linkers. Beads were washed once with 100 µL of PBS, 1% BSA (wash buffer). Primary antibody, anti-HaloTag antibody (Promega), was incubated one hour at 1:500 titer. Beads were washed three times, 2 minutes each, with wash buffer. An anti-mouse phycoerythrin secondary antibody, at a 1:330 titer, was incubated for 30 minutes followed by a single wash. Beads were resuspended in 100 µL wash buffer and read on a BioPlex 200, set to read 50 beads within each bead region.

Capture of HaloTagged fusion proteins directly from wheat germ lysate. The Luminex microspheres coupled with HaloTag linker O4 were tested for their ability to capture HaloTagged proteins directly from the wheat germ translational lysate. Briefly, 3000 of the linker modified beads were distributed to each well of a 96-well plate. Beads were washed once with binding buffer (PBS, 5 mM DTT, 0.05% TritonX-100). Translation lysates were added directly to wells at various volumes ranging from 0-200 µL. Total working volume in all wells was adjusted to 200 µL with binding buffer. Plate was shaken at 300 rcf on plate shaker for two hours in dark. Beads were washed three times with 100 µL binding buffer, five minutes each with shaking. HaloTag was probed using anti-HaloTag antibodies at 1:500 for one hour. Following two washes, anti-mouse phycoerythrin antibodies were added for 30 minutes at 1:330

titer. After a quick wash, beads were resuspended in 100 µL wash buffer and read on a BioPlex 200, set to read 50 beads from each bead region.

Conjugation of Anti C-tag antibodies to Luminex beads. Luminex carboxylated beads were covalently coated with CaptureSelect Anti-C-tag antibodies (ThermoFisher 7103252100) following the standard cookbook procedure with minor adjustments. For all bead activation and coupling steps, buffers were first filtered with a 0.2 µm filter. $1x10^6$ beads of region 21 were placed in a low binding centrifuge tube (Eppendorf LoBind 25000). Beads were washed once with deionized water and then twice with 0.1 M MES pH 4.5, each with 50 µL. After each wash beads were vortexed and sonicated for 20 seconds. Magnetic separator stand was used to pellet beads (Promega MagneSphere Magnetic Separation Stand). Tubes with magnetic bead suspensions were allowed to sit on stand for 90 seconds. After washes, 26.4 µL of 0.1 M MES pH 4.5 was added. Beads were vortexed and sonicated. Sulfo NHS (3.3 µL at 50 mg/µL) was added and tube was gently vortexed followed by EDC addition (3.3 µL at 50 mg/µL). Activation reactions were placed in a dark drawer and gently vortexed every five minutes for 25 minutes. Activated beads were washed twice with 0.1 M MES pH 5.0, 50 µL each. Separately, Anti-C-tag antibodies were mixed with 0.1 M MES pH 5.0 buffer at various concentrations to find optimal antibody concentration needed for saturated coating. Concentrations tested were 0, 2.5, 3.5, 5, 50, and 100 µg/$5.0x10^5$ beads. Optimized conditions were found to be 100 µg of Anti-C-tag antibody mixed with 150 µL 0.1 M MES pH 5.0 (0.4 µg/µL). This solution was added to the activated beads and let incubate with end to end rotation in the dark for two hours. After incubation, beads were washed with freshly mixed PBS-TBN (PBS, 0.1% BSA, 0.02% Tween20, 0.05% Azide).

Detection of Anti-C-tag antibody on beads using SAPE. After beads were coated with anti-C-tag antibodies they were tested for degree of coating. The anti-C-tag antibodies purchased from ThermoFisher contain biotin. To detect the biotinylated antibodies sitting on the beads, streptavidin R-phycoerythrin conjugate (SAPE, ThermoFisher S866) was used. Beads were distributed to 96 well flat bottom plates (Bio-Plex Pro 171025001). Each well contained 3000 beads. Beads were washed once with 100 µL of assay buffer (PBS, 0.1% BSA). For washes, plates were shaken on an IKA MS 3 basic plate shaker at 800 rcf followed by a 90 second magnetic bead settling on the Bio-Plex handheld magnetic washer. Serial dilutions of the SAPE conjugate were made between 1:10 to 1:50,000. To each well 100 µL of titer was added and incubated for 30 minutes with shaking at 800 rcf in the dark. After incubation beads were washed once for three minutes. Beads were resuspended in 100 µL assay buffer and read on a BioPlex 200, set to read 50 beads from each bead region.

Capture of purified C-tag proteins with anti-C-tag antibody coated beads. The anti-C-tag antibody bead complex, in different bead regions, was separately incubated with a C-tagged protein of interest. To verify bead complex formation, C-tag purified *Pf* MSP1-42 and GFP were captured on the beads. For microscale experiments, capture was done directly in the well of a 96 well plate. In each well, 3000 beads were added and washed once with binding buffer (20 mM Tris pH 7.5, 100 mM NaCl). C-tag purified proteins were added at various concentrations. Working volumes were adjusted to 100 µL with binding buffer. Beads were incubated with proteins for two hours in the dark with shaking at 800 rcf. After incubation beads were washed three times for 10 minutes each with assay buffer (PBS, 0.1% BSA). Primary antibody raised against rabbit *Pf* MSP1-42 was incubated for one hour at a titer of 1:2000. Beads were washed three times for 10 minutes each with assay buffer. Anti-rabbit phycoerythrin antibody

(ThermoFisher P-2771MP) was incubated for 30 minutes at a 1:500 titer followed by a single three-minute wash step. Beads were resuspended in 100 µL assay buffer and read on a BioPlex 200, set to read 50 beads from each bead region.

Scale up of protein capturing was later done with $3.0x10^5$ number of anti-C-tag coated beads. Beads were placed in LoBinding tubes and washed twice with binding buffer (20 mM Tris pH 7.5, 100 mM NaCl). Separately, a mixture of 750 ng of purified C-tag *Pf* MSP1-42 or GFP was adjusted to a final volume of 500 µL with binding buffer (1.5 µg/µL). This mixture was added to beads and incubated in dark with end to end rotation for two hours. Beads were washed with freshly prepared PBS-TBN three times with 500 µL, 10 minutes each. Beads were resuspended in 150 µL and final bead count was determined with hemocytometer counting.

Capture of C-tag proteins directly from wheat germ translation with anti-C-tag antibody coated beads. Capture of C-tagged proteins directly from the wheat germ lysate was done similarly to capture of purified C-tag proteins. Initial capture experiments were done on a microscale as with purified proteins. Wheat germ translations of C-tag *Pf* MSP1-42 and GFP were captured on the beads. For microscale experiments, capture was done directly in microtiter wells. In each well, 3000 beads were added and washed once with binding buffer (20 mM Tris pH 7.5, 100 mM NaCl). Lysates were added at various volumes from 0-200 µL. Final working volumes were adjusted to 200 µL with binding buffer. Beads were incubated for two hours in the dark with shaking at 400 rcf. Contrarily, large scale capturing from wheat germ translations was done using one million beads per bead set. Lysate volumes of 5mL were centrifuged at 15,000 rcf for 10 minutes at 4°C. Translation supernatant (5mL) was added to the beads along with 10mL of binding buffer (20 mM Tris pH 7.5, 100 mM NaCl, 0.05% TritonX-100) in a 15 mL Eppendorf tube. Beads were incubated in the dark with end to end rotation for two hours. Beads

were spun at 4,000 rcf for five minutes. Beads formed a small brown pellet and the top 14 mL of supernatant was carefully removed. The final 1mL with beads was transferred to a LoBinding microcentrifuge tube and bead were washed three times with PBS-TBN. Beads were finally stored in PBS-TBN at 4°C.

After incubation, beads were treated just as with purified C-tag antigens (see previous). For bead capture verification rabbit anti *Pf* MSP1-42 antibody was used. Antibodies were incubated for one hour at 1:2000 titer, followed by three washes. Anti-rabbit PE antibody was incubated at 1:500 titer for 30 minutes followed by a single wash. Beads were resuspended in 100 µL assay buffer and read on a BioPlex 200, set to read 50 beads from each bead region.

Plasma sample collection. Patient samples were collected as part of a US National Institutes of Health-sponsored project called Malaria Evolution in South Asia-International Center of Excellence for Malaria Research (MESA-ICEMR). Plasma samples were collected from symptomatic malaria positive patients at Goa Medical College (GMC, India). Written informed consent was obtained from all volunteers. A detailed description of the study site, enrolment and sample processing has been elsewhere published.[119]

Singleplex serum analysis using malaria antigen coated beads. Anti-C-tag antibody coated beads were used for analysis of immune responses in patient sera. After modification and protein capture, beads were distributed in wells at 2000 beads/well in triplicate. Beads were washed twice with assay buffer (PBS, 0.1% BSA). Optimal serum titer was first determined by titration of a single serum with protein coated beads. Titers tested ranged from 1:50 to 1:1500. Working volumes of 100 µL were added to each well. Bound serum antibodies were detected using anti-human IgG-R phycoerythrin conjugate (Sigma P8047). Secondary antibody was incubated for 30 minutes at a titer of 1:500 at a working volume of 100 µL.

Multiplex serum analysis using malaria antigen coated beads. To test the ability of the multiplexing platform designed, 7 malaria patient plasma samples were tested against malaria antigens and a control and immune responses was measured by the BioPlex-200. Different microspheres were separately coated with recombinant *Pf* MSP1-42, *Pf* AMA1, and GFP. A working stock of 100 beads/µL/bead set was made using PBS-TBN. To each well 20 µL of the working stock was added (2000 beads/bead set). Beads were washed once with PBS, 0.1% BSA. Patient plasma samples were added in triplicate at various titers (0, 1:2000, 1:1500, 1:100, 1:500, 1:200, 1:100, 1:50) with a working volume of 100 µL. Bound serum antibodies were detected using anti-human IgG-R phycoerythrin conjugate (Sigma P8047). Secondary antibody was incubated for 30 minutes at a titer of 1:500 at a working volume of 100 µL.

Results

Purified antigen bead modification

For comparison, the traditional method of bead modification using purified protein of interest was done. This method uses carbodiimide chemistry and is represented in Figure 4.1A. Both *Pf* MSP1-42 and control GFP were purified from C-tag columns for the assay. Various concentrations of the purified proteins were added to activated carboxylated beads for amine coupling. Once coupled to beads, antigen coupling levels were determined using anti-C-tag antibodies and a streptavidin PE conjugate. A protein concentration dependent curve is generated in which increasing protein concentration leading to increased mean fluorescence intensities (MFI). There is no significant difference in signal when comparing *Pf* MSP1-42 or GFP coupled assays indicating the coupling efficiency is reproducible from protein to protein. Saturation is observed around 4000 MFI in these microscale experiments. This saturation is reached as low as 8 µg/mL of purified protein.

HaloTag linker bead modification

Bead modification with HaloTag capture linkers was carried out as shown in Figure 4.B. Using carbodiimide chemistry, the carboxylated beads were modified with free amine HaloTag capture linkers. Both linkers tested are shown in Figure 4.3 coupled to the carboxylated multiplexing beads. In Figure 4.3A the linker used was purchased from Promega and in Figure 4.3B the linker was synthesized. Synthesis of this linker is discussed in detail in Chapter 3. Chemical linker capturing was carried out similar to purified protein capture but with some modifications. Beads were activated under identical conditions however coupling of the chemical linker was tested with various buffers and pHs. Coupling was tested with MES pH 4.5, PBS pH 7.4, and boric acid pH 8.5. After coupling, bead modification efficiency was tested by capture of HaloTag standard protein (purchased from Promega) and anti HaloTag antibodies were used for detection. With either chemical linker, concentration dependent MFI signal was only observed when PBS pH 7.4 or boric acid pH 8.5 was used for coupling. Figure 4.3 shows with increasing HaloTag standard protein we see an increase in MFI for both chemical linkers. However, under identical HaloTag standard protein concentrations the purchased chemical linker (Figure 4.3A) gives a maximum signal at 1000 MFI while the synthesized linker gives a maximum signal of 32 MFI (Figure 4.3B). HaloTag protein concentrations tested were 0, 0.25, 2.5, and 25 µg/mL however MFI signals did not correlate.

Subsequent microscale experiments were carried out using the Promega purchased linker modified beads due to the observed difference in signals between purchased and synthesized linker bead modifications. The purchased chemical linker modified beads were used for capture of HaloTag expressed proteins directly from wheat germ translation lysates. Beads were incubated with various volumes of wheat germ lysates of both HaloTag *Pf* MSP1-42 and C-tag

GFP control. Anti HaloTag antibodies were used for detection. In Figure 4.4 a volume dependent MFI signal is observed in the HaloTag *Pf* MSP1-42 curve but not in the C-tag CFP curve. At 200 µL WG lysate/3000 beads a three fold difference is observed between HaloTag *Pf* MSP1-42 and C-tag GFP.

Anti-C-tag antibody bead modification

The final method tested for bead modification was to coat beads with anti-C-tag antibodies. Anti-C-tag antibodies were coupled to carboxylated multiplexing beads using the same carbodiimide chemistry as discussed for purified protein capture. Beads were modified with various concentrations of anti-C-tag antibody to determine optimal antibody concentration needed for maximum signal. Figure 4.5 shows the MFI curves of bead sets modified with various concentrations of anti-C-tag antibody. Concentrations ranged from 0.05-5 µg/50,000 beads. The C-tag antibodies were biotinylated thus antibodies coated on beads were detected using streptavidin PE conjugate (SAPE). From Figure 4.5 it was shown that as anti-C-tag concentration was increased, signal representative of antibody coating also increased.

Next, the ability to capture C-tag proteins using the anti-C-tag antibody coated beads was assessed. First, purified *Pf* MSP1-42 and GFP were captured on modified bead sets at various concentrations ranging from 0-15 µg/mL. Rabbit-anti *Pf* MSP1-42 antibody was used for detection followed by an anti-rabbit IgG PE conjugate. Figure 4.6A-D shows the MFI curves of bead sets modified with various anti-C-tag antibody concentrations. Using bead sets modified with no anti-C-tag antibody both *Pf* MSP1-42 and GFP MFI signals remain at background levels at all tested protein concentrations. As bead coated antibody concentration increases there is an observed increase in *Pf* MSP1-42 signals and significantly less so of GFP. The highest MFI signal difference between *Pf* MSP1-42 and GFP is observed at 50 µg/500K beads (figure 4.6D)

with almost fivefold increase in signal between the two at 2.5 µg/mL protein concentration. An observed MFI signal decrease at high concentrations of *Pf* MSP1-42 is observed in figure 4.6C&D. After anti-C-tag coated beads were tested with purified proteins they were used to asses protein capture ability directly from wheat germ lysate. In figure 4.7 various wheat germ (WG) lysate volumes (0-200 µL) were incubated with bead sets in microscale experiments. Again, where 0 µg of anti-C-tag antibody is coupled to beads both *Pf* MSP1-42 and GFP MFI signals remain at background levels at all tested WG lysate volumes (Figure 4.7A). However, as beads are coated with increasing anti-C-tag antibody MFI signals for *Pf* MSP1-42 increases but MFI signal for GFP remain at or near background levels (Figure 4.7B-D). From Figures 4.7B-D MFI signal saturation is observed at the lowest WG lysate volume tested, 20 µL/well. Unlike the purified protein curves, there is little to no signal decrease at high WG lysate volumes. Instead, a relatively flat line is observed in all the curves.

From Figure 4.6 and 4.7 we observed MFI saturation signals at the lowest concentrations tested. Thus, we felt it was necessary to try and titrate both purified protein and WG lysate at lower concentrations to try and determine the true limit of detection for the C-tag capture assay. Figure 4.8 shows both MFI curves of purified protein and WG lysates of *Pf* MSP1-42 and GFP. There is an observed increase of MFI as concentration of purified protein is added to each reaction well (Figure 4.7A). Signal for *PF* MSP1-42 continually increases until the highest concentration tested, 1500 pg/µL while signal for GFP remains near background levels with a slight increase. In Figure 4.8B there is also an observed increase in MFI signal as volume of WG lysate is increased/well for *Pf* MSP1-42 but not for GFP. GFP MFI signals remain at background levels at all volumes of WG lysate tested. For *Pf* MSP1-42 saturation levels are observed at volumes as low as 15 µL lysate/well. That correlates to 0.68 µL of original wheat germ lysate

used in the translation reactions. By comparison of Figure 4.8 A&B we see that the MFI signals observed do not vary between the use of purified protein capture or protein capture from WG translation lysates.

Further optimization of assay conditions included WG lysate incubation time and number of beads per reaction. In Figure 4.9, varying incubation times of antigen with anti-C-tag antibody coated beads were tested. Capture of C-tag proteins from lysate was monitored at 2 hours and 18 hours. For GFP there is no signal above background for either the 2 or 18-hour curves. Signal increase is observed with increasing volumes of WG lysate of *Pf* MSP1-42. When comparing the 2 hour and 18 hour binding curves of *Pf* MSP1-42 there is not a significant difference in response. A slight decrease in the 18-hour binding signal was observed at high volumes of WG capture. An additional condition tested was the number of beads per reaction well. A series of bead numbers was tested ranging from 500-3000 beads per well (Figure 4.10). In all reaction wells, 20 µL of WG lysates was added. There was no significant difference observed in MFI signal among the bead number tested. During reading of the beads on the BioPlex 200 instrument there was consistently more sampling errors for the low bead reactions (500 and 1000 beads). Sampling errors observed included (1) low bead count (2) bead aggregation detection and (3) classification problem. As bead numbers in the wells increased the likely hood of sampling errors decreased.

Singleplex of human plasma antibody response against *Pf* MSP1-42

The next step in the multiplex assay development of patient sera was to test human plasma samples. Optimization of patient sera titer was first assessed. Two patient plasmas were selected for titration experiments. Patient 42 had previously shown high immune response to *Pf* MSP1-42 and patient 37 had showed low response to *Pf* MSP1-42.[79] Beads were coated with

purified *Pf* MSP1-42 or GFP. Serum titrations were done in a range of 0-1:50 titers against each patient (Figure 4.11). Patient 42 showed MFI signal saturation at 1:200 titer followed by a drop off of signal at higher titers (Figure 4.11A). The control plasma from naïve plasma donors showed similar signal to the GFP background. Patient 37 plasma titer (Figure 4.11B) showed significantly less MFI signal as expected from previous protein array responses (Table 4.1). Unlike patient 42, antibody response for patient 37 decreased rapidly from 1:50 to 1:100 titer and this pattern continued as the titter decreased. In comparison of the MFI signals of patient 42 and 37 at 1:100 titer there is an observed 30-fold difference in signal. Similar analysis of patient antibody responses by protein arrays showed a signal difference of roughly 27-fold (Table 4.1).

Multiplexing of human plasma antibody response against multiple malaria antigens

Multiplexing capabilities of the methods described were tested using two different malaria antigens. Schematic of the assay workflow is shown in Figure 4.12. Unique bead sets coated with *Pf* MSP1, *Pf* AMA1, and GFP control were combined and multiplexed against nine different patient plasma samples along with a single malaria naïve patient. Each patient plasma immune response was tested at a variety of concentrations. Total immune responses from the multiplex assay along with previously reported protein array responses are listed in Table 4.2. GFP background control varied patient to patient representing a range of 170-1194MFI. Few patients showed an immune response above the GFP background control. Against the *Pf* MSP1 antigen patient 42 and patient 136 showed a significantly higher immune response (14 fold or higher). Against the *Pf* AMA1 antigen patient 42, 136 and 30 showed at least a twofold or more signal increase from GFP background. Patient 24 presented a borderline immune response, only slightly over the GFP background. Patient immune responses detected by the multiplexing BioPlex assay were directly compared with previously reported protein array data. Specifically,

the *Pf* MSP1 antigen responses were analyzed (Figure 4.13). By plotting raw bioplex signals versus the raw protein array signals a linear regression analysis can be done. First, signals from the protein array spot with unpurified *Pf* MSP1 was compared to bioplex results and a R^2 value of 0.891 was obtained (Figure 4.13A). For controls, the protein array work also included purified *Pf* MSP1 spots at two different concentrations, 0.1 and 0.3 mg/mL. The same patient immune responses to these purified spots resulted in a better correlation with the bioplex multiplexing results. Comparison of the 0.1mg/mL data versus the bioplex results gave a R^2 value of 0.986 and the 0.3mg/mL data versus the bioplex results gave a R^2 value of 0.994 (Figure 4.13 B & C).

Discussion

As discussed in Chapter 1, there remains a need for a high-throughput assay that can dissect the NAI of malaria patients. The gold standard of dissecting antibody responses has remained protein microarrays. While these traditional arrays have helped identify malaria-specific antibody responses as signatures of transmission and immunity, quality of antigens used on these arrays is questionable and researchers are limited to interrogating a single antigen-antibody interaction at a time. More recently, multiplexing capabilities have become possible and application of such technology to malaria patient immune responses could greatly streamline sera analysis while utilizing minimal precious sample.

Multiplexing using the BioPlex 200 system has previously been used for malaria patient immune response dissection.[70-71, 77, 116-117] Such systems utilize bead-based assays, where spectrally unique bead sets are modified with different malaria antigens of interest. All reports of malaria antigen multiplexing assays utilize the standard bead modification protocols given by the bead manufacturers (Luminex). In such protocols, each antigen is expressed, purified and individually coupled to bead sets. This can add a tremendous amount of time and labor to assay

development. As discussed in detail in Chapter 2, expression and purification of high-quality malaria antigens can be very challenging. As found in the case of just three malaria antigens, optimizing a single purification method and applying to multiple antigens does not always give the same levels of purity in isolated antigens. This forces purification optimization of each antigen of interest separately. Thus, for development of a high-throughput multiplexing assay, purification of every antigen multiplexed is nonideal. Instead, we proposed new chemistries and methods that could be used for the development of high-throughput multiplexing assays of candidate malarial antigens. Here we have compared three different multiplex bead modification and assay strategies: direct protein coupling, HaloTag capture linker coupling, and anti-C-tag antibody coupling.

In determining new bead chemistries for multiplexing assays, we carried out traditional antigen-bead coupling procedures. Antigens were first purified individually and coupled to beads for single plex assays. Here we observed that signal intensities did not depend on the antigen coupled, as both *Pf* MSP1-42 and GFP gave similar MFI curves. Furthermore, a high signal to noise ratio was observed (40-fold). The downside of this method is the need for individual antigen purification and preparation. This makes the assay unappealing wen working with high volumes of antigens.

The second bead modification tested with the multiplexing bead sets was HaloTag capture linker coupling. Previously reported literature utilized the HaloTag capture ability and multiplexing assays for the detection of antibody responses to tumor associated lung cancer antigens.[118] Here we tested two different HaloTag capture linkers: one purchased from Promega that is marketed as a HaloTag capture small molecule, and a second that was synthesized specifically for coupling to carboxylated beads with a HaloTag capture ability (Chapter 4). The

capture of a small molecule onto multiplexing beads was treated differently than the capture of purified proteins. Various coupling buffers at varying pH were tested to try and determine the best coupling conditions for these small molecules. Coupling was successful at higher pHs than with proteins. This is likely due to the relative reactivity of the free amine. For HaloTag capture linkers with a single free amine, it was necessary to increase pH from typical protein coupling pH of 5.0 to a nontraditional pH of 7.4 or 8.5. This ensured that the free amine was in a deprotonated state. The deprotonation favors reactivity with the activated carboxyl groups on the multiplexing beads. Proteins coupled at pHs above 7.4 showed a decrease in coupling efficiency. This is likely because at high pH, stability of carbodiimide intermediate decreases and lead to increased rate of hydrolysis of carboxyl sites. However, under the same coupling conditions, the purchased linker gave a signal to noise ratio of 33 while the synthesized linker gave a signal to noise ratio of roughly 1.4. The difference in coupling efficiency between linkers could be due to inefficient quantity of synthesized linker utilized. Purity of synthesized linker is likely not a problem as LC MS was done on all synthesized linker fractions tested. However, the reasoning behind the failure of synthesized HaloTag capture linker coupling to beads remains unknown. For direct capture from wheat germ lysate only the purchased HaloTag linker modified beads were tested. We found that with little as 20 µL of WG lysate there was a 1.5 fold difference in signal between sample and controls. This indicated that it is possible to modify beads with a HaloTag capture linker and capture HaloTag fused proteins directly from wheat germ lysate. This method acts as a "purification" step where antigens of interest can be separated from unwanted wheat germ background proteins. Although promising the bead modification using the purchased HaloTag capture linker proved to be non-reproducible. Under identical conditions bead modification efficiency varied greatly. The non-reproducible nature of this protocol was

thoroughly investigated but the cause of experimental variability remains unknown. Purchase of new reagents, new buffer stocks, and adjusting scales did not afford positive results. Although this bead chemistry allowed for a streamlined method to separate antigens of interest from a complex translation mixtures it does not seem well suited in the application of high-throughput multiplex assay development due to the variations observed in bead modifications. These findings were surprising as others have reported the use of similar chemistries on carboxylated Luminex beads. However, only one other group has cited the use of the reported HaloTag capture chemistry since the initial development and publication in 2014.[120] This may be an indication of the unreliable nature of such bead chemistries.

The final bead chemistry that was tested for development of a high-throughput multiplexing assay was the coupling of anti-C-tag antibodies to beads. Similar to standard protein coupling procedures, antibodies are coupled directly to the multiplexing beads. These anti-C-tag antibody coated beads showed highly effective C-tag capturing, both from purified and unpurified mixtures. There was a clear correlation between the amount of antibody used for coating, and MFI signal of capture protein. More importantly, when capturing C-tag *Pf* MSP1-42 directly from the wheat germ (WG) lysate we observed a 20-fold signal to noise ratio. This feature, like the HaloTag capture, allows for streamlined multiplex array development. By utilizing these antibody coated beads we have shown we can separate C-tagged antigens from the complex WG translation lysate mixtures. The time-consuming step in multiplex development is the formation of a stable bead-antigen complex. The chemistry developed here can quickly form this complex without purification of each antigen individually. This saves a considerable amount of time and labor compared to the conventional multiplex bead-based assay approach.

The power of the C-tag antibody coated multiplex beads was shown by assessing patient

plasma from malaria patients. Patient sample selection was done based on protein array data and whole genome sequencing information collected from the Malaria Evolution in South Asia-International Center of Excellence for Malaria Research program (MESA-ICEMR, Rathod lab unpublished data).[79] The protein array data included plasma responses of 200 Goan patients infected with either *Plasmodium falciparum* or *Plasmodium vivax*. To replicate protein microarray results, two patient plasmas were selected for singleplex analysis using the C-tag coated bead assay. We observed a strong correlation between the two assays, where the level of patient response using protein microarrays was reproducible using the developed BioPlex method. These findings suggest the C-tag assay on the BioPlex is capable of providing equally sensitive immune responses analysis in comparison to protein arrays, with significantly less assay preparation and sample use.

Finally, the multiplexing capabilities of the designed platform was demonstrated using a select set of malaria patient plasma samples. These patients' immune responses had previously been assessed using traditional protein array methods.[79] Patient samples were multiplexed with *Pf* MSP1, *Pf* AMA1 and GFP control bead sets. Immune responses detected against *Pf* MSP1 were compared with protein array responses. Comparison of the unpurified protein array spot for *Pf* MSP1 correlates with bioplex results with a R^2 value of 0.891. However, purified *Pf* MSP1 was also spotted on the protein arrays as a control and data from these purified spots gave a higher correlation to the bioplex results obtained. The protein array spots representative of 0.1 and 0.3 mg/mL of purified *Pf* MSP1 gave a R^2 correlation value of 0.986 and 0.994, respectively. This indicates that the multiplexing platform designed here is most representative of a true "pure" antigen-antibody response. The ability to capture antigens onto bead sets and separate these antigens from all background translation proteins before immune response analysis affords

purified antigens available for plasma antibody binding. Thus, nonspecific antibody binding onto beads or proteins is reduced leading to results more reflective of true patient immune responses. The results here clearly show the difference in signals obtained when analyzing patient samples against unpurified and purified antigens. These findings further confirm that traditional protein array methodologies may be masking true immune response biomarkers and that the multiplexing platform here can address these technological gaps.

We have shown the successful development of a novel array system utilizing the multiplexing capabilities of the BioPlex 200 along with the epitope binding abilities of the C-tag. Previous works have shown the application of the C-tag solely for purification purposes. The first reports of utilizing the C-tag epitope for malaria antigen purification was for the purification of *Pf* Rh5 from a stable cell line of Drosophila melanogaster.[108] Combining the C-tag capture ability with multiplexing capabilities provides a new assay platform that can be used to dissect NAI responses of malaria patients. Here we have shown both the singleplexing and multiplexing of patient sera against *Pf* MSP1-42, *Pf* AMA1 and GFP. We can now expand studies to take full advantage of the multiplexing capabilities of the platform. Figure 4.12 shows a schematic representation of the envisioned application for the multiplexing platform where a single experiment can output 96 different patient serum immune responses against 100 or more different antigen candidates.

Although BioPlex assays have been implemented to dissect malaria patient immune responses, no such reports have been made using Indian patient samples. Parasites in India are shown to have a large amount of genetic diversity.[119] This genetic diversity is likely reflected in the unique immune responses observed in malaria-infected individuals. Utilizing this new

platform in the study of patient immune responses of Indian patients could help us better understand protective immunity and other disease progression questions.

Chapter 4 Figures

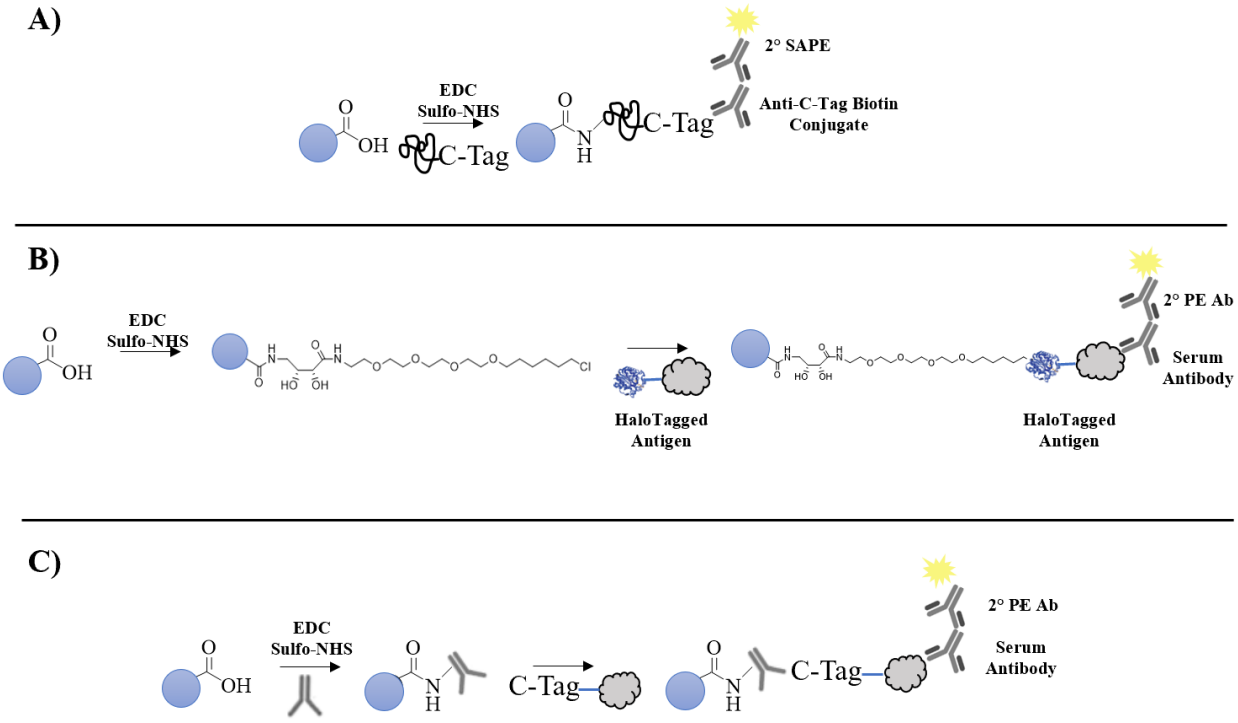

Figure 4.1 Schematic representation of different Luminex bead chemistries tested.

(A)Direct coating of purified C-tag proteins. (B) Chemical modification of beads with HaloTag capture linker. These chemically modified beads capture HaloTagged proteins directly from wheat germ translation lysates. (C) Coating of beads with anti-C-tag antibodies. Antibody coated beads capture C-tagged proteins directly from wheat germ translation lysates.

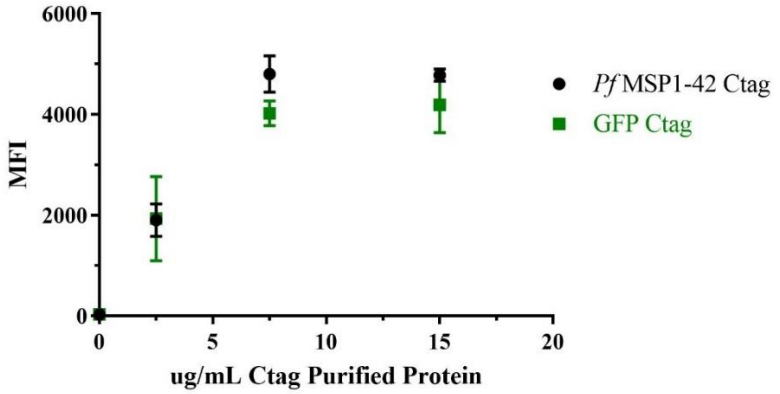

Figure 4.2 Direct coating of C-tag purified proteins to beads. Various concentrations of purified *Pf* MSP1-42 and GFP were coupled with 3000 beads in a single 96-plate well. Mean fluorescent intensity (MFI) represents the signal detected by anti-C-tag antibody on a BioPlex 200 reader.

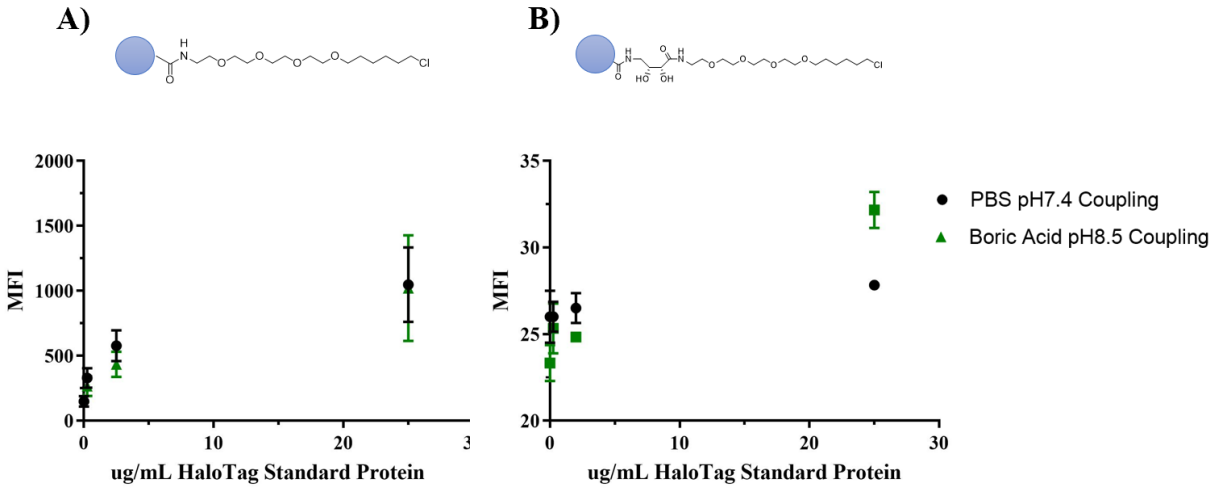

Figure 4.3 Efficiency of bead modification using Halotag capture linkers. Two different HaloTag amine ligands were conjugated on the Luminex microspheres. Structures of HaloTag amine ligands are shown above each respective plot as bead-linker conjugates. The purified HaloTag standard protein was used to detect the efficiency of conjugation in a series of concentrations. The mean fluorescent intensity (MFI) represents the signal detected by anti-HaloTag antibody on a BioPlex 200 reader

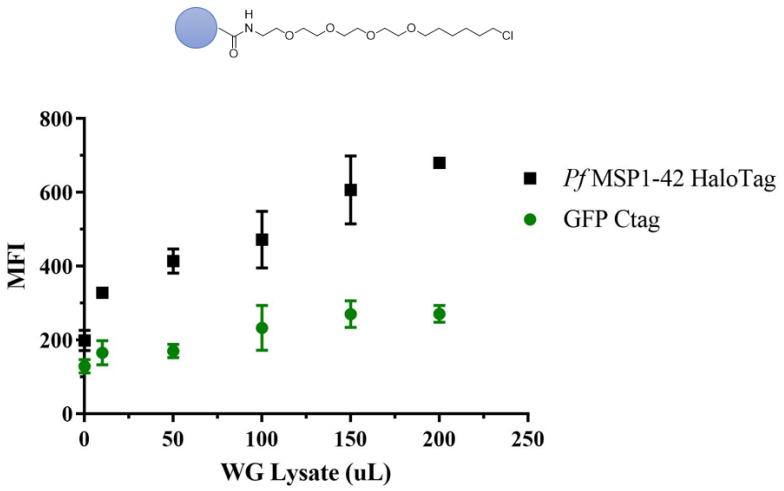

Figure 4.4 Capture of antigens from wheat germ translations using HaloTag linker.

Microspheres modified with purchased Promega HaloTag amine linker were titrated with wheat germ (WG) translation lysate. Each binding was carried out with 3000 beads in a single well of a 96-well plate. The mean fluorescent intensity (MFI) represents the signal detected by anti-HaloTag antibody on a BioPlex 200 reader.

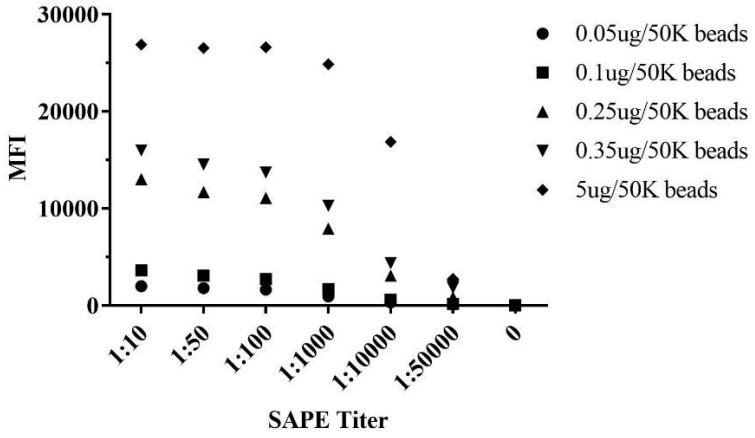

Figure 4.5 Titration of anti-C-tag antibody coupled on the Luminex microspheres. The efficiency of anti-C-tag coating on beads was detected using streptavidin R-Phycoerythrin conjugate in a series of concentrations. The mean fluorescent intensity (MFI) represents the binding signal of the SAPE and was read on a BioPlex200 platform.

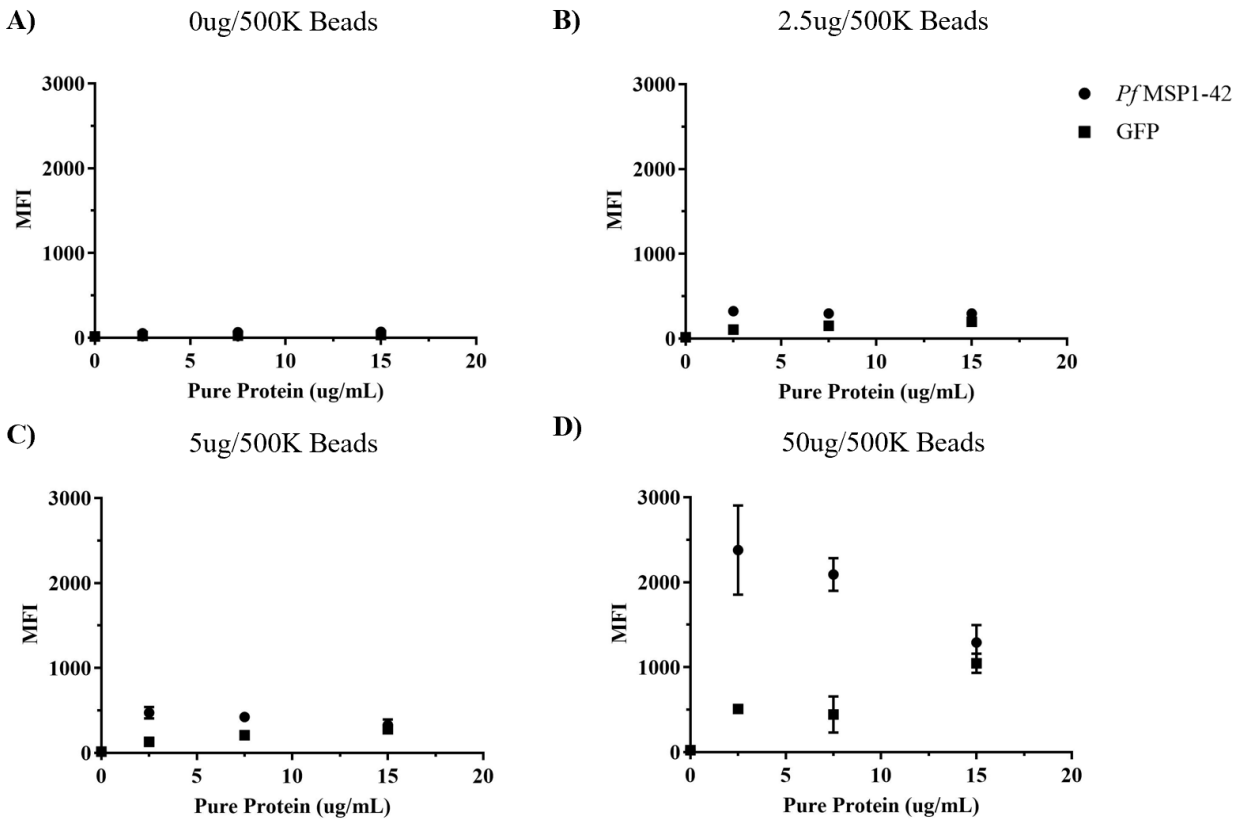

Figure 4.6 Optimization of anti-C-tag antibody bead coating. Anti-C-tag antibodies were conjugated at various concentrations (A-D) on Luminex beads. Each conjugation concentration was tested for capturing ability of C-tag purified proteins, *Pf* MSP1-42 and GFP. Mean fluorescent intensities (MFI) were detected using rabbit anti-*Pf* MSP1-42 antibodies and read on a BioPlex 200 reader.

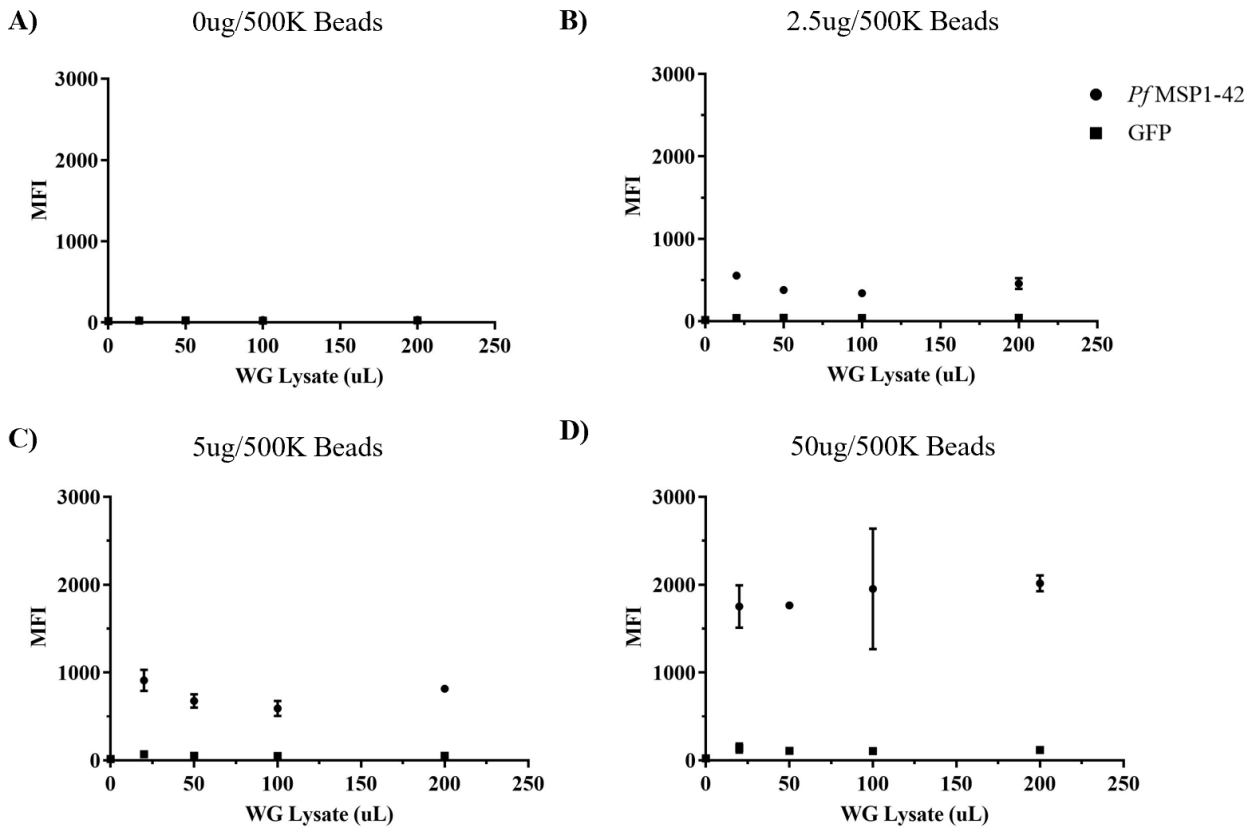

Figure 4.7 Optimization of wheat germ capture to anti-C-tag coated beads. Anti-C-tag antibodies were conjugated at various concentrations (A-D) on Luminex beads. Each conjugation concentration was tested for capturing ability of C-tag *Pf* MSP1-42 and GFP directly from wheat germ (WG) translation lysate. Mean fluorescent intensities (MFI) were detected using rabbit anti-*Pf* MSP1-42 antibodies and read on a BioPlex 200 reader.

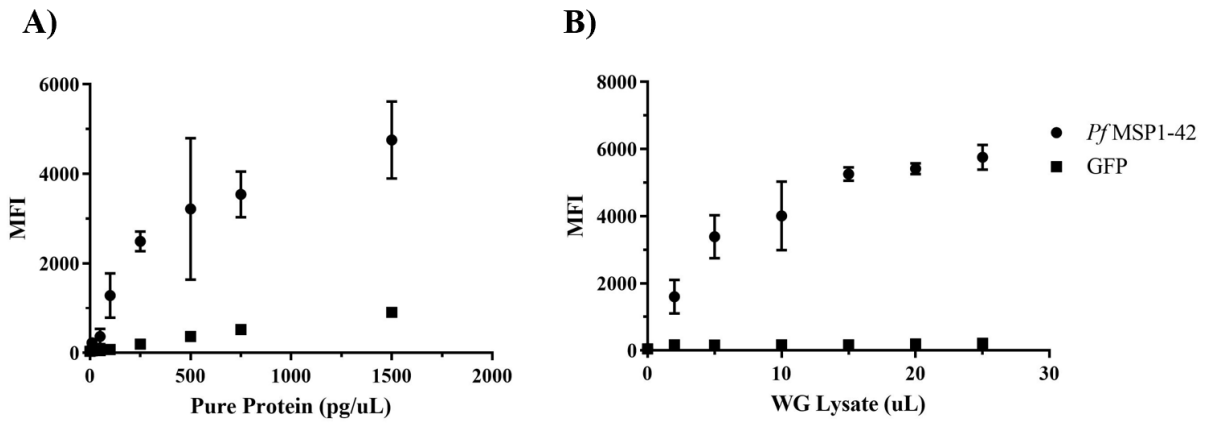

Figure 4.8 Detection of lower limits of C-tag protein binding. Low concentrations of both C-tag purified proteins (A) and wheat germ (WG) lysates (B) were captured to anti-C-tag antibody coated beads. Mean fluorescent intensities (MFI) were detected using rabbit anti-*Pf* MSP1-42 antibodies and read on a BioPlex 200 reader.

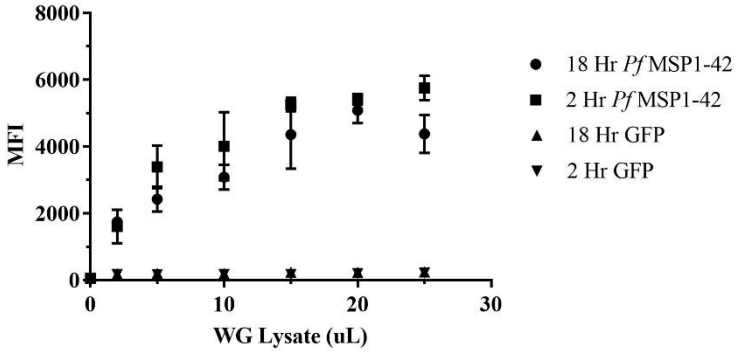

Figure 4.9 Comparison of C-tag protein capture incubation times. Wheat germ (WG) lysates were captured to anti-C-tag antibody coated beads for 18 hours or 2 hours. Mean fluorescent intensities (MFI) were detected using rabbit anti-*Pf* MSP1-42 antibodies and read on a BioPlex.

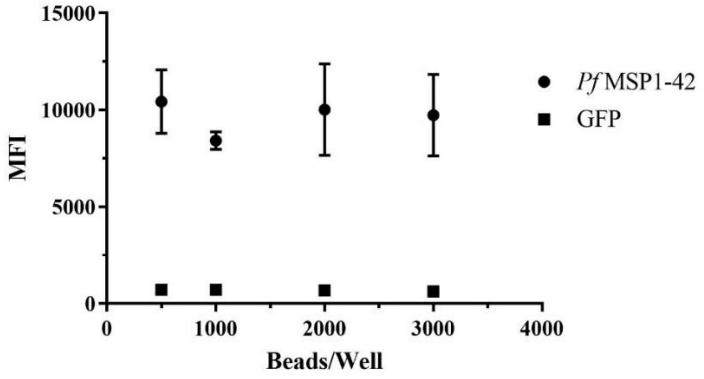

Figure 4.10 Comparison of mean fluorescent intensity (MFI) signals with various bead concentrations. Wheat germ (WG) lysates were captured to anti-C-tag antibody coated beads. Bead number per well was titrated and mean fluorescent intensities (MFI) were detected using rabbit anti-*Pf* MSP1-42 antibodies and read on a BioPlex 200 reader.

Table 4.1 Table of patient sera analysis by protein microarray for comparison.[79] A select set of patients from a previous published study were selected cross examine on the BioPlex platform. Whole genome sequencing (WGS) data results are listed for each patient as number of single nucleotide polymorphisms (SNPs) and specific amino acid (AA) mutations. Protein array responses (Array) against *Pf* MSP1 are shown. Patient history is also listed.

Patient ID	SNPS	Amino Acid Mutations	Array *Pf* MSP1	Sex/Age/Infection
01/42	6	7	49237	M/50/*Pf*
01/136	7	8	31772	M/26/*Pf*
01/25	9	9	14086	M/60/*Pf*
01/30	4	5	12179	M/27/*Pf*
01/81	7	8	4757	M/45/*Pf*
01/31	3	4	4448	M/17/*Pf*
01/24	9	9	3970	M/37/*Pf*
01/45	7	8	2590	M/35/*Pf*
01/37	7	8	1477	M/60/*Pf*

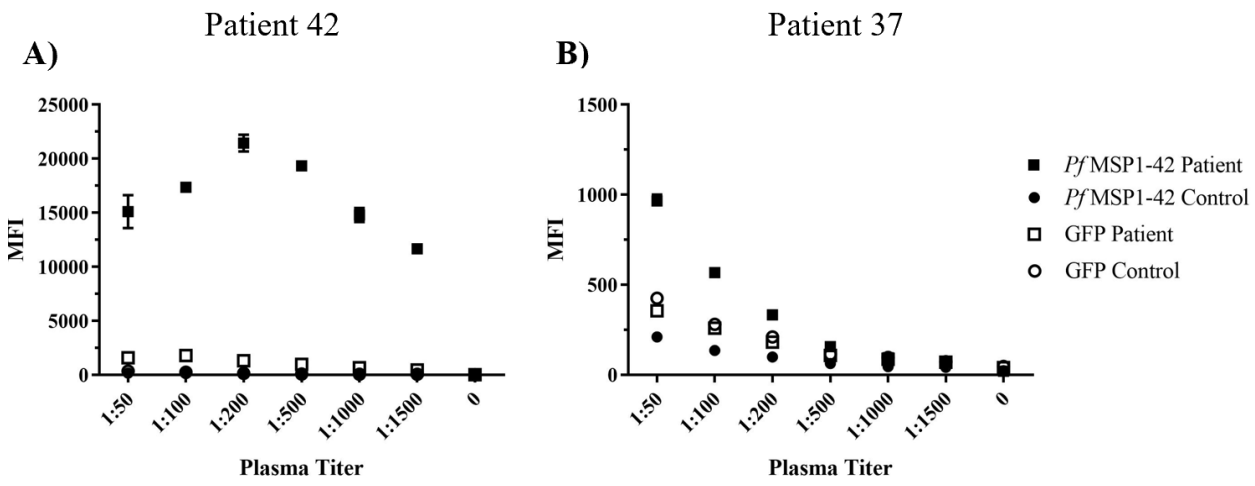

Figure 4.11 Singleplexing of previously determined high and low response patients. Based on previous protein array data, two plasma samples were tested against *Pf* MSP1-42 coated beads. Plasma samples were titrated and mean fluorescent intensities (MFI) were detected using rabbit anti-*Pf* MSP1-42 antibodies and read on a BioPlex 200 reader.

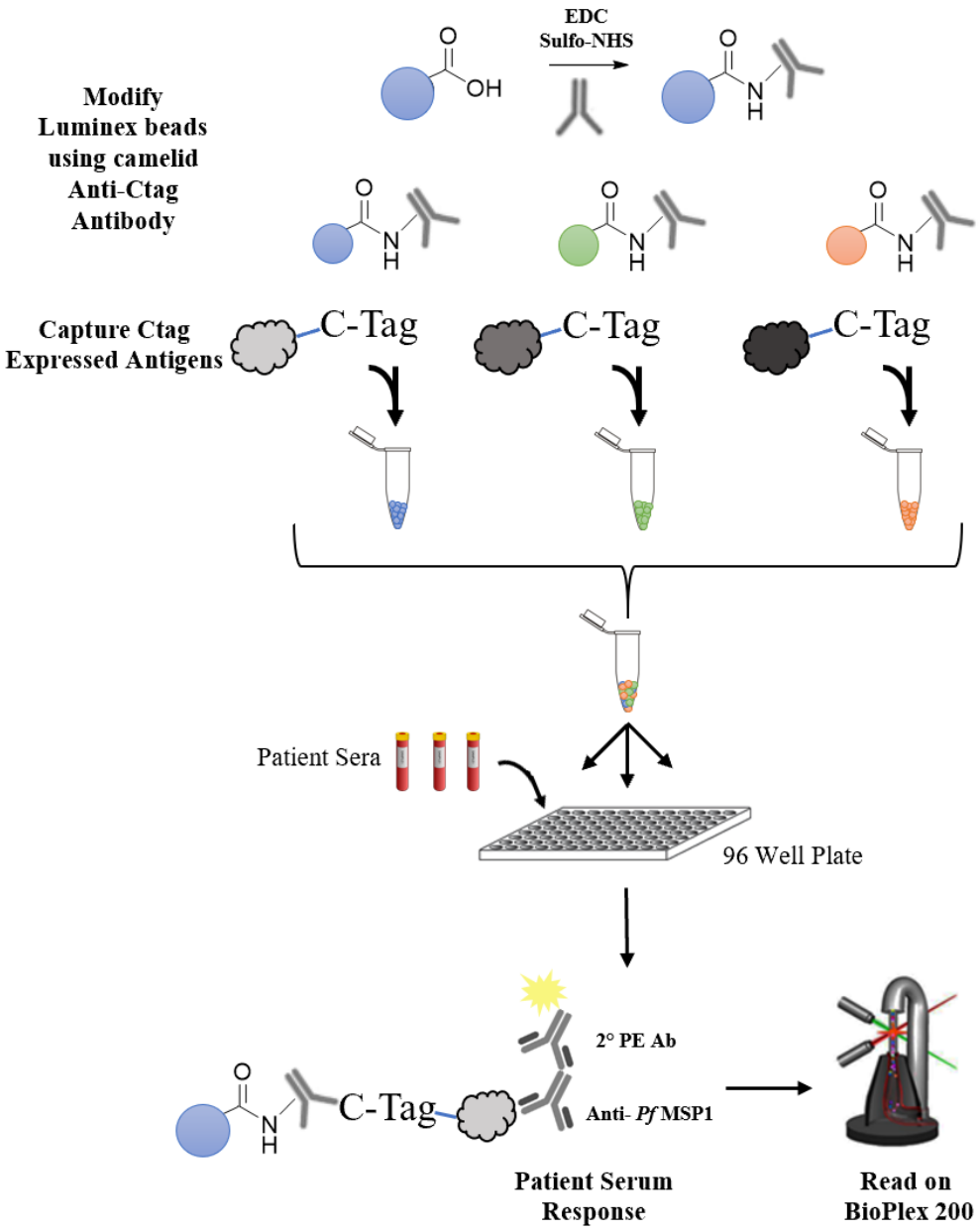

Figure 4.12 Final proposed multiplexing assay design. Luminex beads are modified with anti-C-tag antibodies with carbodiimide coupling. Modified beads capture C-tagged antigens directly from wheat germ lysates. Unique spectral markers make it possible to multiplex antigen-bead complexes in a single well against an individual patient sera.

Table 4.2 Select patient plasma immune responses. The following table represents nine malaria patient immune responses along with a control plasma sample. Responses to *Pf* MSP1, *Pf* AMA1, and GFP were tested. Multiplex signal from the BioPlex-200 reader are displayed (BioPlex Signal) along with previously reported protein array signals (Array Signal).

Antigen	Patient ID	Array Signal	BioPlex Signal
***Pf* MSP1**	01/42	49237	16471
	01/136	31772	14889
	01/25	14086	731
	01/30	12179	608
	01/81	4757	548
	01/31	4448	251
	01/24	3970	616
	01/45	2590	477
	01/37	1477	644
	Control	--	122
***Pf* AMA1**	01/42	41944	7348
	01/136	21220	3167
	01/25	49220	216
	01/30	36952	3416
	01/81	4687	528
	01/31	5203	422
	01/24	4031	1089
	01/45	7131	811.5
	01/37	1458	708
	Control	--	150
GFP	01/42	--	1194
	01/136	--	412
	01/25	--	1339
	01/30	--	1237
	01/81	--	545
	01/31	--	427
	01/24	--	1048
	01/45	--	606
	01/37	--	693
	Control	--	170

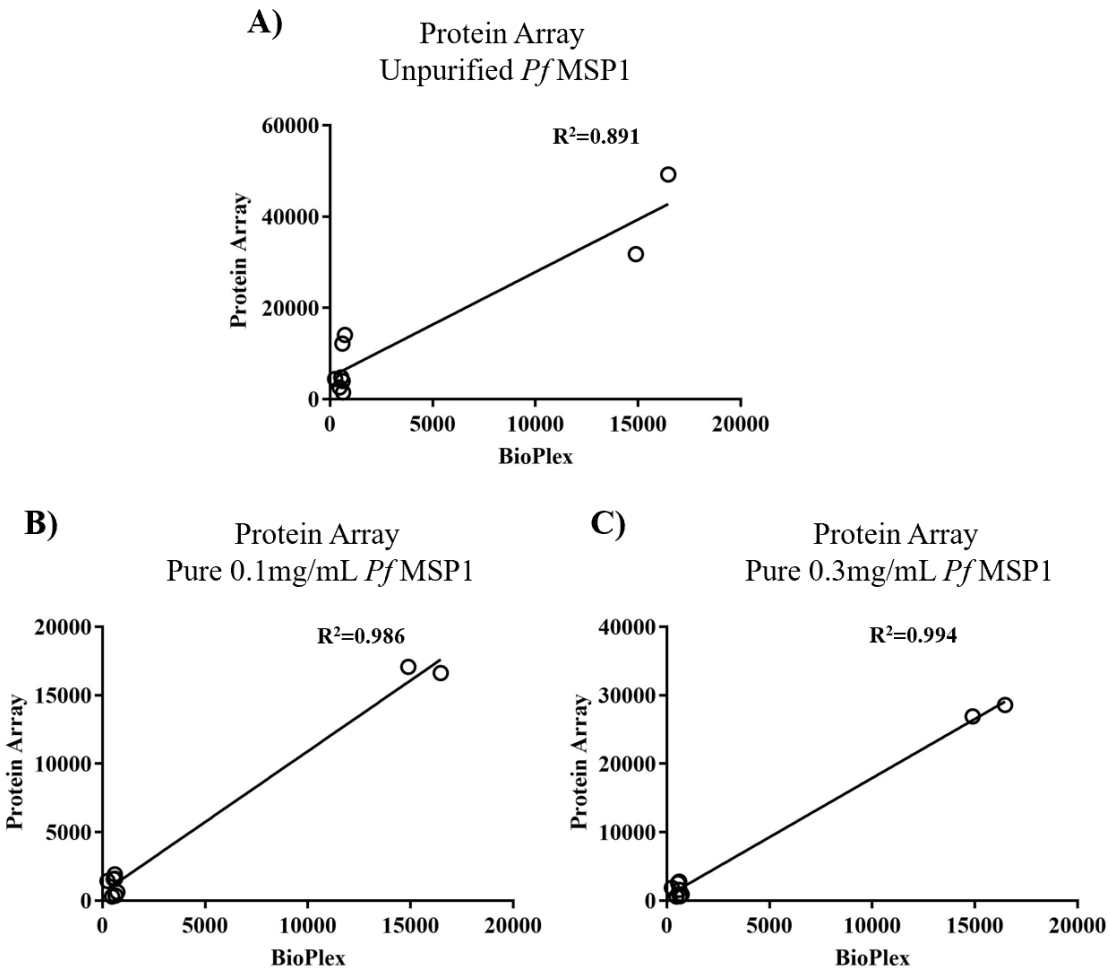

Figure 4.13 Comparison of patient immune responses by protein array and multiplexing platform. Nine patient plasma samples were analyzed by the BioPlex-200 in a multiplexing assay. Signals of patient responses (open circles) to *Pf* MSP1 were directly plotted against previously reported protein array results. Linear regression analysis was fitted to data points and R-squared values are reported on near each fit line.

Chapter 5: Conclusions and Future Work

Conclusion

Malaria, which is caused by various species of the genus Plasmodium, is a major global health problem. Almost half the world's population is at risk for malaria and in 2018 alone there were close to 300 million cases and 600,000 deaths.[1-2] Although antimalarial drugs have been the main force in controlling the disease, parasites eventually evolve resistance to our best compounds. Currently our main defense against the parasite is artemisinin combination therapies, (ACTs) along with basic vector control.[18-19, 24] Although these treatments have proven to be highly effective in most parts of the world, more recent reports from South East Asia have emerged indicating delayed parasite clearance in patients treated with ACTs.[121] While there is a significant amount of money and research devoted to developing a malaria vaccine, currently no FDA approved vaccine is available.[122] It is observed that patients who survive malaria episodes eventually acquire resistance to the disease, confirming the opportunity for vaccine development. This naturally acquired immunity (NAI) has long been studied and it is evident that circulating antibodies play a major role in this protection.[39, 42, 122] Understanding which of the 5,400 parasite antigens evoke the strongest and most protective human immune responses is key to the development of a useful vaccine. Efforts have been made to prioritize these antigen candidates however two main bottlenecks remain: isolation of high-quality parasite antigens for study, and technical design flaws of the arrays used to study these NAI responses. Current antigen prioritization methods utilize traditional protein microarrays.[63, 79] On protein microarrays, antigens are directly spotted on slides without any purification. This can increase the non-specific background interactions that may obscure true binding interactions. To ensure better

results on arrays, antigens should be purified and assayed for correct functional form. However, since these arrays often are interrogating 1000's of antigens at a time, purification of each antigen is extremely laborious. Furthermore, purification of full length and functional malaria proteins remains a major challenge in the field which further hinders the use of such protein array slide assays.

An ideal platform for patient immune response dissection would incorporate two key features. One would utilize high quality antigens in the array itself. Reliable production of highly pure malaria antigens that are expressed in functionally folded form is essential to elicit the correct antigen-antibody binding events on an array. Ideally protein expression and purification would be simplified to a single step purification to help reduce protein loss as well as save time. Second, there remains a need to improve technical approaches to dissecting immune responses. Specifically developing methods that can interrogate multiple antigens in parallel while limiting patient sample use. Additionally, development of a reliable chemistry that can link antigens to the array surface without loss of antigen epitope binding is critical. Implementation of such technical improvements would allow for a high-throughput method of serum analysis compared to traditional arrays, while providing equal or greater sensitivity.

The Rathod Lab has previously shown that the wheat germ cell free system of protein expression yields high quality functional enzymes that can be purified with GST affinity tags. Four potential purification schemes were tested in their ability to isolate highly pure and functional malaria antigens *Pf* MSP1-42, *Pf* MSP1-19, *Pf* AMA1, *Pf* RH5, *Pv* MSP1-42, *Pv* MSP1-19, *Pv* AMA1, *Pv* RH5. The four schemes tested utilized GST and His tags, covalent HaloTag capture, and an epitope tag called C-tag. Schemes using HaloTag and C-tag antigen capture were most successful in producing highly pure antigens. Both yielded antigen

purification above 90% in a single step. The yield of the two varied where HaloTag only recovered 10 µg/mL of translation reaction the C-tag produced 35 µg/mL of translation reaction. This 3.5-fold increase in recovery makes the C-tag system more appealing when large quantities of purified malarial antigen is desired. Testing function of malaria antigens is more challenging than common enzymes as no simple enzymatic study can be done. To show correct folding into the native protein state, antibodies must be raised against purified antigens and shown to inhibit parasite growth in culture. Antibodies raised against C-tag purified *Pf* MSP1-42 showed comparable growth inhibition to literature reports indicating the antigens are being expressed in full length and functionally active form.

In efforts to develop a more high-throughput method of patient sera analysis, the BioPlex multiplexing system platform was utilized. Development of a multiplexing assay required determination of the ideal chemistry for protein binding onto spectrally unique polystyrene beads. Three bead chemistries were demonstrated here: direct protein coupling to beads, capture using HaloTag linker modified beads, and capture using anti-C-tag antibody coated beads. The direct protein capture onto beads is representative of traditional protein microarray surface chemistries. With such chemistries any free amine can react with activated carboxyl groups on the bead surfaces to form an amide bond. This method results in random orientation of proteins and the possible masking, or total loss, of an epitope's binding abilities. Further, antigens must first be individually purified making it challenging to assay many antigens at a time. The second bead chemistry tested was modification of multiplex beads with a HaloTag capture linker. Two linkers were tested: a purchased linker, and a synthesized linker. Although the purchased linker modified beads showed the ability to capture HaloTagged antigens directly from wheat germ lysates the bead chemistry was not reproducible. The goal of a high-throughput system of

immune response dissection requires that a reproducible bead chemistry be used. The last bead chemistry tested was coating of multiplexing beads with anti-C-tag antibodies. This bead chemistry proved to be highly reproducible and was also able to capture expressed malaria antigens directly from the wheat germ lysate. This chemistry eliminates all protein purification steps and provides a streamlined method to produce stable bead-antigen complexes for multiplex assays. Furthermore, the presentation of expressed antigens on the multiplexing beads using the C-tag greatly diminishes the possibility of masking epitope sites.

Combining the multiplexing abilities of the BioPlex platform with the highly specific capture capabilities of the C-tag yields a novel method for dissection of patient antibody immune responses. The true strength of this methodology is shown in the human patient analysis. Select patient immune responses were analyzed on the C-tag multiplexing platform and signals strongly correlated with traditional protein microarray results. Furthermore, multiplex signals correlated highest with purified antigen responses from traditional protein array work indicating the value of using purified antigens when dissecting patient immune responses. This is the first report of such a system and is evidence of how such a system could improve upon traditional protocols. With the capturing ability of the C-tag, protein purification is eliminated. Once an antigen is captured on the beads, it can be multiplexed with over 100 different antigens in a single 96-well plate using as little as 1 µL of patient sera. These features make the system highly valuable for high-throughput analysis of hundreds of malaria patient serum samples.

Future Work

In this thesis we presented a novel method for dissecting patient immune responses. We combined the specificity of the epitope tag C-tag, with the multiplexing capabilities of the BioPlex system. Together a new platform was designed to quickly capture C-tag proteins from a

complex translation mixture onto the spectrally unique beads designed for the BioPlex instrument. Forming these unique bead-antigen complexes allows for the multiplexing of numerous antigens of interest in a single assay. We validated the power of this assay with a select set of patient serum samples and found high correlation of immune responses to *Plasmodium falciparum* MSP1-42 in comparison to traditional protein microarray results. We have also shown the capabilities of multiplexing antigens with the same platform with high correlations to traditional protein array results.

Explorations into malaria patient immune responses using the proposed platform can be expanded. As more proteins are included in the library of multiplexing antigens, universal controls need to be implemented. The wheat germ system expresses proteins in varying yields, thus a fast and reliable method to quantify the degree of antigen coating to each unique bead set is needed. By adding a N-terminal tag to the antigen constructs a dual tagging system could be generated. Dual tags would allow for capture onto the multiplexing beads using the C-tag followed by antigen quantification using antibodies to a N-terminal tag such as His tag or Flag tag. Although introducing new tags may complicate background reactivity with patient serums, a control to compare antigen coating levels among bead sets is necessary to rule out differences in immune responses due to variations in antigen coating levels.

With a universal N terminal tag in place, it will be possible to expand the application of the novel array platform to study hundreds of patient serum samples. Basic questions such as which antigens commonly give rise to the highest immune response can be asked. This will help prioritize antigen candidates using a bead-based assay. Recently published data from the Rathod Lab collaborators at IIT Mumbai show the immune responses of 200 Goan patients against *Plasmodium falciparum* and *vivax* antigens using traditional protein microarrays. These patient

sera have been shared with our lab here in Seattle and we have the capabilities to analyze and compare all 200 patient sera using this multiplexing platform. Although it would be expected that the correlation of high and low responses remains the same between the traditional protein array and multiplexing platform, it may be that interesting contradictions are identified. Such contradictions could give insight into how one array may be better suited over the other. Expanding the patient pool tested would not only confirm the validity of the multiplexing platform but could also allow for new serum reactivity questions to be asked. As previously mentioned, no work has been done to dissect malaria patient immune responses using a multiplexing system in Indian samples.

Using this multiplexing platform, it is possible to start identifying important biomarkers of disease that may be unique to Indian samples. Understanding biomarkers that are associated with factors such as age, sex, home location, or number of previous treatments could aid in better understanding which antigens are crucial to protection. More so, the questions of biomarkers for disease progression is something many have tried to investigate but with little success. These questions can be answered because of the Rathod lab's access to field site hospitals across India having well-characterized patient samples of varying disease severity. Utilizing the multiplexing platform, it may be possible to differentiate biomarkers of severe malaria when compared to non-severe patients.

Finally, the Rathod lab's unique collaborations in India allow us to analyze patient immune responses from across the country. In addition to the patient data, many of the samples collected have undergone whole genome sequencing (WGS). Combining WGS data along with the multiplexing system allows for analysis of immune responses based on specific variants the researcher is interested in. Information about antigenic variants coming from WGS that can help

feed design of multiplex array studies is a powerful tool for the malaria field. To date, no such studies have been conducted. We feel that combining WGS data and multiplex immune response data can help uncover the driving factors of naturally acquire immunity.

References

1. WHO, WHO Malaria report 2018. **2018**.
2. WHO Malaria Report 2018 at a Glance. https://www.who.int/malaria/media/world-malaria-report-2018/en/.
3. Baird, J. K., Evidence and implications of mortality associated with acute Plasmodium vivax malaria. *Clin. Microbiol. Rev.* **2013,** *26* (1), 36-57.
4. Snow, R. W.; Guerra, C. A.; Noor, A. M.; Myint, H. Y.; Hay, S. I., The global distribution of clinical episodes of Plasmodium falciparum malaria. *Nature* **2005,** *434* (7030), 214-7.
5. Sachs J, M. P., The economic and social burden of malaria. *Nature* **2002,** *415* (6872), 680-5.
6. Arrow, K. J., Panosian, C., Gelband, H., Saving Lives, Buying Time: Economics of Malaria Drugs in an Age of Resistance. Washington DC: National Academies Press: 2004. https://www.ncbi.nlm.nih.gov/books/NBK215638/.
7. Bruce-Shwatt, L. J., Alphonse Laverans discovery 100 years ago and today's global fight against malaria. *J. Royal Soc. Med* **1981,** *74*, 531-563.
8. Capanna, E., Grassi vs Ross: who solved the riddle of malaria? *Int. Microbiol.* **2006,** *9*, 69-74.
9. Ross, S.-M. R., On Some Peculiar Pigmented Cells Found In Two Mosquitos Fed On Malarial Blood. *Brit Med J* **1987**, 1786-1788.
10. Liu, W.; Li, Y.; Learn, G. H.; Rudicell, R. S.; Robertson, J. D.; Keele, B. F.; Ndjango, J. B.; Sanz, C. M.; Morgan, D. B.; Locatelli, S.; Gonder, M. K.; Kranzusch, P. J.; Walsh, P. D.; Delaporte, E.; Mpoudi-Ngole, E.; Georgiev, A. V.; Muller, M. N.; Shaw, G. M.; Peeters, M.; Sharp, P. M.; Rayner, J. C.; Hahn, B. H., Origin of the human malaria parasite Plasmodium falciparum in gorillas. *Nature* **2010,** *467* (7314), 420-5.
11. Mller, L. H., Marsh, K., Baruch, D.I., Doumbo, O.K., The Pathogenic Basis of Malaria. *Nat. Inst. Rev.* **2002,** *415*, 673-679.
12. Cowman, A. F.; Tonkin, C. J.; Tham, W. H.; Duraisingh, M. T., The Molecular Basis of Erythrocyte Invasion by Malaria Parasites. *Cell Host Microbe* **2017,** *22* (2), 232-245.
13. Su, X.; Hayton, K.; Wellems, T. E., Genetic linkage and association analyses for trait mapping in Plasmodium falciparum. *Nat Rev Genet* **2007,** *8* (7), 497-506.
14. Cowman, A. F.; Berry, D.; Baum, J., The cellular and molecular basis for malaria parasite invasion of the human red blood cell. *The Journal of cell biology* **2012,** *198* (6), 961-71.
15. Bruce, M. C.; Alano, P.; Duthie, S.; Carter, R., Commitment of the malaria parasite Plasmodium falciparum to sexual and asexual development. *Parasitology* **1990,** *100 Pt 2*, 191-200.
16. Davies, H. M.; Nofal, S. D.; McLaughlin, E. J.; Osborne, A. R., Repetitive sequences in malaria parasite proteins. *FEMS Microbiol. Rev.* **2017,** *41* (6), 923-940.
17. Cowman, A. F.; Crabb, B. S., Invasion of red blood cells by malaria parasites. *Cell* **2006,** *124* (4), 755-66.
18. D'Alessandro, U., Achan, J., et. al. , Quinine An Old Antimalarial Drug in a Modern World Role in the Treatemnt of Malaria. *Mal J.* **2011,** *10* (144), 1-12.
19. Slater, A. F., Chloroquine: mechanism of drug action and resistance in Plasmodium falciparum. *Pharmacol. Ther.* **1993,** *57* (2-3), 203-35.
20. Fidock, D. A., Lakshmanan, V., et. al. , A critical role for PfCRT K76T in Plasmodium falciparum verapamil-reversible chloroquine resistance. *EMBO J.* **2005,** *24*, 2294-2305.
21. Rosenthal, P. J., Rathod, P.K., Cui, L., et. al. , Antimalarial Drug Resistance: Literature Review and Activities and Findings of the ICEMR Network. *Am. J. Trop. Med. Hyg.* **2015,** *93*, 57-68.
22. Laughlin, L. W., Hoffman, S.L., et. al., RII and RIII Type Resistance of Plasmodium Falciparum to Combination of Mefloquine and SulfadoxinePyrimethamine in Indonesia. *The Lancet* **1985**, 1039-1040.

23. Wellems, T. E., Walliker, D., Peterson, D.S., Evidence that a point mutation in dihydrofolate reductase thymidylate synthase confers resisitance to pyrimethamine in falciparum malaria. *Proc. Natl. Acad. Sci. USA* **1988,** *85*, 9114-9118.
24. Krishna, S., Price, R.C., et. al. , Mefloquine resistance in Plasmodium falciparum and increased pfmdr1 gene copy number. *Lancet.* **2004,** *364*, 438-447.
25. Cui, L.; Su, X. Z., Discovery, mechanisms of action and combination therapy of artemisinin. *Expert Rev Anti Infect Ther* **2009,** *7* (8), 999-1013.
26. Nsanzabana, C., Resistance to Artemisinin Combination Therapies (ACTs): Do Not Forget the Partner Drug! *Trop Med Infect Dis* **2019,** *4* (1).
27. Leang, R.; Taylor, W. R.; Bouth, D. M.; Song, L.; Tarning, J.; Char, M. C.; Kim, S.; Witkowski, B.; Duru, V.; Domergue, A.; Khim, N.; Ringwald, P.; Menard, D., Evidence of Plasmodium falciparum Malaria Multidrug Resistance to Artemisinin and Piperaquine in Western Cambodia: Dihydroartemisinin-Piperaquine Open-Label Multicenter Clinical Assessment. *Antimicrob. Agents Chemother.* **2015,** *59* (8), 4719-26.
28. Meshnick, S. R., Artemisinin Mechanism of Action Resistance and Toxicity. *Int. J. Paristol.* **2002,** *32*, 1655-1660.
29. Slutsker, L.; Kachur, S. P., It is time to rethink tactics in the fight against malaria. *Malar J* **2013,** *12*, 140.
30. Kumari, A.; Karnatak, M.; Singh, D.; Shankar, R.; Jat, J. L.; Sharma, S.; Yadav, D.; Shrivastava, R.; Verma, V. P., Current scenario of artemisinin and its analogues for antimalarial activity. *Eur J Med Chem* **2019,** *163*, 804-829.
31. Burrows, J. N.; Burlot, E.; Campo, B.; Cherbuin, S.; Jeanneret, S.; Leroy, D.; Spangenberg, T.; Waterson, D.; Wells, T. N.; Willis, P., Antimalarial drug discovery - the path towards eradication. *Parasitology* **2014,** *141* (1), 128-39.
32. NIAID, N. Malaria Prevention, Treatment, and Control Strategies. https://www.niaid.nih.gov/diseases-conditions/malaria-strategies.
33. Beier, J. C., Benelli, G. , Malaria Prevention, Treatment, and Control Strategies. *Acta. Tropica.* **2017,** *174*, 91-96.
34. Vreysen, M. J. B., Bourtzis, K., et. al. , More than one rabbit out of the hat: Radiation, transgenic and symbiont-based approaches for sustainable management of mosquito and tsetse fly populations. *Acta. Tropica.* **2016,** *157*, 115-130.
35. Doolan, D. L.; Dobano, C.; Baird, J. K., Acquired immunity to malaria. *Clin. Microbiol. Rev.* **2009,** *22* (1), 13-36, Table of Contents.
36. Marsh, K.; Kinyanjui, S., Immune effector mechanisms in malaria. *Parasite Immunol.* **2006,** *28* (1-2), 51-60.
37. Sharma, S., Mannan, B.A., et. al. , How specific is the immune response to malaria in adults living in endemic areas. *J. Vect. Borne. Dis.* **2003,** *40*, 84-91.
38. Butcher, G. A., Cohen, S. , Properties of Protective Malarial Anitbody. *Immunology* **1970,** *19*, 369-384.
39. Cohen, S., McGregor, I.A., Carrington, S. , Gamma Globulin and Acquired Immunity to Human Malaria. *Nature* **1961,** *4804*, 733-737.
40. Fowkes, F. J.; Richards, J. S.; Simpson, J. A.; Beeson, J. G., The relationship between anti-merozoite antibodies and incidence of Plasmodium falciparum malaria: A systematic review and meta-analysis. *PLoS Med* **2010,** *7* (1), e1000218.
41. Borrmann, S.; Matuschewski, K., Protective immunity against malaria by 'natural immunization': a question of dose, parasite diversity, or both? *Curr. Opin. Immunol.* **2011,** *23* (4), 500-8.
42. Riley, E. M., Stevenson, M.M, Innate Immunity to Malaria. *Nat. Rev. Imm.* **2004,** *4*, 169-180.

43. Muellenbeck, M. F.; Ueberheide, B.; Amulic, B.; Epp, A.; Fenyo, D.; Busse, C. E.; Esen, M.; Theisen, M.; Mordmuller, B.; Wardemann, H., Atypical and classical memory B cells produce Plasmodium falciparum neutralizing antibodies. *The Journal of experimental medicine* **2013,** *210* (2), 389-99.
44. Schats, R.; Bijker, E. M.; van Gemert, G. J.; Graumans, W.; van de Vegte-Bolmer, M.; van Lieshout, L.; Haks, M. C.; Hermsen, C. C.; Scholzen, A.; Visser, L. G.; Sauerwein, R. W., Heterologous Protection against Malaria after Immunization with Plasmodium falciparum Sporozoites. *PLoS One* **2015,** *10* (5), e0124243.
45. Sauerwein, R. W.; Roestenberg, M.; Moorthy, V. S., Experimental human challenge infections can accelerate clinical malaria vaccine development. *Nat Rev Immunol* **2011,** *11* (1), 57-64.
46. Hoffman, S. L.; Vekemans, J.; Richie, T. L.; Duffy, P. E., The march toward malaria vaccines. *Vaccine* **2015,** *33 Suppl 4*, D13-23.
47. Mahmoudi, S.; Keshavarz, H., Efficacy of phase 3 trial of RTS, S/AS01 malaria vaccine: The need for an alternative development plan. *Hum Vaccin Immunother* **2017,** *13* (9), 2098-2101.
48. Freeman, R. R., Trejdosiewicz, A.J., Cross, G.A.M., Protective monoclonal antibodies recognising stage-specific merozoite antigens of a rodent malaria parasite. *Nature* **1980,** *284* (5754), 366-368.
49. Freeman, R. R., Holder, A.A., Trejdosiewicz, A.J., Cross, G.A. , The Host-Invader Interplay. H, V. D. B., Ed. Elsevier: Amsterdam, 1980.
50. Freeman, R. R., Holder, A.A. , Immunization against blood stage rodent malaria using purified parasite antigens. *Nature* **1981,** *361-364*.
51. Mitchell G. H., T. A. W., Alderson T., Deans J.A., Rat monoclonal antibodies which inhibit the in vitro multiplication of Plasmodium knowlesi. *Clin. exp. Immunol* **1982,** *49*, 297-309.
52. Cohen, S., Alderson, T., Thomas, A.W., Deans, J.A., Biosynthesis of a putative protective Plasmodium knowlesi merzoite antigen. *Mol. Biochem. Parasitol.* **1984,** *11*, 198-204.
53. Kemp, D. J., Brown, G.V., et. al. , The expression of Plasmodiu falciparum bloodstage antigens in Escherichia coli. *Phil. Trans. R. Soc. Lond.* **1984,** *307*, 179-187.
54. Hadley, T. J., Camus, D., A plasmodium falciparum antigen that binds to host erythrocytes and merzoites. *Science* **1985,** *230*, 553-556.
55. Kan S., S., W.A., et. al. , Merzoite surface coat precursor protein completely protects Aotus monkeys against Plasmodium falciparum malaria. *Proc. Natl. Acad. Sci. USA* **1987,** *84*, 3014-3018.
56. Felgner, P. L., Doolan, D.L., et. al. , Profiling Humoral Immune Responses to P falciparum Infection with Protein Microarrays. *Proteomics* **2008,** *8* (22), 4680-4694.
57. Barrell, B., Gardner, M.J. et. al. , Genome sequence of the human malaria parsite Plasmodium falciparum. *Nature* **2002,** *419*, 1-34.
58. MacBeath, G., Schreiber, SL., Printing proteins as microarrays for high-throughput function determination *Science* **2000,** *289* (5485), 1760-1763.
59. Emili A.Q., C., G. , Large-scale functional analysis using peptide or protein arrays. *Nat. Biotechnol.* **2000,** *18* (4), 393-397.
60. Vigil, A., Davies, D.H., Felgner, Defining the humoral immune response to infectious agebts using high density protein mmicroarrays. *Future Microbiol.* **2010,** *5* (2), 241-251.
61. Doolan, D. L. B., A.E., et. al. , The stability and Complexity of Antibody Responses to the Major Surface Antigen of Plasmodium falciparum. *Mol. and Cell. Proteom. 10.11* **2011,** *Authors Choice* 1-12.
62. Yan, G., Baum, E., et. al. , Protein Microarray Analysis of Antibody Responses to Plasmodium falciparum in western Kenyan Highland Sites with Differing Transmission Levels. *PLoS One* **2013,** *8*, 1-15.
63. Das, J., Uplekar, S., et. al. , Characterizing Antibody Responses to Plasmodium vivax and Plasmodium falciparum Antigens in India Using Genome-Scale Protein Microarrays. *PLoS Negl Trop Dis* **2017,** *2017*, 1-17.

64. Kim, K., Kessler, A. et. al., Convalescent Plasmodium falciparum-specific seroreactivity does not correlate with paediatric malaria severity or Plasmodium antigen exposure. *Mal. J.* **2018,** *17* (178), 1-15.
65. Stillman, B. A.; Tonkinson, J. L., FAST slides: a novel surface for microarrays. *Biotechniques* **2000,** *29* (3), 630-5.
66. Shriver-Lake, L. C.; Anderson, G. P.; Taitt, C. R., Oriented Peptide Immobilization on Microspheres. *Methods Mol. Biol.* **2016,** *1352*, 183-97.
67. Sciences, B. C. L., History of Flow Cytometry. https://www.mybeckman.in/resources/fundamentals/history-of-flow-cytometry.
68. E. Engvall, K. J., P. Perlmann, Quantitative assay of protein antigen immunoglobulin G by means of enzyme labelled antigen and antibody coated tubes. *BBA* **1971,** *251* (3), 427-434.
69. Graham, H.; Chandler, D. J.; Dunbar, S. A., The genesis and evolution of bead-based multiplexing. *Methods* **2019**.
70. Fouda, G. G.; Leke, R. F.; Long, C.; Druilhe, P.; Zhou, A.; Taylor, D. W.; Johnson, A. H., Multiplex assay for simultaneous measurement of antibodies to multiple Plasmodium falciparum antigens. *Clin Vaccine Immunol* **2006,** *13* (12), 1307-13.
71. Yman, V.; White, M. T.; Asghar, M.; Sundling, C.; Sonden, K.; Draper, S. J.; Osier, F. H. A.; Farnert, A., Antibody responses to merozoite antigens after natural Plasmodium falciparum infection: kinetics and longevity in absence of re-exposure. *BMC Med* **2019,** *17* (1), 22.
72. Varela, M. L.; Mbengue, B.; Basse, A.; Loucoubar, C.; Vigan-Womas, I.; Dieye, A.; Toure, A.; Perraut, R., Optimization of a magnetic bead-based assay (MAGPIX((R))-Luminex) for immune surveillance of exposure to malaria using multiple Plasmodium antigens and sera from different endemic settings. *Malar J* **2018,** *17* (1), 324.
73. Rouhani, M.; Zakeri, S.; Mehrizi, A. A.; Djadid, N. D., Comparative analysis of the profiles of IgG subclass-specific responses to Plasmodium falciparum apical membrane antigen-1 and merozoite surface protein-1 in naturally exposed individuals living in malaria hypoendemic settings, Iran. *Malar J* **2015,** *14*, 58.
74. Fernandez-Becerra, C.; Sanz, S.; Brucet, M.; Stanisic, D. I.; Alves, F. P.; Camargo, E. P.; Alonso, P. L.; Mueller, I.; del Portillo, H. A., Naturally-acquired humoral immune responses against the N- and C-termini of the Plasmodium vivax MSP1 protein in endemic regions of Brazil and Papua New Guinea using a multiplex assay. *Malar J* **2010,** *9*, 29.
75. Perraut, R.; Richard, V.; Varela, M. L.; Trape, J. F.; Guillotte, M.; Tall, A.; Toure, A.; Sokhna, C.; Vigan-Womas, I.; Mercereau-Puijalon, O., Comparative analysis of IgG responses to Plasmodium falciparum MSP1p19 and PF13-DBL1alpha1 using ELISA and a magnetic bead-based duplex assay (MAGPIX(R)-Luminex) in a Senegalese meso-endemic community. *Malar J* **2014,** *13*, 410.
76. Fonseca, A. M.; Quinto, L.; Jimenez, A.; Gonzalez, R.; Bardaji, A.; Maculuve, S.; Dobano, C.; Ruperez, M.; Vala, A.; Aponte, J. J.; Sevene, E.; Macete, E.; Menendez, C.; Mayor, A., Multiplexing detection of IgG against Plasmodium falciparum pregnancy-specific antigens. *PLoS One* **2017,** *12* (7), e0181150.
77. Dodoo, D.; Atuguba, F.; Bosomprah, S.; Ansah, N. A.; Ansah, P.; Lamptey, H.; Egyir, B.; Oduro, A. R.; Gyan, B.; Hodgson, A.; Koram, K. A., Antibody levels to multiple malaria vaccine candidate antigens in relation to clinical malaria episodes in children in the Kasena-Nankana district of Northern Ghana. *Malar J* **2011,** *10*, 108.
78. Cham, G. K.; Kurtis, J.; Lusingu, J.; Theander, T. G.; Jensen, A. T.; Turner, L., A semi-automated multiplex high-throughput assay for measuring IgG antibodies against Plasmodium falciparum erythrocyte membrane protein 1 (PfEMP1) domains in small volumes of plasma. *Malar J* **2008,** *7*, 108.
79. Venkatesh, A.; Jain, A.; Davies, H.; Periera, L.; Maki, J. N.; Gomes, E.; Felgner, P. L.; Srivastava, S.; Patankar, S.; Rathod, P. K., Hospital-derived antibody profiles of malaria patients in Southwest India. *Malar J* **2019,** *18* (1), 138.

80. Young, R.; Bremer, H., Polypeptide-chain-elongation rate in Escherichia coli B/r as a function of growth rate. *The Biochemical journal* **1976,** *160* (2), 185-94.
81. Jorstad, C. M.; Morris, D. R., Polyamine limitation of growth slows the rate of polypeptide chain elongation in Escherichia coli. *J. Bacteriol.* **1974,** *119* (3), 857-60.
82. Vedadi, M.; Lew, J.; Artz, J.; Amani, M.; Zhao, Y.; Dong, A.; Wasney, G. A.; Gao, M.; Hills, T.; Brokx, S.; Qiu, W.; Sharma, S.; Diassiti, A.; Alam, Z.; Melone, M.; Mulichak, A.; Wernimont, A.; Bray, J.; Loppnau, P.; Plotnikova, O.; Newberry, K.; Sundararajan, E.; Houston, S.; Walker, J.; Tempel, W.; Bochkarev, A.; Kozieradzki, I.; Edwards, A.; Arrowsmith, C.; Roos, D.; Kain, K.; Hui, R., Genome-scale protein expression and structural biology of Plasmodium falciparum and related Apicomplexan organisms. *Mol. Biochem. Parasitol.* **2007,** *151* (1), 100-10.
83. Anders, R. F.; Crewther, P. E.; Edwards, S.; Margetts, M.; Matthew, M. L.; Pollock, B.; Pye, D., Immunisation with recombinant AMA-1 protects mice against infection with Plasmodium chabaudi. *Vaccine* **1998,** *16* (2-3), 240-7.
84. Wu, X.; Jornvall, H.; Berndt, K. D.; Oppermann, U., Codon optimization reveals critical factors for high level expression of two rare codon genes in Escherichia coli: RNA stability and secondary structure but not tRNA abundance. *Biochem. Biophys. Res. Commun.* **2004,** *313* (1), 89-96.
85. Gardner, M. J.; Hall, N.; Fung, E.; White, O.; Berriman, M.; Hyman, R. W.; Carlton, J. M.; Pain, A.; Nelson, K. E.; Bowman, S.; Paulsen, I. T.; James, K.; Eisen, J. A.; Rutherford, K.; Salzberg, S. L.; Craig, A.; Kyes, S.; Chan, M. S.; Nene, V.; Shallom, S. J.; Suh, B.; Peterson, J.; Angiuoli, S.; Pertea, M.; Allen, J.; Selengut, J.; Haft, D.; Mather, M. W.; Vaidya, A. B.; Martin, D. M.; Fairlamb, A. H.; Fraunholz, M. J.; Roos, D. S.; Ralph, S. A.; McFadden, G. I.; Cummings, L. M.; Subramanian, G. M.; Mungall, C.; Venter, J. C.; Carucci, D. J.; Hoffman, S. L.; Newbold, C.; Davis, R. W.; Fraser, C. M.; Barrell, B., Genome sequence of the human malaria parasite Plasmodium falciparum. *Nature* **2002,** *419* (6906), 498-511.
86. Mudeppa, D. G.; Rathod, P. K., Expression of functional Plasmodium falciparum enzymes using a wheat germ cell-free system. *Eukaryot Cell* **2013,** *12* (12), 1653-63.
87. Mudeppa, D. G.; Kumar, S.; Kokkonda, S.; White, J., 3rd; Rathod, P. K., Topoisomerase II from Human Malaria Parasites: Expression, Purification, and Selective Inhibition. *The Journal of biological chemistry* **2015,** *33* (290), 20313-24.
88. Rui, E.; Fernandez-Becerra, C.; Takeo, S.; Sanz, S.; Lacerda, M. V.; Tsuboi, T.; del Portillo, H. A., Plasmodium vivax: comparison of immunogenicity among proteins expressed in the cell-free systems of Escherichia coli and wheat germ by suspension array assays. *Malar J* **2011,** *10*, 192.
89. Tsuboi, T.; Takeo, S.; Iriko, H.; Jin, L.; Tsuchimochi, M.; Matsuda, S.; Han, E. T.; Otsuki, H.; Kaneko, O.; Sattabongkot, J.; Udomsangpetch, R.; Sawasaki, T.; Torii, M.; Endo, Y., Wheat germ cell-free system-based production of malaria proteins for discovery of novel vaccine candidates. *Infect. Immun.* **2008,** *76* (4), 1702-8.
90. Chen, J. H.; Jung, J. W.; Wang, Y.; Ha, K. S.; Lu, F.; Lim, C. S.; Takeo, S.; Tsuboi, T.; Han, E. T., Immunoproteomics profiling of blood stage Plasmodium vivax infection by high-throughput screening assays. *J Proteome Res* **2010,** *9* (12), 6479-89.
91. Janssen, D. B., Evolving haloalkane dehalogenases. *Curr. Opin. Chem. Biol.* **2004,** *8* (2), 150-9.
92. Los, G. V.; Encell, L. P.; McDougall, M. G.; Hartzell, D. D.; Karassina, N.; Zimprich, C.; Wood, M. G.; Learish, R.; Ohana, R. F.; Urh, M.; Simpson, D.; Mendez, J.; Zimmerman, K.; Otto, P.; Vidugiris, G.; Zhu, J.; Darzins, A.; Klaubert, D. H.; Bulleit, R. F.; Wood, K. V., HaloTag: a novel protein labeling technology for cell imaging and protein analysis. *ACS Chem Biol* **2008,** *3* (6), 373-82.
93. Ohana, R. F.; Encell, L. P.; Zhao, K.; Simpson, D.; Slater, M. R.; Urh, M.; Wood, K. V., HaloTag7: a genetically engineered tag that enhances bacterial expression of soluble proteins and improves protein purification. *Protein Expr. Purif.* **2009,** *68* (1), 110-20.
94. De Genst, E. J.; Guilliams, T.; Wellens, J.; O'Day, E. M.; Waudby, C. A.; Meehan, S.; Dumoulin, M.; Hsu, S. T.; Cremades, N.; Verschueren, K. H.; Pardon, E.; Wyns, L.; Steyaert, J.; Christodoulou, J.; Dobson,

C. M., Structure and properties of a complex of alpha-synuclein and a single-domain camelid antibody. *J. Mol. Biol.* **2010,** *402* (2), 326-43.
95. de Marco, A., Biotechnological applications of recombinant single-domain antibody fragments. *Microb Cell Fact* **2011,** *10*, 44.
96. Sharma, S.; Pathak, S., Malaria vaccine: a current perspective. *Journal of vector borne diseases* **2008,** *45* (1), 1-20.
97. Birkenmeyer, L.; Muerhoff, A. S.; Dawson, G. J.; Desai, S. M., Isolation and characterization of the MSP1 genes from Plasmodium malariae and Plasmodium ovale. *The American journal of tropical medicine and hygiene* **2010,** *82* (6), 996-1003.
98. Holder, A. A.; Blackman, M. J.; Burghaus, P. A.; Chappel, J. A.; Ling, I. T.; McCallum-Deighton, N.; Shai, S., A malaria merozoite surface protein (MSP1)-structure, processing and function. *Mem. Inst. Oswaldo Cruz* **1992,** *87 Suppl 3*, 37-42.
99. Remarque, E. J.; Faber, B. W.; Kocken, C. H.; Thomas, A. W., Apical membrane antigen 1: a malaria vaccine candidate in review. *Trends in parasitology* **2008,** *24* (2), 74-84.
100. Sawasaki, T.; Morishita, R.; Gouda, M. D.; Endo, Y., Methods for high-throughput materialization of genetic information based on wheat germ cell-free expression system. *Methods Mol. Biol.* **2007,** *375*, 95-106.
101. Spirin, A. S.; Baranov, V. I.; Ryabova, L. A.; Ovodov, S. Y.; Alakhov, Y. B., A continuous cell-free translation system capable of producing polypeptides in high yield. *Science* **1988,** *242* (4882), 1162-4.
102. Shevchenko, A.; Tomas, H.; Havlis, J.; Olsen, J. V.; Mann, M., In-gel digestion for mass spectrometric characterization of proteins and proteomes. *Nature protocols* **2006,** *1* (6), 2856-60.
103. Guild, K.; Zhang, Y.; Stacy, R.; Mundt, E.; Benbow, S.; Green, A.; Myler, P. J., Wheat germ cell-free expression system as a pathway to improve protein yield and solubility for the SSGCID pipeline. *Acta Crystallogr Sect F Struct Biol Cryst Commun* **2011,** *67* (Pt 9), 1027-31.
104. Woehlbier, U.; Epp, C.; Kauth, C. W.; Lutz, R.; Long, C. A.; Coulibaly, B.; Kouyate, B.; Arevalo-Herrera, M.; Herrera, S.; Bujard, H., Analysis of antibodies directed against merozoite surface protein 1 of the human malaria parasite Plasmodium falciparum. *Infect. Immun.* **2006,** *74* (2), 1313-22.
105. Mudeppa, D. G.; Pang, C. K.; Tsuboi, T.; Endo, Y.; Buckner, F. S.; Varani, G.; Rathod, P. K., Cell-free production of functional Plasmodium falciparum dihydrofolate reductase-thymidylate synthase. *Mol. Biochem. Parasitol.* **2007,** *151* (2), 216-9.
106. Tohmoto, T.; Takashima, E.; Takeo, S.; Morita, M.; Nagaoka, H.; Udomsangpetch, R.; Sattabongkot, J.; Ishino, T.; Torii, M.; Tsuboi, T., Anti-MSP11 IgG inhibits Plasmodium falciparum merozoite invasion into erythrocytes in vitro. *Parasitol Int* **2019,** *69*, 25-29.
107. Tachibana, M.; Miura, K.; Takashima, E.; Morita, M.; Nagaoka, H.; Zhou, L.; Long, C. A.; Richter King, C.; Torii, M.; Tsuboi, T.; Ishino, T., Identification of domains within Pfs230 that elicit transmission blocking antibody responses. *Vaccine* **2019,** *37* (13), 1799-1806.
108. Jin, J.; Hjerrild, K. A.; Silk, S. E.; Brown, R. E.; Labbe, G. M.; Marshall, J. M.; Wright, K. E.; Bezemer, S.; Clemmensen, S. B.; Biswas, S.; Li, Y.; El-Turabi, A.; Douglas, A. D.; Hermans, P.; Detmers, F. J.; de Jongh, W. A.; Higgins, M. K.; Ashfield, R.; Draper, S. J., Accelerating the clinical development of protein-based vaccines for malaria by efficient purification using a four amino acid C-terminal 'C-tag'. *Int. J. Parasitol.* **2017,** *47* (7), 435-446.
109. Promega HaloTag® Ligands. https://www.promega.com/en/products/protein-expression/protein-labeling-and-detection/halotag-fluorescent-ligands (accessed April 1).
110. North, S. H.; Wojciechowski, J.; Chu, V.; Taitt, C. R., Surface immobilization chemistry influences peptide-based detection of lipopolysaccharide and lipoteichoic acid. *J Pept Sci* **2012,** *18* (6), 366-72.
111. Ayoglu, B.; Szarka, E.; Huber, K.; Orosz, A.; Babos, F.; Magyar, A.; Hudecz, F.; Rojkovich, B.; Gati, T.; Nagy, G.; Schwenk, J. M.; Sarmay, G.; Prechl, J.; Nilsson, P.; Papp, K., Bead arrays for antibody and

complement profiling reveal joint contribution of antibody isotypes to C3 deposition. *PLoS One* **2014,** *9* (5), e96403.
112. Heubach, Y.; Planatscher, H.; Sommersdorf, C.; Maisch, D.; Maier, J.; Joos, T. O.; Templin, M. F.; Poetz, O., From spots to beads-PTM-peptide bead arrays for the characterization of anti-histone antibodies. *Proteomics* **2013,** *13* (6), 1010-5.
113. Malaprade, L., A study of the action of polyalcohols on periodic acid and alkaline periodates. *Bull. Soc. Chim. Fr.* **1934,** *3* (1), 833.
114. Kamiya, T.; Saito, Y.; Seki, H.; Hashimot.M, Hypocholesterolemic Alkaloids of Lentinus-Edodes (Berk)Sing .2. Novel Synthesis of Eritadenine. *Journal of Heterocyclic Chemistry* **1972,** *9* (2), 898-906.
115. Benink, H.; McDougall, M.; Klaubert, D.; Los, G., Direct pH measurements by using subcellular targeting of 5(and 6-) carboxyseminaphthorhodafluor in mammalian cells. *Biotechniques* **2009,** *47* (3), 769-74.
116. Priest, J. W.; Plucinski, M. M.; Huber, C. S.; Rogier, E.; Mao, B.; Gregory, C. J.; Candrinho, B.; Colborn, J.; Barnwell, J. W., Specificity of the IgG antibody response to Plasmodium falciparum, Plasmodium vivax, Plasmodium malariae, and Plasmodium ovale MSP119 subunit proteins in multiplexed serologic assays. *Malar J* **2018,** *17* (1), 417.
117. Ambrosino, E.; Dumoulin, C.; Orlandi-Pradines, E.; Remoue, F.; Toure-Balde, A.; Tall, A.; Sarr, J. B.; Poinsignon, A.; Sokhna, C.; Puget, K.; Trape, J. F.; Pascual, A.; Druilhe, P.; Fusai, T.; Rogier, C., A multiplex assay for the simultaneous detection of antibodies against 15 Plasmodium falciparum and Anopheles gambiae saliva antigens. *Malar J* **2010,** *9*, 317.
118. Jia, J.; Wang, W.; Meng, W.; Ding, M.; Ma, S.; Wang, X., Development of a multiplex autoantibody test for detection of lung cancer. *PLoS One* **2014,** *9* (4), e95444.
119. Chery, L.; Maki, J. N.; Mascarenhas, A.; Walke, J. T.; Gawas, P.; Almeida, A.; Fernandes, M.; Vaz, M.; Ramanan, R.; Shirodkar, D.; Bernabeu, M.; Manoharan, S. K.; Pereira, L.; Dash, R.; Sharma, A.; Shaik, R. B.; Chakrabarti, R.; Babar, P.; White, J., 3rd; Mudeppa, D. G.; Kumar, S.; Zuo, W.; Skillman, K. M.; Kanjee, U.; Lim, C.; Shaw-Saliba, K.; Kumar, A.; Valecha, N.; Jindal, V. N.; Khandeparkar, A.; Naik, P.; Amonkar, S.; Duraisingh, M. T.; Tuljapurkar, S.; Smith, J. D.; Dubhashi, N.; Pinto, R. G.; Silveria, M.; Gomes, E.; Rathod, P. K., Demographic and clinical profiles of Plasmodium falciparum and Plasmodium vivax patients at a tertiary care centre in southwestern India. *Malar J* **2016,** *15* (1), 569.
120. Hussain, S.; Saxena, S.; Shrivastava, S.; Arora, R.; Singh, R. J.; Jena, S. C.; Kumar, N.; Sharma, A. K.; Sahoo, M.; Tiwari, A. K.; Mishra, B. P.; Singh, R. K., Multiplexed Autoantibody Signature for Serological Detection of Canine Mammary Tumours. *Sci Rep* **2018,** *8* (1), 15785.
121. Noedl, H.; Se, Y.; Schaecher, K.; Smith, B. L.; Socheat, D.; Fukuda, M. M., Evidence of artemisinin-resistant malaria in western Cambodia. *The New England journal of medicine* **2008,** *359* (24), 2619-20.
122. Immunity to Malaria. https://www.immunopaedia.org.za/immunology/special-focus-area/4-immunity-to-malaria/.